ÅBO AKADEMI

FAKULTETEN FÖR
NATURVETENSKAPER OCH
TEKNIK

FACULTY OF
SCIENCE AND
ENGINEERING

Johan Gadolin
processkemiska centret

Johan Gadolin
Process Chemistry Centre

REPORT 16-01

Chemical Changes in Biomass during Torrefaction

Tooran Khazraie Shoulaifar

Doctoral Thesis

Laboratory of Inorganic Chemistry

REPORT 16-01

Chemical Changes in Biomass during Torrefaction

Tooran Khazraie Shoulaifar

Tooran Khazraie Shoulaifar

Laboratory of Inorganic Chemistry

Department of Chemical Engineering

Åbo Akademi University

Supervisors

Professor Mikko Hupa

Åbo Akademi University

D.Sc. Nikolai DeMartini

Åbo Akademi University

Opponent

Professor Leonardo Tognotti

University of Pisa, Italy

Reviewers

Professor Jenny Jones

University of Leeds, England

D.Sc. Vesna Barisic

Foster Wheeler Company, Finland

Acknowledgement

of love, concern and support during all these years. Very special thanks go to my loving mother and sister who were with me day in day out despite the long geographical distance. I dedicate this dissertation to my father who must be smiling now in the heavens to see me fulfilling his dreams. My heartiest gratitude to Shakiba, my lovely daughter, and Mehdi, my husband, who were the source of inspiration and made my time in Finland full of joy and warmth.

Tooran Khazraie Shoulaifar
January 2016, Turku, Finland

Abstract

Torrefaction is moderate thermal treatment (~200-300 °C) of biomass in an inert atmosphere. The torrefied fuel offers advantages to traditional biomass, such as higher heating value, reduced hydrophilic nature, increased its resistance to biological decay, and improved grindability. These factors could, for instance, lead to better handling and storage of biomass and increased use of biomass in pulverized combustors. In this work, we look at several aspects of changes in the biomass during torrefaction. We investigate the fate of carboxylic groups during torrefaction and its dependency to equilibrium moisture content. The changes in the wood components including carbohydrates, lignin, extractable materials and ash-forming matters are also studied. And at last, the effect of K on torrefaction is investigated and then modeled.

In biomass, carboxylic sites are partially responsible for its hydrophilic characteristic. These sites are degraded to varying extents during torrefaction. In this work, methylene blue sorption and potentiometric titration were applied to measure the concentration of carboxylic groups in torrefied spruce wood. The results from both methods were applicable and the values agreed well. A decrease in the equilibrium moisture content at different humidity was also measured for the torrefied wood samples, which is in good agreement with the decrease in carboxylic group contents. Thus, both methods offer a means of directly measuring the decomposition of carboxylic groups in biomass during torrefaction as a valuable parameter in evaluating the extent of torrefaction. This provides new information to the chemical changes occurring during torrefaction.

The effect of torrefaction temperature on the chemistry of birch wood was investigated. The samples were from a pilot plant at Energy research Center of the Netherlands (ECN). And in that way they were representative of industrially produced samples. Sugar analysis was applied to analyze the hemicellulose and cellulose content during torrefaction. The results show a significant degradation of hemicellulose already at 240 °C, while cellulose degradation becomes significant above 270 °C torrefaction. Several methods including Klason lignin method, solid state NMR and Py-GC-MS analyses were applied to measure the changes in lignin during torrefaction. The changes in the ratio of phenyl, guaiacyl and syringyl units show that lignin degrades already at 240 °C to a small extent. To investigate the changes in the extractives from acetone extraction during torrefaction, gravimetric method, HP-SEC and GC-FID followed by GC-MS analysis were performed. The content of acetone-extractable material increases already at 240 °C torrefaction through the degradation of carbohydrate and lignin. The molecular weight of the acetone-extractable material decreases with increasing the torrefaction temperature. The formation of some valuable materials like syringaresinol or vanillin is also observed which is important from biorefinery perspective.

To investigate the change in the chemical association of ash-forming elements in birch wood during torrefaction, chemical fractionation was performed on the original and torrefied birch samples. These results give a first understanding of the changes in the association of ash-forming elements during torrefaction. The most significant changes can be seen in the distribution of calcium, magnesium and manganese, with some change in water solubility seen in potassium. These changes may in part be due to the destruction of carboxylic groups. In addition to some changes in water and acid solubility of phosphorous, a clear decrease in the concentration of both chlorine and sulfur was observed. This would be a significant additional benefit for the combustion of torrefied biomass.

Another objective of this work is studying the impact of organically bound K, Na, Ca and Mn on mass loss of biomass during torrefaction. These elements were of interest because they have been shown to be catalytically active in solid fuels during pyrolysis and/or gasification. The biomasses were first acid washed to remove the ash-forming matters and then organic sites were doped with K, Na, Ca or Mn. The results show that K and Na bound to organic sites can significantly increase the mass loss during torrefaction. It is also seen that Mn bound to organic sites increases the mass loss and Ca addition does not influence the mass loss rate on torrefaction. This increase in mass loss during torrefaction with alkali addition is unlike what has been found in the case of pyrolysis where alkali addition resulted in a reduced mass loss. These results are important for the future operation of torrefaction plants, which will likely be designed to handle various biomasses with significantly different contents of K. The results imply that shorter retention times are possible for high K-containing biomasses.

The mass loss of spruce wood with different content of K was modeled using a two-step reaction model based on four kinetic rate constants. The results show that it is possible to model the mass loss of spruce wood doped with different levels of K using the same activation energies but different pre-exponential factors for the rate constants. Three of the pre-exponential factors increased linearly with increasing K content, while one of the pre-exponential factors decreased with increasing K content. Therefore, a new torrefaction model was formulated using the hemicellulose and cellulose content and K content. The new torrefaction model was validated against the mass loss during the torrefaction of aspen, miscanthus, straw and bark. There is good agreement between the model and the experimental data for the other biomasses, except bark. For bark, the mass loss of acetone extractable material is also needed to be taken into account. The new model can describe the kinetics of mass loss during torrefaction of different types of biomass. This is important for considering fuel flexibility in torrefaction plants.

Referat

Torrefiering (eng. Torrefaction) är mild värmebehandling (~200-300 °C) av biomassa i syrefri atmosfär. Torrefierad biomassa har flera fördelar jämfört med obehandlad biomassa såsom högre värmevärde, mindre hydrofil karaktär, förbättrad resistans mot biologisk nedbrytning och förbättrad malbarhet. Dessa faktorer kan ge förbättrade förvaringsmöjligheter och ökad användning av biomassa, framförallt inom pulveriserad förbränning av biomassa. I avhandlingen studeras hur biomassa förändras i och med torrefiering. I avhandlingen undersöks hur koncentrationen av karboxylgrupper förändras under torrefiering samt hur fukthalten vid jämvikt med omgivningen beror på koncentrationen av karboxylgrupperna. Dessutom studeras förändringar i biomassans beståndsdelar såsom kolhydrater, lignin, extraktivämnen och askbildande material. Slutligen undersöks hur kaliumhalten inverkar på torrefiering.

Karboxylgrupperna förklarar till stor del den hydrofila karaktären hos biomassan. Dessa förstörs delvis under torrefiering. I avhandlingen används två metoder för bestämning av koncentrationen av karboxylgrupper i torrefierad granved: absorption av metlyenblå samt potentiometrisk titrering. Metodernas resultat överensstämde väl sinsemellan. För de torrefierade träproven noterades en minskning av fukthalten vid jämvikt jämfört med de obehandlade träproven, vilket överensstämmer med minskningen av koncentrationen av karboxylgrupperna. Avhandlingen visar att båda metoderna kan användas för att studera koncentrationsförändring av karboxylgrupper i biomassa under torrefiering, vilket i sin tur kan utnyttjas för att mäta graden av torrefiering och för att få en ökad förståelse för de kemiska förändringar som sker under torrefiering.

I avhandlingen undersöks även hur torrefieringstemperaturen inverkar på kemin hos björkved. Torrefierad björkved togs från en pilotanläggning vid Energy research Center of the Netherlands (ECN). Följaktligen representerade proven industriellt framställda prov. Analys av olika sockerarter användes för att bestämma koncentrationen av hemicellulosor och cellulosa under torrefiering. Resultaten visar att nedbrytning av hemicellulosorna är betydande redan vid 240 °C, medan nedbrytningen av cellulosa är betydande först vid 270 °C. Flera experimentella metoder såsom den s.k. Klason lignin metoden, fastfas-NMR och Py-GC-MS-analyser användes för att bestämma förändringen av ligninhalten under torrefiering. Förändringar i förhållandet av fenyl, guaiacyl och syringylenheter visar att ligninets nedbrytning påbörjas redan vid 240 °C. För att undersöka förändringar i extraktivämnen från acetonextraktion under torrefiering gjordes gravimetriska experiment, HPSEC och GC-FID-analyser följt av GC-MS-analyser. Halten av aceton-extraherbart material ökar redan vid 240 °C i och med nedbrytning av kolhydrater och lignin. Molekylvikten av det acetonextraherbara materialet minskar som funktion torrefieringstemperaturen. Dessutom observerades att kommersiellt värdefulla material som syringaresinol eller vanillin bildades, vilket är viktigt utifrån ett bioraffinaderiperspektiv.

Kemisk fraktionering av obehandlade prov och av torrefierade prov av björkved utfördes för att undersöka förändringen i specieringen i askbildande element. Resultaten ger en första förståelse för förändringar i specieringen för askbildande element under torrefiering. De mest signifikanta förändringarna observerades i distributionen av kalcium, magnesium och mangan. Dessutom observerades små förändringar i vattenlösligheten av kalium. Förändringarna kan delvis förklaras från degraderingen av karboxylgrupper. Förutom förändringar i vatten och syralösligheten av fosfor observerades en tydlig

koncentrationsminskning av klor och svavel. Även detta kunde vara fördelaktigt vid förbränning av torrefierad biomassa.

Ett annat mål med avhandlingen var att undersöka hur organiskt bundet kalium, natrium, kalcium och mangan inverkar på viktminskningen av biomassan under torrefiering. Dessa element inverkar katalytisk på viktiga kemiska reaktioner som sker vid pyrolys och förgasning och är därför viktiga med avseende på torrefiering. I avhandlingen syratvättades olika typers biomassor för att separera askbildande material, varefter organiska säten dopades med kalium, natrium, kalcium eller mangan. Resultaten visar att organisk bundet kalium och natrium kan öka viktminskningen signifikant vid torrefiering. Resultaten visar dessutom att organiskt bundet mangan ökar viktminskningen medan kalcium inte påskyndar viktminskningen vid torrefiering. Den ökade viktminskningen vid torrefiering som funktion av ökad alkalikoncentration överensstämmer inte med vad som tidigare observerats under pyrolysexperiment, enligt vilka viktminskningen minskar som funktion av ökad alkalikoncentration. Dessa resultat är viktiga att beakta i framtida torrefieringsanläggningar som designas för att fungera för biomassor med olika koncentrationer av kalium. Resultaten indikerar att kortare uppehållstider kan uppnås för biomassor med höga kaliumkoncentrationer.

Viktminskningen för prov av granved med olika koncentrationer av kalium modellerades med en s.k. tvåstegsmodell som baserar sig på fyra kinetiska hastighetskonstanter. Resultaten visar att det är möjligt att modellera viktminskningen av granved dopat med olika mängder av kalium med samma aktiveringsenergi men med olika frekvensfaktorer för de fyra hastighetskonstanterna. Tre av frekvensfaktorerna ökar linjärt med ökad kaliumkoncentration, medan en av frekvensfaktorerna minskar som funktion av ökad kaliumkoncentration. Utifrån detta utvecklades en ny modell för beskrivningen av viktminskning vid torrefiering endast beroende på halten hemicellulosor, cellulosa och koncentrationen av kalium. Den nya kinetiska torrefieringsmodellen validerades gentemot torrefieringsexperiment med asp, miskantus och bark. Modellerade resultat överensstämde med experimentella resultat för samtliga bränslen utom bark. För bark måste även acetonextraherbart material tas i beaktande. Den nya modellen kan beskriva viktminskning vid torrefiering för olika typers biomassor. Detta har praktisk betydelse för att förstå hur olika typers bränslen kan tas i beaktande i framtida torrefieringsanläggningar.

Nyckelord: torrefiering, biomassa, pyrolys, alkalimetall, hemicellulosor, cellulosa, lignin, extraktivämnen, askbildande element, klor

List of Publications

This thesis is based on the following original publications, which are referred to in the text as I-V.

I <u>T. Khazraie Shoulaifar</u>, N. DeMartini, A. Ivaska, P. Fardim, M. Hupa. Measuring the Concentration of Carboxylic Acid Groups in Torrefied Spruce Wood; Bioresource Technology, **2012** 123, pp. 338–343.

II <u>T. Khazraie Shoulaifar</u>, N. DeMartini, S. Willför, A. Pranovich, A. Smeds, T. Virtanen, S. L. Maunu, F. Verhoeff, J. Kiel, M. Hupa. Impact of Torrefaction on the Chemical Structure of Birch Wood; *Energy Fuels*, **2014**, *28* (6), pp. 3863–3872.

III <u>T. Khazraie Shoulaifar</u>, N. DeMartini, M. Zevenhoven, F. Verhoeff, J. Kiel, M.Hupa. Ash Forming Matter in Torrefied Birch Wood: Changes in Chemical Association; *Energy Fuels*, **2013**, *27* (10), pp. 5684–5690.

IV <u>T. Khazraie Shoulaifar</u>, N. DeMartini, O. Karlström, M. Hupa. Impact of Organically Bonded Potassium on Torrefaction: Part 1. Experimental; *Fuel,* **2016,**165, pp. 544–552.

V <u>T. Khazraie Shoulaifar</u>, N. DeMartini, O. Karlström, J. Hemming, M. Hupa. Impact of Organically Bonded Potassium on Torrefaction: Part 2. Modeling; *Fuel,* **2016,**168, pp. 107–115.

Author's Contribution

In all the papers Tooran Khazraie Shoulaifar was responsible for writing the manuscripts. Khazraie, Dr. DeMartini and Professor Hupa planned the experimental matrix.

Paper I: Professor Fardim and Professor Ivaska provided the author with technical advice over methylene blue sorption technique and potentiometric titration, respectively.

Paper II: Dr. Smeds performed GC-MS and Py-GC-MS, and Dr. Pranovich and Professor Willför gave technical advice for lignin, extractable materials and sugar analyses. Professor Maunu and Dr. Virtanen performed the solid state NMR.

Paper III: Torrefaction was performed at ECN and the samples were received from Professor Kiel and Engineer Verhoeff. Dr. Zevenhoven gave technical advice in fuel fractionation.

Paper V: Dr. Karlström wrote the MATLAB codes for the model and helped to develop the model. Mr. Hemming performed the fiber analysis.

Other Publications by the author

1. S. B. Saleh, J. P. Flensborg, <u>T. Khazraie Shoulaifar</u>, Z. Sárossy, B. B. Hansen, H. Egsgaard, P. A. Jensen, P. Glarborg, K. Dam-Johansen, N. DeMartini. Release of Cl and S during biomass torrefaction and pyrolysis. *Energy Fuels*, **2014**, *28* (6), pp. 3738–3746.

2. <u>T. Khazraie Shoulaifar</u>, N. DeMartini, O. Karlström, M. Hupa. "Catalytic Effect of Potassium on Torrefaction" in Bioenergy from Forest **2014**, September 15-18, Helsinki, Finland – Oral presentation.

3. <u>T. Khazraie Shoulaifar</u>, N. DeMartini, M. Zevenhoven, S. Willför, A. Pranovich, A.Smeds, T. Virtanen, S. L. Maunu, F. Verhoeff, J. Kiel, M. Hupa. "Impact of Torrefaction on Chemical Structure of Woody Biomass" in American Chemical Society (ACS), Fall **2013**, September 8-12, Indianapolis, IN, US –Oral presentation.

4. <u>T. Khazraie Shoulaifar</u>, N. DeMartini, M. Zevenhoven, F. Verhoeff, J. Kiel, M. Hupa. "Ash Forming Matter in Torrefied Birch Wood" in Impacts of Fuels Quality on Power Production and the Environment Conference in **2012**, September 23-27, Puchberg, Vienna, Austria – Oral presentations.

Table of Contents

Chapter One: Introduction

Biomass, as a carbon-neutral fuel, is one source of renewable energy. One option is to partially or fully replace coal with biomass in coal fired boilers. There are important differences between coal and biomass and how to efficiently replace coal with biomass is an important area of research. Coal has a much higher heating value than biomass, so generally more biomass is needed for the same heat input. Storage of biomass has different requirements than coal. In open environments, biomass absorbs water and starts to biodegrade. Additionally for pulverized fuel combustion, the grinding of raw biomass requires more energy to obtain a similar particle size distribution as coal, due to the long polymeric chains in the biomass structure.

Torrefaction[1] can alter some of the characteristics of biomass for combustion applications. During torrefaction, biomass is heated up to a temperature of 200-300 ˚C in an inert atmosphere. A part of the original biomass is released as volatiles and the remaining char can be used as a fuel. The properties of torrefied biomass are more similar to coal: it absorbs less water [1], it is resistant to biodegradation [2], it has higher heating value and its grinding is easier [3]. Thus, torrefaction may be a useful technology for increased use of biomass in power plants.

Torrefaction is currently a technology trying to emerge. There are operating pilot plants and demonstration plants, but torrefied biomass has not become an important fuel source in power boilers burning biomass. The focus of former researches, conducted on woody and herbaceous biomasses, mostly deal with physical properties of biomass, including mass loss, changes in heating values as well as changes to storage and handling properties. These researches, however, have not profoundly taken the chemical changes in torrefied biomass into account. I have laid my focus on two main elements: Firstly, the chemical changes that occurs during torrefaction. A better view of these changes is important to understanding the physical properties in biomass and finding new application for torrefied biomass rather than mere fuel. Secondly, how torrefaction conditions would need to be changed to handle different types of feedstock.

---

[1] The term "torrefaction" originates from French, meaning roasting. Torrefaction was used when the coffee beans were roasted.

1.1. Principles

1.1.1. Heating Stages in Torrefaction

During torrefaction, biomass partially degrades and part of its mass releases. This results in the chars and volatiles. The volatiles include condensable compounds and non-condensable gas. The resulting char contains some of the original components as well as newly formed compounds that are a product of sugar and lignin degradations. Condensable phase of the volatiles contains water and tar – organic high molecule compounds like lipids and phenols. The non-condensable gas contains CO_2, CO and very light hydrocarbons.

The process of torrefaction occurs in a number of stages which are shown in Figure 1. It starts with drying in which the moisture inside the biomass evaporates. The volatilization of some light organic compounds in biomass, including a number of so-called extractives such as terpenes [4] also overlaps with the evaporation. At higher temperatures of 180 ˚C lignin starts to be softened and becomes more amorphous. Finally, the breakage of the some bonds between hydrogen, oxygen and carbon occurs, and the biomass starts to thermally degrade and torrefied biomass is produced. In practice, the released volatiles, called torgas, burn to totally/partially supply the required heat for the continuation of torrefaction.
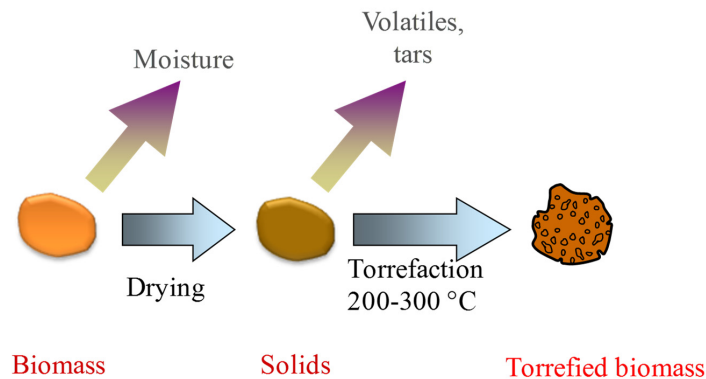
Figure 1. The steps in the process of torrefaction

1.1.2. Proximate and Ultimate Analyses

The proximate analysis shows that the torrefied biomass has higher fixed carbon and lower volatile matter than the original biomass. The higher content of fixed carbon in torrefied biomass is closer to coal. The increase in the fixed carbon is attributed to a partial volatilization, which occurs during torrefaction [5].

The ultimate analysis of torrefied biomass shows that more H and O are released compared to C during torrefaction. Consequently, the atomic ratios of O/C and H/C of torrefied biomass are smaller than that of the raw biomass. This can be illustrated in Van Krevelen diagram, Figure 2. It is seen in Figure 2 that the chemical composition of torrefied wood is close to peat.
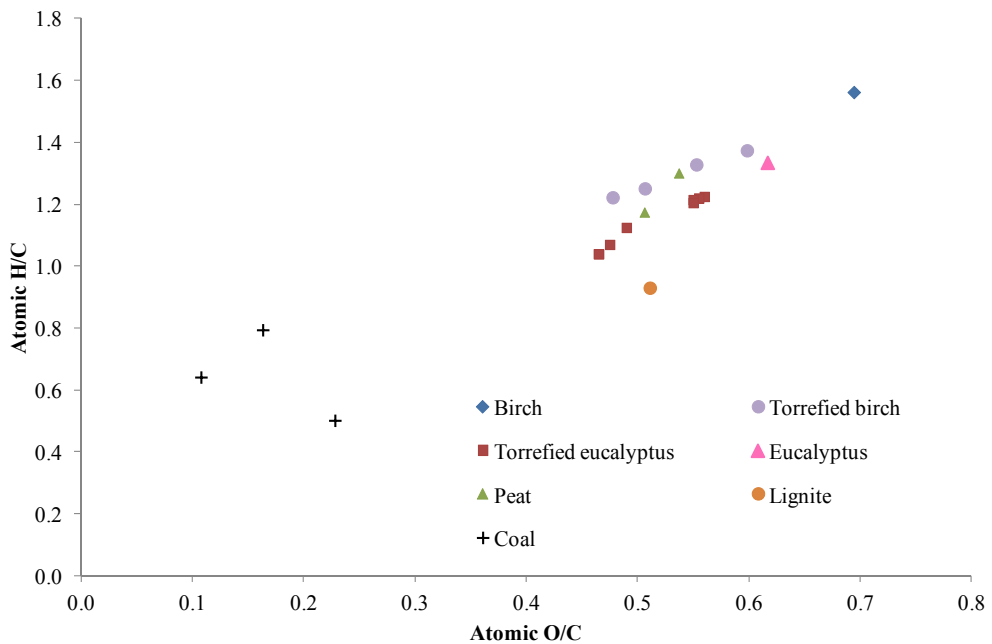
Figure 2. Torrefied biomass at Van Krevelen diagram (data from [6]**)**

1.1.3. Mass Loss

The changes in the content of biomass can be shown by mass loss or mass yield of the biomass during torrefaction, equation (1&2) [7,8]:

$$L_{mass}\% = \frac{(Initial\ Mass - Final\ Mass)}{Initial\ Mass} \times 100 \qquad\qquad \text{equation (1)}$$

where L_{mass} is mass loss.

$$Y_{mass}\% = \frac{Final\ Mass}{Initial\ Mass} \times 100 = 100 - L_{mass}\% \qquad\qquad \text{equation (2)}$$

where Y_{mass} is mass yield.

The final mass and the initial mass are usually provided on a dry basis. In practice, it is not common to provide the mass loss or mass yield of torrefaction on the ash free basis.

The mass loss depends on the temperature and residence time. The value of the mass loss varies widely, for instance, it is reported that the mass loss for the wood residues are between 6 and 57% [9], and particularly 5-63% [10] for pine. It was proposed that the mass loss from torrefaction could be correlated to the fuel properties like heating value and Equilibrium Moisture Content (EMC) [11].

1.1.4. Energy Yield

The energy yield describes the amount of biomass energy retained in the torrefied biomass [12]. The energy yield is defined as the ratio of the total energy still in the torrefied biomass to the energy content of raw biomass, equation (3) [12]:

$$Y_{energy}\% = \frac{energy\ in\ torrefied\ biomass}{energy\ in\ raw\ biomass} = (1 - L_{mass}) \times \frac{LHV_{torr}}{LHV_{raw}} \times 100 \qquad \text{equation (3)}$$

where Y_{energy} = energy yield and LHV= lower heating value. The energy yield is expressed on dry basis.

The value of the energy yield, depending on the temperature and residence time, can vary widely. For example, the energy yield for wood residues is reported between 50-97% [9] and for pine particularly 52.4-99.8% [10].

Equation (4) can be derived from equation (3):

$$\frac{LHV_{torr}}{LHV_{raw}} = \frac{Y_{energy}}{(1 - L_{mass})} \qquad\qquad \text{equation (4)}$$

For instance, one of the best reported scenarios for torrefaction of wheat straw at 290 °C is an energy yield of about 66% and a mass yield of about 55%, resulting in an LHV that is 20% higher compared to raw wheat straw [5].

The energy released in the gaseous products, torgas, is used to continue the process of torrefaction. If the energy in torgas is enough to conduct the torrefaction process, the operation is defined as autothermal operation [12]. Less energy in the torgas results in the need for the external heater equipment.

1.1.5. Equilibrium Moisture Content (EMC)

Biomass inherently contains moisture, which normally varies between 10-50% [13]. The moisture in biomass causes some problems: increases the storage and handling costs [14], and makes it susceptible to biodegradation during storage.

The moisture in biomass exists both in bonded and non-bonded forms. Non-bonded moisture exists in the surface and cavities of biomass; whereas bonded water is attracted to the biomass structure by forming hydrogen bonds between the biomass and water. Vasquez and Coronella [15] found that bonded water is not affected by the environment's relative humidity; however, non-bonded water in biomass is increased by increasing the relative humidity of surrounding atmosphere.

The moisture in biomass can be quantified by measuring the Equilibrium Moisture Content (EMC), showing the amount of moisture that biomass has absorbed at a specific temperature, pressure and humidity.

$$EMC\% = \frac{(M_e - M_d)}{M_d} \times 100 \qquad \text{equation (5)}$$

Where M_e is the mass of the sample at equilibrium with a humid atmosphere and M_d is the mass of dry sample.

The EMC values for torrefied biomass are lower than raw biomass. This is due to lower hydrophilic characteristic of torrefied biomass. Increasing the torrefaction temperature decreases the hydrophilic characteristic of biomass [16]. Torrefied pellet also has lower EMC compared to raw pellet made of the same biomass [17]. In that work, the raw and torrefied

pellets of biomass were inserted in water and as a result, the fast disintegration of raw biomass was observed; however, torrefied pellet resisted deformation in the first few minutes of being in water.

Björk and Rasmuson [18] attributed the moisture sorption in biomass foremost to hemicellulose and then to the amorphous cellulose. They believed that crystalline cellulose and lignin in biomass absorb limited amounts of moisture. A number of researchers [17,19] attributed the decrease in hydrophilic characteristic of biomass during torrefaction to the decrease in the hemicellulose content. Hemicellulose is rich in hydroxyl groups, and therefore the reduction in the hydrophilic characteristic of biomass can be attributed to the decrease in any type of hydroxyl groups of hemicellulose in biomass.

1.1.6. Grindability

Due to its polymeric structure, biomass needs high amount of energy to grind and produce fine particles. Torrefaction as a pretreatment can decrease the tenacious characteristic of biomass and produce a more brittle material [20-23].

Bergman and Kiel [24] observed the reduction in the energy required to grind the torrefied biomass 70-90% compared to raw biomass. This reduction depends on the severity of torrefaction and biomass type. Therefore, the grinding characteristic of torrefied biomass becomes closer to coal, so that the existing grinding mill for coal can be used for torrefied biomass as well.

Repellin et al. [20] observed that the increase in mass loss up to 8%, as a result of torrefaction, decreased the grinding energy significantly; however for higher mass losses, the grinding energy decreased only slightly. However, increase in the mass loss resulted in a linear decrease in the mean particle size distribution for torrefied spruce and beech.

Phanphanich and Mani [21] observed that the required energy to grind the pine chips and logging residues decreased already after torrefaction at 225 °C; however a decrease in the mean particle size became significant at higher torrefaction temperatures. Increasing the severity of torrefaction, by increasing the temperature and residence time, results in the formation of finer particles in the final product [3,25,26].

The grindability of torrefied biomass, usually measured by Hardgrove Grindability Index (HGI) [22,26], is primarily used in the coal industry. Increasing the torrefaction temperature plus residence time result in a higher value of the HGI, which shows better grindability of torrefied biomass [22,23]. In this method, the grinding energy is not measured although the HGI of severely torrefied wood and coal show very close values [26]. The better grindability of biomass during torrefaction has been attributed to the removal of hemicellulose [22].

1.1.7. Resistance to Biodegradation

The biodegradation of heat treated wood[2] is studied more than torrefied biomass, but they can be applicable for torrefied biomass. Heat treatment of biomass increases the resistance of biomass to fungal degradation [27-29]. A number of mechanisms explain the better resistance of torrefied biomass, which are as follows:

- Low tendency of heat treated biomass to absorb water results in improved resistance against different types of fungi [28].

- The formation of toxic compounds during heat treatment could also result in a fuel resistant to biodegradation. The extractable material increases during heat treatment, which can explain the resistance of biomass against fungal attack [30].

- The chemical modification of biomass components also prevents the fungi to degrade torrefied biomass. It is proposed that some compounds, such as furfural arising from heat treatment, form a network with lignin. Similarly, acetic acid released from hydrolysis of hemicellulose modifies cellulose by esterification. The mentioned compounds prevent fungi from recognizing the wood's matrix and decaying it [31].

- Torrefaction results in decrease in the amount of pentosans which are important nutrients for fungi [30,31].

Overall, the heat treatment of biomass at torrefaction temperature protects biomass to some extent from biodegradation. This results in a more resistant fuel which improves the storage properties of torrefied biomass.

---

[2] Wood is heat treated at temperatures below 200 °C for the preservation purposes.

1.2. Technology

1.2.1. Utilization of Torrefied Biomass

Due to the mentioned advantages of torrefied biomass to raw biomass, torrefied biomass is utilized in the following applications:

Co-firing in Pulverised Coal Power Plants: Pulverized coal combustors are one of the important power plants which produce energy. Nowadays, the designs of these plants are modified in order to use raw biomass as a renewable fuel. Torrefied biomass, the properties of which are more similar to coal, can replace coal or be co-fired without changing the plants' design [12,32]. A higher heating value, better grindability and a lower tendency to absorb water result in a better fuel compared to raw biomass for use in pulverized fuel boilers [33].

Gasification: Particle size and moisture content of the fuel are key factors during gasification. Therefore, torrefied biomass, due to its lower moisture content, good grindability and higher heating value, is an interesting fuel to be utilized for gasification [25]. A uniform and small particle size of torrefied biomass improves the flow properties of the feedstock and results in higher H_2 and CO formation which consequently improves the efficiency of the entrained-flow gasifiers [34,35]. Torrefier and gasifier can be integrated in a plant so that the released volatiles from the torrefaction can be used in gasifiers [36]. Improved fluidization of torrefied biomass can also increase its usage in fluidized bed gasifiers [37].

The concentration of alkali metals is higher in the torrefied biomass than raw biomass [38]. Alkali metals catalyze the char gasification reaction [39], and thus char gasification from ash-forming matter perspective might be slightly more rapid.

Prior to Pyrolysis: Torrefied biomass can be employed as the fuel of the pyrolyzer in order to produce bio-oil. The studies show that utilization of the torrefied biomass as a fuel prior to pyrolysis has two main advantages. First, as a fuel its storage, handling and grindability are facilitated, and second the properties of the final product are improved: lower water content, lower acidity (decrease in acetic and propanoic acids specifically) of the bio-oil and higher energy content [40].

Pellet Production: Pellet production from milled torrefied biomass has some advantages and some disadvantages compared to raw biomass [41,42]. Torrefied biomass can be milled

easier; however, it requires more energy to produce pellets. This can be attributed to the changes in the lignin during torrefaction which reduces its thermal softening. In order to produce pellets from torrefied biomass, higher temperature of operating condition and/or binders is needed [43]. There are a number of studies on wood and torrefied wood which indicates that producing the pellets is an area that needs more work; however, some studies show that it is both economical and efficient [44,45].

Blast Furnaces: Torrefied biomass can be considered for the application in blast furnaces, since it is a renewable fuel with lower net emission of CO_2. It can be added to coal blends during coke making [46] or can be utilized as injectant into the blast furnace [47]. However, the high content of alkali metals and high amount of volatile matters in torrefied biomass limit its usage in blast furnaces. Therefore, the steel industry's priority is carbonized biomass, and the application of torrefied biomass seems limited [35].

1.2.2. Torrefaction Reactor Types

Commercial development of torrefaction is still in its early stages. Several companies are working to design the torrefaction reactors; though the torrefier in these companies are chiefly on the pilot scale or demonstrated scale [35]. The designing of commercial scale torrefier comes primarily from existing industrial driers [48]. Therefore, they are broadly designed on two main principles of heating: direct and indirect heating methods. In the directly heated torrefier, biomass is in direct contact with hot gas. The origin of the hot gas could be torgas or flue gas from the boiler. In the indirectly heated torrefier, the heating gas is not in a direct contact with biomass, and thus biomass is heated by heat exchanging through reactor's wall [49]. The primary designs are: rotating drum, fluidized bed, moving bed, screw reactor, microwave and multiple hearth furnace reactors [48], which are explained below.

1. ***Rotary drum*** is filled with biomass and rotates around an axis. The heating can be direct or indirect. Andritz/ACB has intended to design an indirectly heated torrefaction reactor with the capacity of 50,000-250,000 ton/year. The biomass is dried in an external dryer and then feed into the rotary drum reactor. The temperature can vary in the range of 250-300 °C with a residence time of about 30 min. The demonstration plant is in Frohnleiten, Austria with a capacity of 1 ton/hr [50].
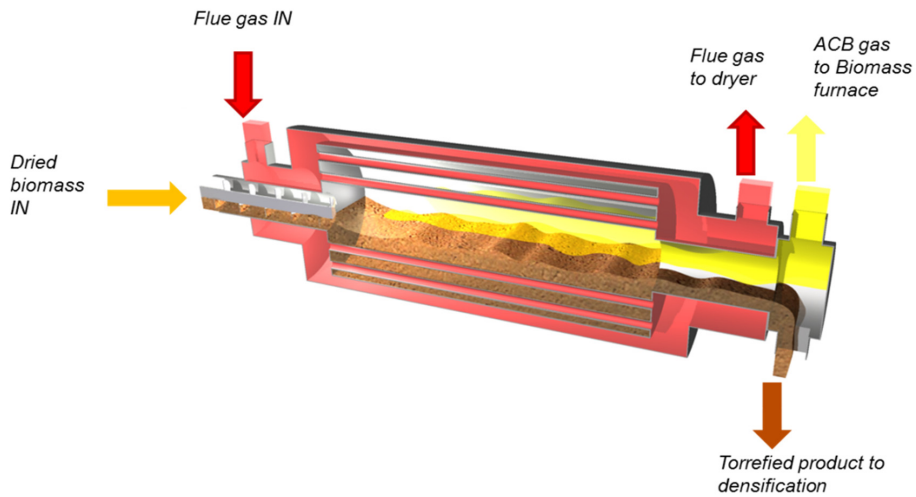
Figure 3. Rotating drum reactor, designed by Andritz located in Austria [51]

In the Andritz/ACB torrefaction reactor, the flows of biomass and hot gas are co-current, Figure 3. In the combination of torrefaction and combustion plants, the flue gas from the boiler can be used to indirectly torrefy the feedstock.

2. The concept of *fluidized bed* reactor is used in TORBED reactor designed by Topell Energy. In this reactor, the biomass and hot gas contact directly for a short period of time (100 s) where a small size of reactor is needed to create a fluidized bed. The maintenance cost in this reactor is expected to be relatively lower than for the other reactors with moving parts [50,52].

3. *Moving bed* is another type of torrefaction reactor; examples include designs by Thermya in France and Andritz in Denmark. TORSPYD is the torrefaction reactor designed by Thermya. They have demonstrated the plant with the capacity of 20,000 ton/year. In this reactor, biomass enters to the reactor, and it is heated in the reactor directly. The operation is a continuous counter-current flow in which the solids flow down in the reactor. And the hot gas is inserted from the bottom of the reactor [53]. The lower investment of this reactor, compared to the other reactors, is a significant advantage in the moving bed reactor [54].

Andritz with Energy research Center of the Netherlands (ECN) plans to design a pressurized torrefaction reactor with the capacity of 700,000 ton/year. The chips are fed with high pressure of two bars into the reactor. The reactor's design is the combination of moving bed

and multiple hearth furnace concepts. It can be seen in Figure 4, the heating process consists of two stages: cross-flow-current, followed by counter-current heating at the bottom of the reactor. The demo plant with the capacity of 1 ton/h is in Stenderup, Denmark [50].
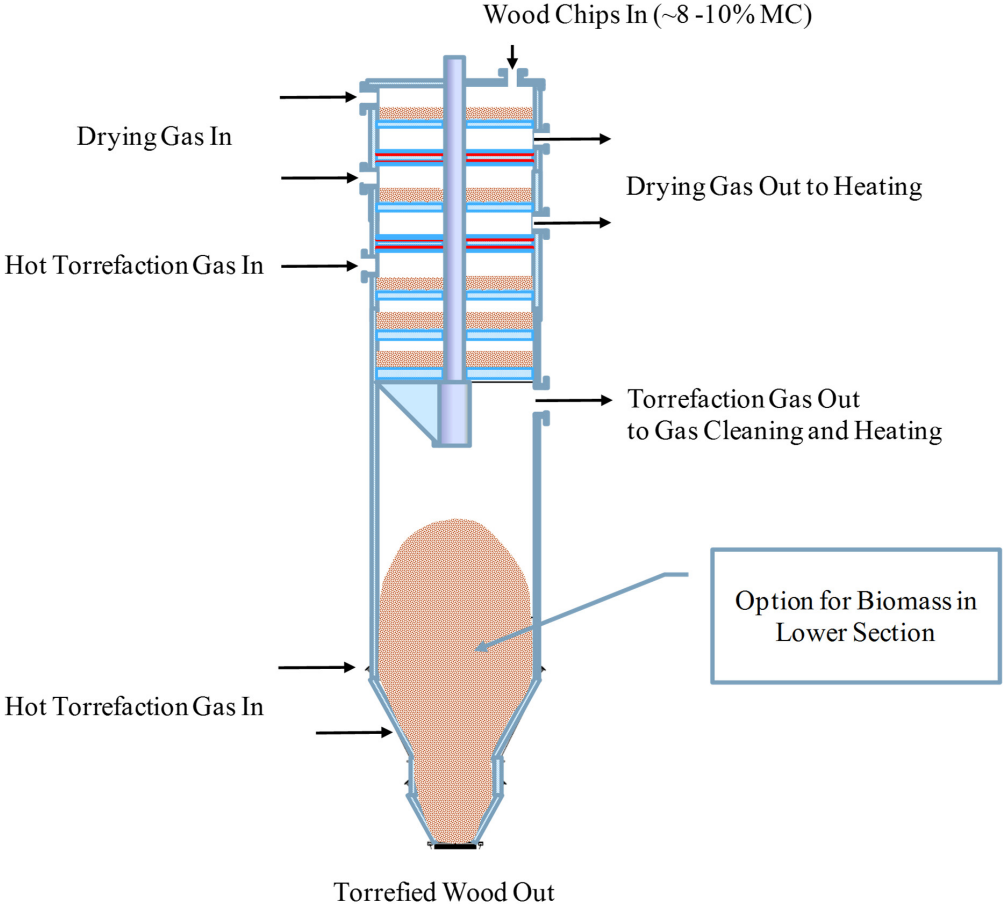
Figure 4. Andritz pressurized reactor concept [51]

4. In the *screw conveyor* reactor, which is a continuous reactor, a wide range of chip sizes can be used. In this type of reactor, biomass can be heated directly through a hot gas or indirectly heated through the walls and shafts of the reactor. Although the latter reactor is more common, char is usually formed on the hot surfaces of the reactor. The maintenance cost of a screw conveyor is relatively high due to several moving parts [48,50].

5. In a *microwave reactor*, biomass is heated by electromagnetic waves of about 2.45 GHz frequency. The main advantage of this method is fast and uniform heating even for large chips

[55]. In this method, the residence time is short. The Rotawave Company has microwave reactor in British Columbia with the capacity of 11000 ton/year of biomass [56].

6. **Multiple hearth furnace** is a continuously counter-current reactor in which biomass enters from the top, and the hot gas flows from the bottom of reactor. The reactor consists of a series of hearths, placed one above the other while a vertical shaft carrying arms rotates through the centre of the cylindrical reactor. Good mixing and a wide range of residence time and biomass particle size are the advantage of this reactor [50].

1.3.   Chemistry of Torrefaction

Biomass, particularly ligno-cellulosic biomass in this study, is composed of hemicellulose, cellulose and lignin [57]. In addition to the main biomass components, biomass contains extractives and ash-forming matters. The content of these components is relatively different depending on biomass type, Table 1.

Table 1: Carbohydrate analysis of different raw biomasses [58]

Components (wt% dry)	Straw (agricultural)	Miscanthus (herbal)	Spruce (softwood)	Beech (hardwood)	Spruce bark
Hemicellulose	25.4	20.1	18.4	21.2	12.9
Cellulose	42.7	45.8	45.0	40.8	24.1
Lignin	17.3	22.4	27.6	23.8	36.8
Ash	5.6	2.3	0.3	0.6	5.0
Extractives	3.2	4.3	1.0	1.0	5.7
Residues	5.8	2.4	7.7	12.6	15.5

1.3.1. Hemicellulose

The portion of hemicellulose in biomass depends on the type of biomass; for instance, woody biomass contains 20-30% hemicellulose, and herbaceous biomass contains 20-35% of hemicellulose [59].

The degree of polymerization in hemicellulose is about 100-200 [60], where the general formula is presented by $(C_5H_8O_4)_n$. This low degree of polymerization is due to the branched

and amorphous structure of hemicellulose [59]. The monomers in the polymeric structure of hemicellulose are sugar units. These monomers include six-carbon sugars, hexoses, and five-carbon sugars, pentoses. Hexoses include glucose (Glu), mannose (Man) and galactose (Gal), and pentoses include xylose (Xyl), arabinose (Ara) and Rhamnose (Rha) [61]. The content of these sugars can help to distinguish the type of biomass. Mostly, softwood contains galactoglucomannan – a polymer mainly consists of Gal, Glu and Man – and hardwood contains xylan – a polymer mainly consists of Xyl [62].

In addition to the above mentioned sugars, hemicellulose contains small amounts of weak acids known as uronic acids including glucuronic acid (GlcA); galacturonic acid (GalA), mainly in pectin; and 4-O-methyl-D-glucuronic acid (4-*O*-Me GlcA). All these acids have carboxyl groups and can carry a negative charge to form a bond to metal ions. Carboxylic groups in hemicellulose are important due to their acidic characteristic, tendency to bind to metal ions and hydrophilic characteristic in the biomass.

During heat treatment, hemicellulose is the most reactive biomass component which decomposes in the temperature range of 225-325 °C, Figure 5. At about 225 °C, hemicellulose undergoes rapid decomposition, producing condensable light volatile organics, non-condensable gases like H_2O, CO_2 and CO and char [63]. Though, hemicellulose containing five-carbon sugars is more sensitive to temperature than the one containing six-carbon sugars [16,64]. Experiments show that at the same conditions, mass loss of hardwood is more than the softwood [65]. This can be explained by higher degradation of xylan than glucomannan in hemicellulose.
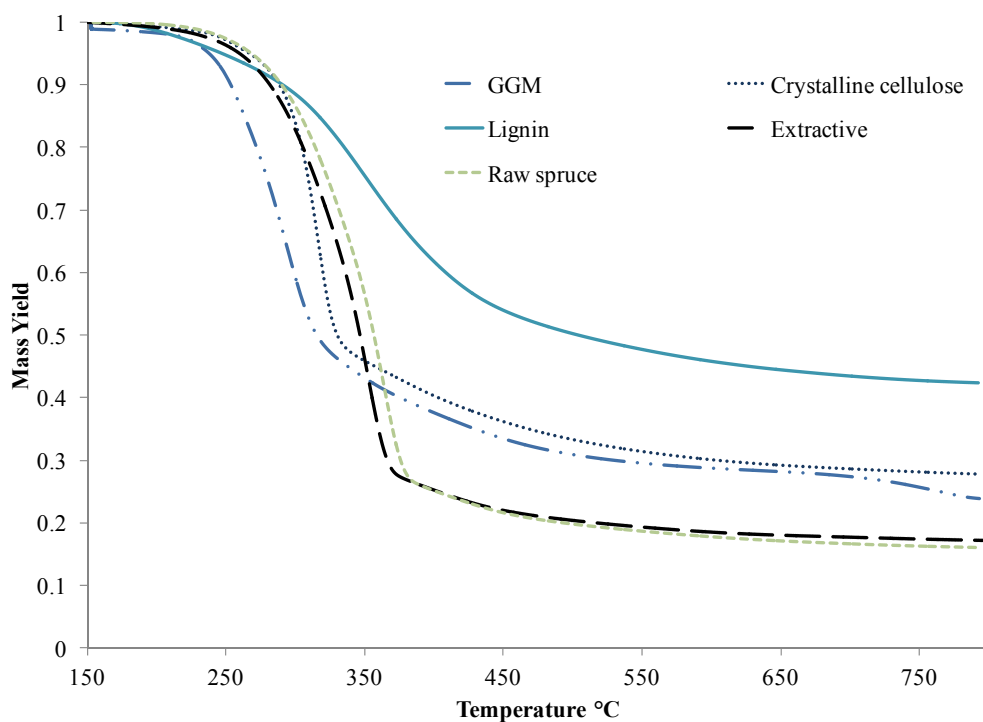
Figure 5. Degradation of raw spruce and its components during heat treatment, run by TG (Data from Paper IV)

The condensable volatiles from torrefaction in hardwood are mainly water and acetic acid (torrefaction of willow at 270 °C : water/acetic acid= 7.5%/3% [65]) plus smaller amounts of methanol, formic acid, lactic acid, furfural, hydroxyl acetone and traces of phenol, while softwood releases chiefly water and formic acid (torrefaction of larch at 270 °C : water/acetic acid= 3%/0.25% and water/formic acid= 3%/1% [65]). The amount of acetic acid increases in hardwood by increasing the torrefaction temperature [66], and the total amount of condensable volatiles from softwood is smaller than hardwood [65].

The total amount of non-condensable volatiles in hardwood is always higher than softwood [65]. This also indicates higher degradation of five-carbon sugars than six-carbon sugars during torrefaction. The gases formed are mainly CO_2 and then CO plus traces of H_2 and CH_4. The formation of CO_2 can be attributed to decarboxylation of acidic group in hemicellulose [67].

1.3.2. Cellulose

Cellulose is the most abundant biopolymer, represented by the general formula $(C_6H_{10}O_5)_n$. The share of this biomass component, for instance in woody biomass, is about 40-45% [59]. Cellulose has a long chain of glucose with a high degree of polymerization (<10000). The tendency of forming intra and inter-molecular hydrogen bonds by hydroxyl groups results in a crystalline structure which gives strength to cellulose. Crystalline cellulose accounts for 60-75% of total cellulose and the rest is amorphous cellulose [59]. The amorphous cellulose is more hydrophilic than crystalline cellulose due to more non-bonded hydroxyl groups.

The degree of polymerization decreases in cellulose in the temperature range of 150-190 °C [68]. As low as 220 °C, a little formation of water results in a small weight loss [69]. This becomes more pronounced at 250 °C, Figure 5. Patai and Halpern [70] found that during isothermal heat treatment of crystalline and amorphous cellulose at 250 °C for about 2 h the mass loss varies between 2-18% depending on the crystallinity index. The major products from cellulose degradation are char, CO_2, H_2O and a very small amount of CO. At temperatures above 250 °C, the cellulose chain starts to decompose, forming condensable volatiles along with non-condensable gases [71].

1.3.3. Lignin

Lignin is an amorphous polymer composed of phenylpropane units. It is highly branched and complex. Phenylpropanes appear in three main forms, including p-hydroxyphenyl, guaiacyl and syringyl units. Softwood lignin contains mainly guaiacyl units and small amounts of p-hydroxyphenyl units. Hardwood lignin is composed primarily of syringyl and guaiacyl units with small amounts of p-hydroxyphenyl units. In contrast, herbaceous lignin contains a higher content of p-hydroxyphenyl units, in addition to both guaiacyl and syringyl units. These groups are predominantly bonded together by C-O-C (ether) or C-C linkages.

At temperatures below 200 °C, some thermal softening of lignin is observed without any significant weight loss. Over a wide range of temperature 240-420 °C, lignin devolatilizes. In torrefaction, lignin is more stable than the other components and produces more char.

Muller-Hagedorn [72] observed higher reactivity of syringyl groups to thermal treatment at 100-290 °C compared to guaiacyl group, and they concluded that softwood lignin is more thermally stable than hardwood lignin. This was shown in TG curves of both types of lignins

[73]. Therefore, the char yield from hardwood lignin is likely slightly lower than softwood lignin.

1.3.4. Extractives

The extractive content in woody biomass varies between 2-15% while the content in bark is about 20-40% [60,74]. Extractives comprise a large number of substances in biomass such as volatile matters like terpenes, resins, fats, waxes, tannins, lignan and carbohydrates [75]. By definition, they can be subdivided to polar and non-polar materials. They impart color, odor and taste to biomass. Extractives can protect the biomass from microbial and insect attacks [76]. Furthermore, extractives supply energy for biological activities in biomass [59].

During heat treatment of biomass at relatively low temperature of about 150 °C, the volatile extractives like monoterpenes are released from biomass without major structural decomposition [4]. Increasing the temperature results in degradation and devolatilization of extractives. Significant degradation and devolatilization of acetone extractable material for raw spruce occurs between 250-350 °C, Figure 5.

1.3.5. Ash-forming Elements

In addition to the organic components, biomass also contains mineral matters. When biomass is used as fuel, these matters are called ash-forming matters since they form ash during combustion. Some are partly released like sulfur or chlorine [77]. Ash-forming elements are important in combustion applications due to the problems they cause in boilers such as fouling and slagging.

Ash-forming elements in biomass exist in different forms. For instance, some of alkali and alkaline earth metals are linked to anionic inorganics, producing inorganic salts. Some alkali and alkaline earth metals are bound to organic structures in biomass, such as carboxylic and/or phenolic groups, whereas some other ash-forming elements, such as chlorine and sulfur, have covalent bonds in the organic structure [78].

Ash-forming elements in biomass can be chemically active during pyrolysis. For example, the presence of alkali metals affects the char yield as well as the ratio of the condensable to non-condensable volatiles [79]; while Ca affects the temperature of maximum degradation rate of

pyrolysis [80]. It is found that the addition of K salt to the demineralized biomass increases the char yield [81,82]. Some earlier researches showed that K decreases the content of levoglucosan in tar to smaller molecular weight compounds [83]. K also affects the concentration of gas phase during pyrolysis where cracking the tar results in higher amount of CO_2 and CO [84]. Although a significant number of studies deal with the pyrolysis process, there is dearth of information on the effect of metals on torrefaction.

Saleh et al. [58] measured some increase in mass loss of torrefaction when the K salt is added physically to biomass. However, Saddawi et al. [85] observed that washing the mineral matters from biomass results in increase in the volatile matter of torrefied biomass. Prins et al. [65] hypothesized that the increase in the release of carbon monoxide in straw during torrefaction can be attributed to the higher amount of ash-forming elements in straw.

In general, torrefaction of woody biomass results in an increase in the concentration of ash-forming elements [9,21]. This is because most of these elements are retained during torrefaction.

Chlorine release has been observed for some woody and herbaceous biomasses at 250 ˚C by 20% to methyl chloride [86]. During torrefaction to 300 ˚C, the release of chlorine in straw is 50% [87] and in switchgrass is about 25% [88]. The release of sulfur during torrefaction has been observed in straw at 250 ˚C [86], corn stover at 250 and 280 ˚C [89] and during wet torrefaction of pine to 260 ˚C [90].

1.4. Effect of Torrefaction Process Parameters

1.4.1. Temperature

Torrefaction occurs in the temperature range of 200-300 ˚C when the residence time varies between 10-45 min, in practice. Increasing temperature and residence time results in higher mass loss of biomass during torrefaction. Temperature has been found to have a large impact on the degradation of biomass than residence time [91,92]. The impact of temperature and residence time on torrefaction is shown in Figure 6.
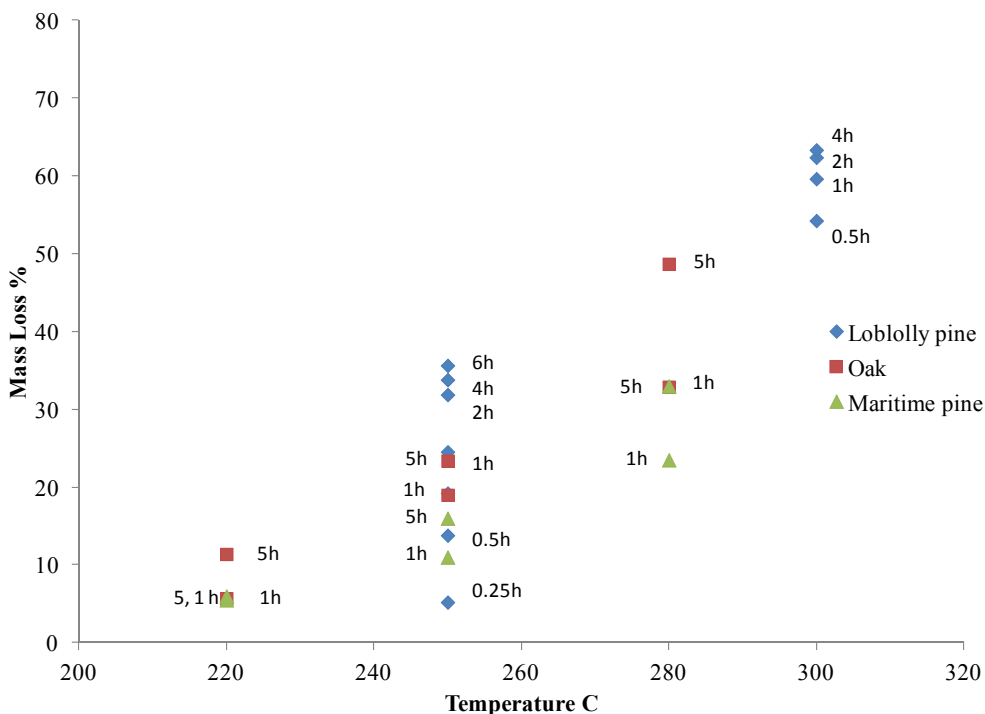
Figure 6. Effect of temperature and residence time on mass loss: loblolly pine [10]**, Oak and Maritime pine** [93]

It is worth noting that increasing the torrefaction temperature does not continuously lead to higher LHV. For instance, during torrefaction of willow at 250 °C in 30 min, the LHV of the torrefied biomass is 16.9 MJ/kg original willow whereas during the torrefaction of the same biomass at 300 °C in 30 min, the LHV of the torrefied biomass is 14.0 MJ/kg original willow [36]. Therefore, the energy balance over the torrefaction system is done to find the optimum condition.

1.4.2. Pressure

Pressure affects the torrefaction of biomass in both closed and open pressurized reactors. In a closed pressurized reactor, biomass is torrefied in a sealed high pressure reactor. In this type of reactor, increasing the pressure decreases the mass loss [94,95]. Increasing the pressure to 40 bar decreases the mass loss from 46 to 36% during torrefaction of woody biomass (leucocephala) at 250 °C, when the residence time is 30 min [94]. Therefore, it can be

concluded that the secondary reactions during high pressurized torrefaction in a closed system are remarkable.

On the other hand, in the open pressurized system where the pressurized atmosphere is flowing through the biomass, increasing the pressure from atmospheric pressure to 20 bar increases the mass loss [96].

1.4.3. Particle Size

Increasing the particle size decreases the mass loss during torrefaction. It is found that torrefaction of cylinder beech (d=5mm, L=10 mm and weight~90 mg) at 280 °C resulted in 28.9% mass loss; However torrefaction of the same beech ground to a particle size of 0.125-0.250 mm resulted in 32.5% mass loss [96].

Particle size of biomass can control the heat and mass transfer during torrefaction. If the particle size of biomass is small enough, the heat transfer to and within biomass are fast. Therefore, the internal temperature of the biomass particle is similar to the environment's temperature. With regard to mass transfer, the volatiles, which are easily released, leave the biomass in small particles with a limited chance for secondary reaction. In order to assure that the heat and mass transfer are not the limiting factors, Biot and Pyrolysis numbers can be calculated [19].

1.4.4. Atmosphere

Torrefaction can be carried out in an inert gas or gases containing CO_2, O_2 or H_2O [5,19,97]. Using an inert atmosphere prevents any reaction between the atmospheric gas and biomass during torrefaction. In practice, in industrial scale reactors, it is not economical to use these expensive gases. The volatiles released from torrefaction, called torgas, air or flue gas from boilers are used in industrial torrefaction reactor with direct heating.

The presence of an oxidative medium in the process of torrefaction has been found to result in higher mass loss [98-101]. For instance, at 250 °C during the torrefaction of oil palm fiber, the mass loss increased by 33.1% when air was used instead of nitrogen [99].

The main non-condensable volatile gas from torrefaction, CO_2, can be used as a torrefaction medium. In a number of recent works, the effect of CO_2 on torrefaction has been investigated

[102,103]. For example, torrefaction of hardwood (Juniper) in CO_2 at 300 °C resulted in an increase of 4.3% in mass loss compared to an N_2 atmosphere [102]. In addition to higher mass loss in presence of CO_2, the grindability of torrefied wood improved. There is lack of information on the impact of steam on torrefaction.

1.5. Kinetics

Modeling biomass decomposition during heat treatment can help predict the mass yield at any specific residence time. Thermal decomposition of biomass has been modeled with a variety of kinetic models, specifically at high temperatures [104,105]. All of these models are based on the thermal degradation of biomass components and then determination of rate constants including activation energies and pre-exponential factors. Di Blasi et al [104] modeled xylan degradation for low temperature pyrolysis as a two-step reaction. The mass loss for the pyrolysis of beech wood at temperatures 255-311 °C was modeled using two reactions in series [106]. They assumed that the extractives and reactive hemicellulose degraded in the first step, and a fraction of cellulose and the rest of hemicellulose degraded in the second step.

Rousset et al. [107] began with three parallel reactions for hemicellulose, cellulose and lignin degradation during torrefaction and then concluded that hemicellulose degradation was more significant than the other components at 210 and 250 °C. Repellin et al. [20] and Chen et al. [108] by applying slightly different mechanisms found the same conclusion about the degradation of biomass components during torrefaction.

Prins et al. [19] used a two-step reaction model to describe the torrefaction reaction kinetics for willow. In this model, biomass (B) decomposes to volatiles (V_1) and intermediate product (C). Then, the intermediate product (C) decomposes to final char (D), and volatiles (V_2) are formed (reaction (1a-d)).

$$B \xrightarrow{k_C} C \qquad\qquad\qquad \text{reaction (1a)}$$

$$B \xrightarrow{k_{V1}} V_1 \qquad\qquad\qquad \text{reaction (1b)}$$

$$C \xrightarrow{k_D} D \qquad\qquad\qquad \text{reaction (1c)}$$

$$C \xrightarrow{k_{V2}} V_2 \qquad\qquad\qquad \text{reaction (1d)}$$

Using this two-step reaction mechanism, Prins et al. [19] determined the rate constants for the torrefaction of willow. The obtained activation energy of the first step and the second step reactions were 76.0 and 151.7 kJ/mol, for k_C and k_D reactions. Shang et al. [109] used the same reaction mechanism to model wheat straw. They obtained similar activation energies for k_C and k_D. The values were 71.0 and 76.6 kJ/mol, respectively.

Recently, it has been observed that potassium (K) influences the extent of degradation during torrefaction [58,110]. However, this is not been taking into account in any model in torrefaction before this PhD work.

1.6. Objectives

In this work, changes in the chemistry of biomass during torrefaction, depending on the torrefaction conditions, are investigated. These changes in the chemistry of torrefaction can explain some physical and chemical characteristics of torrefied biomass. A better understanding of the possibilities of using torrefaction in biorefinery concepts can result in a valuable source of fine chemicals rather than its application for fuel upgrading. Additionally, it is considered whether any ash-forming elements affect the mechanism of torrefaction, which can help predict the biomass behavior. This information will be useful for choosing torrefaction conditions as well as designing and operating the industrial reactors.

This work concentrates on the chemistry of biomass during torrefaction and the effect of alkali metals. Accordingly, it consists of two parts: in the first part, changes in hemicellulose, cellulose, lignin and the distribution of extractable materials and ash-forming elements are given, applying different methods. In the second part, the effect of alkali metals on the mass loss, with a focus on potassium (K), is investigated. Then, the torrefaction reaction is modeled; the dependence of the kinetic parameters on the concentration of K is taken into account.

In **Paper I**, we investigate how decrease in hydrophilic characteristic can be explained by the changes in content of functional groups in biomass. Hydroxyl groups, including carboxylic and phenolic groups in biomass, can form hydrogen bond with water. Therefore, in this paper, the changes in the amount of carboxylic groups are measured by two different methods, including methylene blue sorption technique and potentiometric titration. In addition, the equilibrium moisture contents of torrefied biomass are determined. The hydrophilic

characteristic of biomass is likely due to the content of carboxylic groups, the measuring of which functions as an indirect but faster method of measuring hydrophilic characteristic. Therefore, measuring the changes in carboxylic groups during torrefaction, which is a key reaction, can provide a tool to measure the extent of torrefaction.

Chemical changes of biomass components during torrefaction can explain some of the characteristics of torrefied biomass. Although there are some scattered information about changes in the main wood components, changes in the extractable materials and ash-forming elements are very limited. Thus, changes in the chemistry of biomass during torrefaction have been investigated in **Paper II** and **Paper III**. In **Paper II**, the changes in the chemistry of hemicellulose, cellulose, lignin and extractable materials during torrefaction are investigated, while in **Paper III** the changes in the chemical association of ash-forming elements are studied. Sugar analyses, including acid methanolysis and acid hydrolysis, are applied to measure the changes in the hemicellulose and cellulose contents. To investigate the changes in lignin, the Klason-lignin method is used to measure the total content of acid-insoluble materials, while Pyrolysis Gas Chromatography Mass Spectrometry (Py-GC-MS) and Cross-Polarization Magic Angle Spinning Nuclear Magnetic Resonance (13C CP-MAS NMR) spectroscopy were applied to analyze changes in the lignin structure.

The total content of acetone extractable materials is measured by a gravimetric method; while the chemical composition of low-molar-mass extractable materials is determined by GC-MS. High Performance Size Exclusion Chromatography (HP-SEC) also analyzes the molar mass distribution of extractable material. Formation and/or degradation of extractable materials would be interesting from a biorefinery perspective when valuable fine chemicals are produced.

In **Paper III**, we explore the form of ash-forming elements during torrefaction. Chemical fractionation is applied to measure the distribution of ash-forming elements in biomass during torrefaction. Ion Chromatography is utilized to measure the chloride, nitrate, phosphate, sulfate and oxalate in the leachates from biomass and torrefied biomass. Coulometry is applied to measure the carbonate in the solid biomass and torrefied biomass. Carboxylic group sites are also measured, because they can bind to cations. All these measurements provide new information on the fate of metals as well as chlorine and sulfur during torrefaction.

Earlier works have shown the clear effect of alkali metals on pyrolysis. In **Paper IV** we investigate whether alkali metals affect torrefaction. The catalytic effect of alkali metals is studied with a focus on the effect of potassium (K) on biomass during torrefaction. Biomass is acid washed and then doped with K, Na, Ca or Mn. Additionally, K_2CO_3 is also added to biomass components, including hemicellulose, cellulose and lignin, and then the effect of K is investigated on them during torrefaction. These results are important for the future operation of torrefaction plants which will likely be designed to handle various biomasses with significantly different contents of alkali metals.

By knowing that K affects the process of torrefaction, we want to find out in what ways this effect can be modeled during torrefaction. In **Paper V**, kinetic parameters are established to model the mass loss during torrefaction of different biomasses. The unique feature of this model is taking into account the influence of potassium on the mass loss during torrefaction. The model is validated and compared to experimental data for straw, miscanthus, aspen and bark. In the model, the reactive components are assumed hemicellulose and cellulose. Since this model does not take the volatilization of extractives into account, it is valid for wood or herbaceous biomass with low levels of acetone extractable material; however, it is not for bark.

Chapter Two: Methods

The spruce, pine, aspen, spruce bark [111], straw and miscanthus [86] were the same samples studied in the earlier works. The commercial birch wood chips were supplied to the Energy research Center in the Netherlands (ECN).

2.1. Torrefaction

The biomasses were torrefied in three different reactors: thermogravimetric analyzer, single particle reactor, and pilot scale reactor at ECN. The details of the reactors are described below:

2.1.1. TGA

About 10 mg of biomass – spruce, pine, aspen, straw, miscanthus and spruce bark – ground and sieved to a particle size of 125-250 μm, was loaded in an alumina sample holder, and then inserted into the Thermogravimetric Analyzer (TGA). The heating rate was 20 °C/min, and N_2 flow of 100 NmL/min was used to prevent any oxidation reactions during the experiments. The applied torrefaction temperatures were between 240 and 280°C. When the TGA reached the torrefaction temperature, the temperature was held for 30 min. Some conditions were repeated 5 times to establish the experimental variations. Spruce doped with 0.12 wt.% K torrefied at 280°C resulted in the average mass loss of 29.3% and standard deviation of 0.4%. TGA analysis of acid washed spruce had an average mass loss of 24.5% and a standard deviation of 0.3%.

2.1.2. Single Particle Reactor

Single particle reactor is a quartz reactor inside an electric heated furnace and is described elsewhere [112]. Spruce wood was ground and sieved to a particle size of 125-250 μm and then dried prior to torrefaction. Accurately weighed samples of 80 ± 5 mg were placed on a quartz sample holder (15 mm in diameter). The sample holder, containing the biomass, was kept in the unheated flow of N_2 for a few seconds before insertion into the heated reactor. This was done, so that the concentration of the oxygen in the hot furnace dropped to zero, before the sample was inserted.

The samples were kept in the reactor for 30 min at 180, 200, 240, 260, 280 or 300°C. The gas through the reactor was 100% N_2, 220 NL/h. In order to investigate the temperature profile of the biomass versus time, the tip of K-type thermocouple – 0.5 mm bead size – was inserted in the center of the wood samples. Thus, the time-temperature history was recorded at 180 and 300°C. It took less than 5 min for the center of the samples to reach the reactor temperature at the both lowest and highest temperatures, Figure 7.

The initial and the final mass of the dried samples were recorded to determine the mass loss. Multiple torrefaction runs were made at each condition to provide enough samples for the methylene blue sorption and potentiometric measurements. Torrefied samples were kept in desiccators before analysis by methylene blue sorption or potentiometric titration.
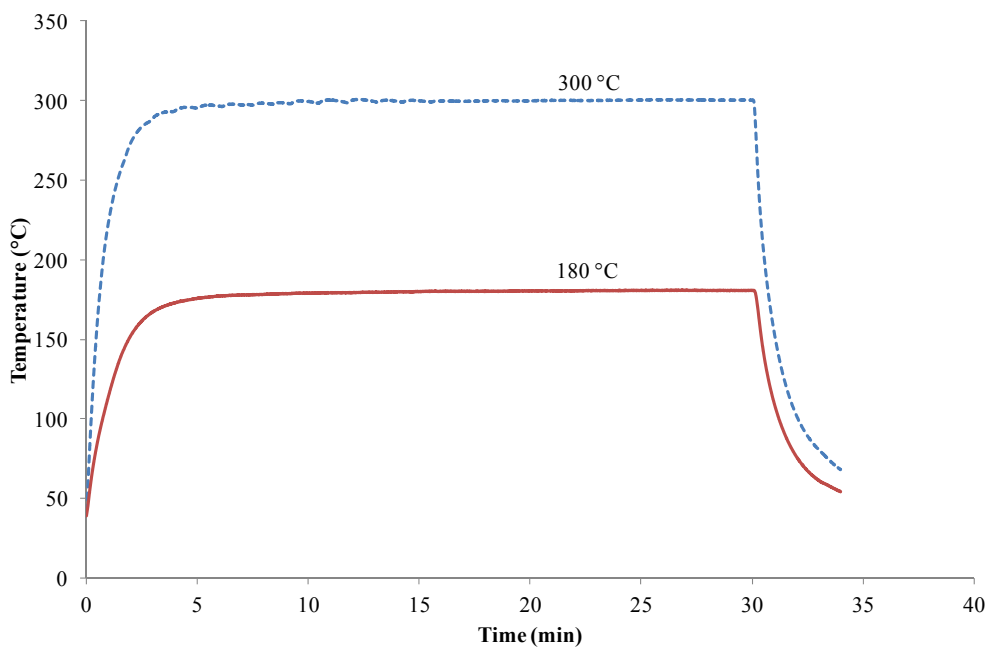

Figure 7. Time – Temperature history of the sample in the single particle reactor (Paper I)

2.1.3. Pilot Scale Reactor at ECN

The pilot scale moving bed reactor at ECN was used to torrefy commercial birch chips. The birch wood chips were smaller than 40×40×2 mm. Dust with particle sizes smaller than 1 mm was removed before torrefaction.

An external drier was used to dry the chips fed to the reactor to below 15% moisture before torrefaction [113]. The reactor uses both direct and indirect heating. The chips were heated indirectly by a central element while the bed was moving. In addition, recycled torrefaction gas (torgas) was used to heat the biomass directly in the reactor. The birch chips were inside the continuous reactor between 35 and 45 min. The residence time was calculated based on the volumetric flow of the inlet feed stock and the total volume of the reactor. The torrefaction temperatures were 240, 255, 270 and 280°C. The reactor's capacity is 80 kg/h. The temperature given is the ingoing torgas temperature which controls the torrefaction. Kotilainen et al. [91] showed that at least at 220 °C, the temperature has a much larger impact on the extent of the chemical changes in wood than time or environment atmosphere, and thus, the slight variability of the residence time in the pilot unit in this study is not expected to overly influence the results. For analysis, the wood chips samples were taken after the drier (before torrefaction) and after torrefaction at 240, 255, 270 or 280 °C. All samples were analyzed for CHNO, ash and HHV. The ultimate and proximate analyses of the raw and torrefied birch samples are shown in Table 2.

Table 2. Ultimate and proximate analysis of raw and torrefied birch. All the values are given on a dry fuel basis. * Raw birch values are the average of analysis for two separate samples which has each been analyzed twice, for other samples duplicate analysis given in parenthesis. **This is the analyzed oxygen content. n.a.: not analyzed; b.d. below detection. (Paper III)

Torrefaction temp	Raw Birch	at 240°C	at 255°C	at 270°C	at 280°C
Ash (at 550°C)	0.19-0.21	0.23	0.35	0.33	0.38
Moisture content	8.1-7.9	3.20	3.00	2.90	2.70
Volatiles	88-87	81.00	76.00	75.50	72.00
HHV(MJ/kg)	19.07-18.99	21.07	21.53	22.08	22.73
C %	48.8-48.75*	52.5(52.3)	54.30(54.10)	55.3(55.0)	56.45
H %	6.4-6.3*	6.00(6.00)	6.00(6.00)	5.7(5.8)	5.8(5.7)
N %	0.13-0.13*	0.15(0.15)	0.15(0.15)	0.15(0.15)	0.15(0.15)
O %**	44.15-45.15*	41.7(41.9)	39.9(40.0)	37.1(37.4)	36.0(35.9)
S %	0.0072	0.0051	n.a	n.a	0.0050
Cl %	b.d.	b.d.	n.a.	n.a.	b.d.

2.2. Analytical Methods

2.2.1. Determination of Carboxylic Groups

Sample Preparation: The wood sample was ground and sieved to a size of 125–250 µm, and then dried at 105°C for 24 h. This wood was then split into two parts. Part of the wood was torrefied without any additional pretreatment. Another part of the sample was treated to remove extractives and metals before torrefaction. For removal of the extractives, the wood was first washed with acetone in a Soxhlet apparatus for 6 h at 60 °C and then washed with distilled water for 1 h. Mass loss during acetone extraction was 4.0 wt.% on a dry mass basis. After removal of the extractives, the wood was added to a solution of Na-EDTA and HCl (both 0.01 M) respectively, for 2 h to remove metals. The acid, EDTA and metals were washed away with ultrapure water. The acid-washed wood was then oven dried at 105 °C for 24 h. Both the original wood and acid-washed wood were analyzed by ICP-AES (Inductivity Coupled Plasma Atomic Emission Spectrometers), which showed a nearly complete removal of the ash-forming matter. Then, they were torrefied in the single particle reactor.

Two different methods were applied to measure the carboxylic groups in the biomass including acid-base titration and a methylene blue sorption technique.

Titration: The base used for titration was prepared from Merck, titrisol 1M NaOH, which was diluted to 0.1 M using degassed ultra pure water. The exact concentration of the NaOH solution was determined by titration of potassium hydrogen phthalate [114]. Sodium nitrate was added to the solution of NaOH where its concentration was 0.1 M. This is done to maintain the ionic strength of the solution containing the wood during titration.

Prior to titration, in some cases, the acetone extraction pre-treatment plus acid washing were performed on the samples. For the titrations, 1.5g of dry accurately weighed sample was added to 150ml of 0.1M $NaNO_3$ solution in a glove box with a flow of N_2. The $NaNO_3$ solution was prepared fresh for each test from ultrapure water which was boiled to release dissolved CO_2 gas. The boiled water was cooled down in the N_2 purged glove box before the salt was added. The suspension was acidified with 1.5 ml of 0.5M HNO_3 (resulting in a pH of 2) to begin with all of the carboxylic acids in the protonated form. The solution was then titrated with 0.1M NaOH using an automatic Metrohm Tiamo titrator. The potential stability criterion (signal drift) during the automatic titration was 0.1 $mV.min^{-1}$ with a maximum

waiting time of 10 min. between dosages. A blank titration test was performed first, in which 1.5 ml of HNO_3 was added to 150 ml of 0.1 M $NaNO_3$ solution and was titrated with the base until pH≈11. The difference in the inflection point of the blank titration curve and the inflection point for the titration of the suspension containing biomass sample was considered to be the amount of carboxylic acid groups which were neutralized. Because the inflection point may also be somewhat affected by phenolic groups as well as carboxylic acids, this approach is not fully exclusive only for carboxylic acid sites.

Titration of the spruce wood in triplicate showed good repeatability, giving values of 80, 93, and 86 µmol/g dry wood. However, for the torrefied samples of the untreated spruce wood at 260 °C and above, the titration curve actually moves to the left of the blank. This is likely due to the presences of alkali and alkaline earth salts in the torrefied wood. When the HNO_3 was added to the sample solution prior to titration, these alkaline salts consumed some of the acid, thereby shifting the inflection point to the left of the blank. Therefore, to obtain the concentration of carboxylic acid sites for the torrefied wood samples, it was necessary to acid wash the chars from torrefaction prior to titration to remove the metals and protonate the acid groups.

Methylene Blue Sorption Technique: Methylene blue sorption measurements were carried out to measure the acidic groups in the biomass. For each experiment, eight samples of 50 mg were accurately weighed. Three mL of deionized water was added to each dried biomass samples and then mixed for an hour. Different volumes of 0.4 mM Methylene Blue (MB) solution – 5, 10, 15, 20, 25, 30, 35, 40ml – in which the pH was adjusted to 7.8-8 with a 0.6mM barbital solution, were added to the suspensions. Then, the whole suspensions were mixed for 20 min. The time had been studied earlier and found to be sufficient for pulps [115]. We also established that 20 min was sufficient for our samples.

After 20 min. of stirring at room temperature, the suspensions were filtered through a glass filter. The filtrate was then diluted 25 times using a 0.6 mM barbital solution. The diluted solution was analyzed by UV-Vis spectrophotometry at a wavelength of 664nm. These results then provided a sorption diagram, which was used to determine the total content of acid sites in wood with a pKa less than 7.8. Two blank tests were performed to measure the amount of methylene blue that is absorbed to the glass filter and wall. To ensure the repeatability of the

methylene blue results, the test was repeated three times for torrefied wood at 260°C with 22, 22, and 23 µmol/g obtained for the three analyses.

2.2.2. Determination of Equilibrium Moisture Content

The humidity absorption study was conducted by a static desiccator method [116]. The humidity of the desiccator is maintained using saturated salt solutions [117]. Different relative humidity (RH) levels including 11%, 37%, 60%, 75% and 98% were used with LiCl, $MgCl_2$, $Mg(NO_3)_2$, NaCl, K_2SO_4 salts, respectively. Excess salt was added to the sealed box to ensure that the humidity was constant. The temperature was room temperature, 23°C. Dried samples of 90±10 mg were put in small bottles in sealed boxes containing the saturated salt solutions to give different humidity in the boxes. The samples were then weighed at intervals over 2 weeks. No additional weight gain was observed between day 7 and day 14 and this was taken to be the equilibrium moisture content.

2.2.3. Determination of Hemicellulose

In order to do the chemical analysis, the samples were ground and sieved to a size of 125-250 µm. The samples were dried overnight at 105°C. They were kept in a desiccator prior to analysis. In order to measure the hemicellulose content in the biomass, acid methanolysis was performed to quantify and qualify the sugar unit contents in the hemicellulose.

Acid Methanolysis: About 20-40 mg of the freeze-dried sample, depending on the severity of torrefaction, was accurately weighed. Acid methanolysis followed by Gas Chromatography (GC) analysis was performed to quantify the sugar contents [62,118]. During acid methanolysis, hemicellulose and pectins were degraded to their sugar units. To detect the produced sugars by GC, they were silylated. The samples were left overnight, and then the sugar units were detected by GC [118].

2.2.4. Determination of Cellulose

The biomasses were ground and sieved to 125-250 µm and then dried an overnight in the oven at 105 °C.

Acid Hydrolysis: Acid hydrolysis followed by silylation and GC analysis [118] was applied to quantify the cellulose. About 10±0.1 mg of freeze-dried sample was used for acid hydrolysis.

With this method, the total amount of glucose from both cellulose and hemicellulose was quantified. To calculate the cellulose amount, the glucose from the hemicellulose was subtracted from the total amount.

2.2.5. Determination of Lignin

The samples were ground and sieved to 125-250 μm and dried at 105 °C. Three methods are performed to characterize the lignin. The Klason lignin method determined the content of acid soluble and insoluble lignin, while Dipolar Dephasing NMR (DD NMR) and Pyrolysis-Gas Chromatography-Mass Spectrometry (Py-GC-MS) qualified the changes in the structure of the lignin.

Klason Lignin: The acid-insoluble lignin content in acetone extracted raw and torrefied birch wood was determined by the Tappi Standard method, T 222 om-98. The acid-soluble lignin content was quantified according to Tappi standard method UM 250.

Solid State NMR: DD NMR was performed on the raw and torrefied birch samples from ECN. In DD NMR, the high power proton decoupling was switched off for a short period of time, allowing the signal from the protonated carbons, excluding methyl carbons, to become dephased. Only the signals from the quaternary and methyl carbons were then detected, making interpretation of the spectra from the lignin aromatic region more reliable. The measurements were carried out at Helsinki University.

Pyrolysis-Gas Chromatography-Mass Spectrometry: Py-GC-MS was used to determine the changes in the content of *p*-hydroxyphenyl, guaiacyl and syringyl units of lignin. Acetone extraction pretreatment was performed on the samples prior to Py-GC-MS. The samples were pyrolyzed at 650 ˚C for 2 s. The details of the method have been described by Smeds et al. [119].

2.2.6. Determination of Extractable Materials

The biomass was ground and sieved to 125-250 μm and then dried overnight in the oven at 105 °C. Acetone extraction of biomass was performed using acetone/water (v/v: 95/5) as solvent in an Accelerated Solvent Extractor (ASE-300) [120]. Accurately weighed freeze-dried samples of about 2 grams were placed in the extraction vials and the vials were filled

with carefully washed inert quartz sand. The operating temperature was 100°C and the operating pressure was 10.34 MPa. Three static cycles were applied with each cycle lasting 5 min. The extracted liquids were collected in a glass tube, and the levels of all extraction liquids were adjusted to 50 mL with acetone. The extracted materials were quantified by three different ways. In the first step, the total extracted materials were quantified by weighing the sample after evaporating the solvent to dryness at 50°C in the nitrogen atmosphere. In the second step, the low-molar-mass compounds were analyzed by GC-FID and GC-MS. In the third step, the molar mass distribution of the extractable materials was analyzed by High Performance Size Exclusion Chromatography (HPSEC).

Gravimetric Analysis: In the first method, the total amount of extractable material in the acetone solution, which was about 50 mL, was exactly adjusted to 50 mL by acetone [121]. After shaking the solution, 10 mL of the extractable material solution was accurately weighed in the test tubes. Then the solution was dried under nitrogen flow at 50 ˚C until it became nearly dry. The almost dried extractable materials were fully dried in a vacuum desiccator at 7 Pa and 40 ˚C for 2 h. The extractable materials, kept in a desiccator, were weighed in between several times until a constant weight was obtained. The final mass was the concentration of acetone-extractable material.

Gas Chromatography-Flame Ionization Detector and Mass Spectrometry (GC-FID and GC-MS): In the second method, GC-FID was applied to quantify the low-molar-mass compounds of extractable materials according to the method first described somewhere else [122]. To identify the compounds in the extractable materials, GC-MS was used.

High Pressure Size Exclusion Chromatography (HPSEC): In the third method, HPSEC was applied to analyze the molar mass distribution of the extractable material. The specific volume of extractable materials in acetone solution was dried under nitrogen atmosphere, to get about 5 mg of the dried extractable materials. 1mL of acetylation solution (acetic anhydrate/ pyridine 50/50 v/v) was added to the 5 mg of the dried extractable material. The mixture was left in a dark place at room temperature. After 5 days, 2mL of ethanol was added to the solution and the solution was dried in a flow of nitrogen at 40°C. Then, 5mL of tetrahydrofuran (THF) was added to the dried acetylated extractable material. The result was a clear transparent solution. After filtration of the solution into a vial, the HPSEC analysis was performed. The details of the method have been described in another study [123]. Shimadzu

GPC for CLASS VP software was used to process the HPSEC data. The peak area of the chromatograms was calibrated by analyzing triglyceride, steryl esters, fatty acids and resin acids, each at 0.5 mg/mL. It should also be noted that the molar mass scale is calibrated based on different molecular weight polystyrene, and thus not very accurate for the unknown complex mixtures of extractable materials; however, polystyrene is commonly used for the general purpose of molar mass calibration.

2.2.7. Determination of Ash-forming Elements

The samples used in this work were the birch wood chips torrefied at ECN in pilot scale reactor. Only the raw birch, 240 and 280 °C were analyzed by fuel fractionation to determine if there are changes in the distribution of ash-forming elements during torrefaction.

Chemical Fractionation Method: The fuel fractionation was based on three leaching steps: water; a solution of 1M ammonium acetate; and for the last step 1M hydrochloric acid [124]. The wood chips were ground to less than 5 mm for chemical fractionation. Samples of about 100 g were added to water and shaken for one day, after which the whole suspension was filtered and rinsed. The rinsed residue from the water was suspended in 1M ammonium acetate. After one day, the sample was filtered and rinsed and then this step was repeated two more times for one day each. The three ammonium acetate solutions were blended for analysis. During the last step, the residue was leached two separate times in a 1M hydrochloric acid solution at about 70°C for one day each [78]. The ratio of the solutions to biomass was 5 to 1 on a mass basis for each step.

Induced Coupled Plasma (ICP) Test: The initial biomass, the solid final residue of fuel fractionation, as well as the three leachates were sent to an external laboratory where samples were analyzed using Induced Coupled Plasma - Atomic Emission Spectrometry (ICP-AES) and Induced Coupled Plasma - Sector Field Mass Spectrometry (ICP-SFMS) according to EPA 200.7 and EPA 200.8 standards, respectively[125,126].

Ion Chromatography (IC) Experiment: IC with a conductivity detector was used to quantify the concentration of Cl^-, NO_3^-, SO_4^{2-}, PO_4^{3-}, and $C_2O_4^{2-}$, in the three liquid leachates (water, ammonium acetate and acid). A Metrosep A SUPP-5 column was used with an eluent of 1.0 mM $NaHCO_3$ and 3.2 mM Na_2CO_3 in ultra-pure water. For the identification and

quantification of the anions, standard solutions of the anions were prepared from the respective high purity (p.a.) sodium salts.

Carbonate Experiment: The concentration of carbonate was determined in the original wood and the torrefied wood at 240 and 280 °C by coulometric determination. The experiments were performed in a certified external laboratory.

2.3. Impact of K on Torrefaction

The applied samples in this work consisted of three woody biomasses, spruce and pine as soft woods and aspen as a hardwood, and a grassy miscanthus. In addition to these biomasses, isolated constituents of spruce –galactoglucomannan, crystalline cellulose and lignin– and Whatman ash free filter paper were used. The biomasses were ground and sieved so that the dimensions of the biomasses were between 125-250 μm.

The biomass samples demineralized with a two-step process. First the biomass was added to a 0.01 M sodium EDTA aqueous solution for 2 hours at room temperature. The washed sample was then rinsed with water and then washed with 0.01 M HCl for 2 hours. Finally the samples were rinsed with ultra pure water [127]. According to an earlier study [79], changes in the organic structure of the biomass were negligible using mild condition to wash and then absorb the inorganics.

The acid-washed biomass was doped with K, Na, Ca or Mn by adding 1.5 g of dried biomass to 50 ml of a 0.05 M metal nitrate solution for 24 hours. The pH of the solution was adjusted to 5, 8 or 12 by the addition of the metal hydroxide. The suspension was filtered and the biomass was washed with ultrapure water. The biomass was then dried for an overnight in the oven at 105°C.

About three grams of dried acid-washed spruce were impregnated in 50 mL of 0.003M potassium carbonate aqueous solution. The suspension was stirred for 60 min and the aqueous solution was filtered. The impregnated sample was then dried overnight at 105 °C.

Table 3. Content of K, Na, Ca and Mn in raw, acid-washed, doped and impregnated biomass feedstock analyzed by ICP (Paper IV)

Biomass/content (ppm)	K	Ca	Mn	Na
spruce, raw	220	720	100	10
spruce acid-washed		7		
spruce K-low	1200	12		
K_2CO_3 impregnated spruce	3300	64		
spruce K-medium	6000			
spruce K-high	12000	10		
spruce Ca-medium		2500		
spruce Ca-high		4600		
spruce Mn-low		30	1100	
miscanthus, raw	4300	1200	100	40
miscanthus acid-washed		50		
miscanthus K-low	1300	30		
miscanthus K-medium	2300	30		
miscanthus K-high	6400	40		
aspen, raw	1370	1000		15
aspen acid-washed	0	40		
aspen K-low	1500	40		
aspen K-medium	2400	40		
aspen K-high	8200	200		100
aspen Na-low		70		710
aspen Na-medium		60		1400
aspen Na-high		90		5100
raw spruce K-low	1380	340	40	40
raw spruce K-medium	2180	470	73	20
raw spruce K-high	6830	990	100	50
pine, raw	407	640	80	15
raw pine K-high	6340	650	40	30

Impregnation of hemicellulose, cellulose and lignin was performed by mixing 1 g of biomass component in 50mL of 0.003M K_2CO_3 aqueous solution for 60 min. The solution was placed in a freeze-drier and the dried cellulose, hemicellulose or lignin was kept in a desiccator before using. Freeze-drying was used instead of oven drying for the biomass components,

because the final dried component was fluffier and could be more easily ground. The metal content of the K_2CO_3 impregnated biomass was analyzed by burning samples in a TGA at 540 °C and measuring the weight. This was converted to K as the ash is K_2CO_3.

The indigenous metal ions are almost completely removed from biomasses during the acid-washing process, while impregnation and doping add the desired cations to the biomass selectively. As it is expected, the pH during doping affects the content of the absorbed alkali and alkaline earth metals. Table 3 shows the ICP results of raw, acid washed and metal-loaded biomass samples. As seen in the table, K-low refers to the acid washed samples and doped without adjusting pH; K-medium refers to the samples acid washed and then doped at pH=8 and K-high refers to the biomasses acid washed and then doped at pH=12. This is the same for the Na, Ca and Mn.

2.4. Kinetic Modeling

Carbohydrate analyses were conducted to determine the hemicellulose and cellulose contents, Table 4. There is some variation in the hemicellulose and cellulose contents with spruce bark having much lower cellulose content than the other biomass samples.

Table 4. Carbohydrate analysis of the biomasses (Paper V)

Components (wt% dry)	Hemicellulose	Cellulose
Straw	34	30
Miscanthus	26	45
Spruce	25	35
Aspen	27	42
Spruce Bark	27	18

Some of the samples were used raw but the others were demineralized by acid washing and then loaded with K cations. The contents of the elements were analyzed by ICP, and the results are shown in Table 3.

The samples used to calculate the rate constants for the model in this work were about 10 mg of acid-washed spruce, K-low, medium and high loaded spruce with 0.12, 0.6 and 1.2 wt.% K

and K_2CO_3 impregnated spruce which contains 0.33 wt.% K. The samples were dried at 105 °C overnight after loading and then stored in sealed containers in the laboratory.

The mass yield curve of the samples during torrefaction was obtained using a thermo gravimetric analyzer (TGA). The heating rate was 20 °C/min with an isothermal step of 30 min. at 240, 250, 260, 270 or 280 °C.

The rate constants obtained from the spruce runs were validated against mass loss curves for raw aspen, K-high aspen (0.82% K), raw miscanthus, K-high miscanthus (K=0.64%), raw straw, and raw bark. All the biomasses were torrefied at 240 and 280 °C, except K-high miscanthus, which was torrefied at 240, 250, 260, 270 and 280 °C, and K-high aspen, which was torrefied at 240, 260 and 280 °C.

2.4.1. Calculations

The model used is two-step in series [19,109].

$$B \xrightarrow{k_C} C \qquad\qquad\qquad\qquad \text{reaction (1a)}$$

$$B \xrightarrow{k_{V1}} V_1 \qquad\qquad\qquad\qquad \text{reaction (1b)}$$

$$C \xrightarrow{k_D} D \qquad\qquad\qquad\qquad \text{reaction (1c)}$$

$$C \xrightarrow{k_{V2}} V_2 \qquad\qquad\qquad\qquad \text{reaction (1d)}$$

In steps (1a) and (1b) the reactive biomass is denoted 'B' which is converted to an intermediate solid C with a reduced degree of polymerization. The intermediate solid C reacts to form the final solid residue D. In reactions (1b) and (1d), '$V1'$ and '$V2'$ are volatiles.

The reaction rates are given by:

$$r_B = -(k_C + k_{v1}) \times [B] \qquad\qquad\qquad\qquad \text{equation (6)}$$

$$r_C = k_C \times [B] - (k_D + k_{v2}) \times [C] \qquad\qquad\qquad\qquad \text{equation (7)}$$

$$r_D = k_D \times [C] \qquad\qquad\qquad\qquad \text{equation (8)}$$

where k is the rate constant for each step, and is expressed as s^{-1}, [B] and [C] show the concentrations.

The rate constants are expressed as:

$$k_B = A_B\, e^{-E_B/RT} \qquad\qquad \text{equation (9a)}$$

$$k_C = A_C\, e^{-E_C/RT} \qquad\qquad \text{equation (9b)}$$

$$k_{V1} = A_{V1}\, e^{-E_{V1}/RT} \qquad\qquad \text{equation (9c)}$$

$$k_{V2} = A_{V2}\, e^{-E_{V2}/RT} \qquad\qquad \text{equation (9d)}$$

Here, A is pre-exponential factor (s^{-1}), E is activation energy (kJ/mol), R is the gas constant (J/mol K) and T is temperature (K).

The mass yield at any given time is calculated from the experimental data by the equation:

$$Y_{exp}\,\% = \frac{m_t - m_{ash}}{m_0 - m_{ash}}\,x100 \qquad\qquad \text{equation (10)}$$

Where Y_{exp} is the experimental mass yield, m_t is the total mass at time t, m_{ash} is mass of ash in the initial samples and m_0 is initial total mass. The calculated mass yield, equation (11) can be expressed as the sum of the three solid mass compounds B, C and D plus non-reactive solid mass compounds at time t.

$$Y_{mod}\,\% = (B+C+D+ (1-hemicellulose-cellulose))x100 \qquad\qquad \text{equation (11)}$$

where Y_{mod} is the modeled mass yield.

To model the mass yield curve, measured by the TGA, activation energies (E_B, E_C, E_{V1}, E_{V2}) and pre-exponential factors (A_B, A_C, A_{V1}, A_{V2}) were determined by comparing the modeled mass yield with experimental mass yield. The numerical approach by MATLAB codes, fminsearch, was used to fit all the kinetic parameters using the nonlinear least square method by minimizing the sum of the squares in equation (12):

$$\sum_i (\%Y_{exp_i} - \%Y_{mod_i})^2 \qquad\qquad \text{equation (12)}$$

in which subscript i denotes the measured data points. The initial guess for the kinetic parameters were the values for the torrefaction of willow reported by Prins et al. [19].

In determining the kinetic parameters, the non-isothermal part from 200 °C to the final temperature was included as well as the 30 min isothermal part of the torrefaction experiments. All the mass yield curves are plotted on a dry and ash-free basis. The weight at 200 °C is set at the initial mass yield of 1. Time 0 on the x-axis is the time when the sample reaches 200 °C. Up to 200 °C is assumed all the mass loss is attributed to water evaporation.

Chapter Three: Results and Discussion

3.1.   Mass Loss

The degradation of biomass components results in mass loss, which is an effective indicator for showing the severity of torrefaction [97]. In this work, as discussed in the method section, three different reactors have been used to torrefy biomass. One of the variables measured is mass loss.

3.1.1. Thermo Gravimetric Analyzer (TGA)

The different biomasses, including spruce, aspen, pine, spruce bark, straw and miscanthus, were torrefied in the TGA where the residence time was 30 min. The mass loss values are shown in Table 5. It is seen that increasing the torrefaction temperature increases the mass loss for different types of biomass. For instance, the mass loss of aspen at 240 °C is 11.1%, while at 280 °C it is 30.0%. The increase in the mass loss can be explained by the enhanced degradation of biomass components at higher torrefaction temperatures.

Table 5 also shows that mass loss in aspen at a similar torrefaction temperature is higher than the mass loss of spruce. This might be due to the higher degradation of hemicellulose, compared to other wood components during torrefaction [128]. The aspen sample used contains 27 % hemicellulose, while spruce sample contains 25% hemicellulose, Table 4. Overall, deciduous biomass shows higher degradation, and hence higher mass loss compared to coniferous biomass during torrefaction at the same condition.

Table5. Mass loss of some biomasses on dried solid basis by TG (data from Paper IV)

Biomass type	Torrefaction at 240 °C	Torrefaction at 260 °C	Torrefaction at 280 °C
spruce	7.5		25.7
pine	9.7		
aspen	11.1	21.4	30.0
miscanthus	12.0		41.3
straw	13.1		39.3
spruce bark	12.5		26.7

3.1.2. Single Particle Reactor

Torrefaction of raw spruce in single particle reactor also resulted in a mass loss of 9.8±1.7% and 22.4±1.3% at 240 and 280 °C, Table 6. These values are in agreement with the values for the same spruce wood torrefied in TGA, Table 5, which is 7.5% at 240°C (reaction time: 30 min) and 25.7% at 280° C. At high torrefaction temperature of 280 °C, the mass loss in the TGA is to a small extent higher than in the single particle reactor. This can be attributed to minor secondary reactions likely to happen in the single particle reactor due to larger amount of sample.

Torrefaction of acid washed spruce was carried out at 260 and 300 °C, giving mass losses of 12.9±1.4% and 31.0±1.5%, respectively, Table 6. The mass loss of the acid washed spruce is less than that of the untreated spruce. The difference in the percentage of mass loss between the untreated and acid washed spruce can be primarily explained by the 4 wt.% mass loss during acetone extraction prior to acid washing. Assuming all the extractives degraded and volatilized during torrefaction at 260 and 300 °C, the mass loss for the acid washed and raw wood is similar at both temperature.

However, non-isothermal pyrolysis of spruce extractives indicates that not all the extractives are decomposed at this temperature [110]. Additionally, we found that potassium increases biomass degradation during torrefaction compared to untreated spruce [110]. Therefore, the lower mass loss of acetone extracted acid washed spruce compared to untreated spruce can be attributed to the combination of changes in the amount of extractives and the presence of potassium.

Table 6. Mass loss at different torrefaction temperature for untreated and acetone-extracted acid-washed spruce, *n.m. not measured (Paper I)

Temperature °C	180	200	240	260	280	300
Untreated (%)	5.5±0.3	6.1±0.7	9.8±1.7	16.2±2.0	22.4±1.3	34.1±1.1
Acetone extracted then acid-washed (%)	n.m*	n.m.	n.m.	12.9±1.4	n.m.	31.1±1.5

3.1.3. Pilot Scale Reactor at ECN

Torrefaction of raw birch chips were performed in a pilot scale reactor in ECN. The residence time was 35-45 min. Increasing the temperature from 240 to 280 °C increases the mass loss from 19% to 35%, Table 7.

Table 7. Mass loss of birch wood torrefied in a pilot scale reactor, ECN. The values are given on a dry wood basis (data from Paper II)

Torrefaction temperature °C	240	255	270	280
Mass loss %	19	24	30	35

Torrefaction of birch in pilot scale reactor compared to aspen in TG at 240 °C shows higher degradation of birch than aspen, 19% compared to 11.1%. Torrefaction of these biomasses at 280 °C shows slightly higher degradation of birch than aspen, 35% compared to 30%. This could be due to higher content of hemicellulose in birch than aspen, 30% compared to 27%, and longer residence time in pilot reactor than TG, 35-45 min compared to 30 min, despite the effect of particle size, birch wood chips compared to ground aspen.

3.2.   Carboxylic Groups

Two methods including a methylene blue sorption technique and potentiometric titration were applied to measure the carboxylic groups in spruce wood.

3.2.1. Methylene Blue Sorption Technique

The methylene blue sorption technique was used to determine the concentration of carboxylic acid groups in the raw and torrefied spruce wood samples. The carboxylic groups with a $pK_a \leq 7.8$ were dissociated in the buffered methylene blue solution, so that they were in their anionic forms. Methylene blue cations, which gave blue color to the solution, bonded to the carboxylic group, and as a result, the color of the solution became lighter and more transparent. The bonding between methylene blue and anionic carboxylic groups continued until all the anionic carboxylic groups became saturated. Beyond the saturation point, further addition of methylene blue did not result in more adsorption and a plateau was reached, Figure 8. The measured content of carboxylic groups in untreated spruce wood was 90µmol/g,

which was consistent with the values from methylene blue sorption of 86±7 µmol/g reported by Werkelin et al. [129] for the same sample and 92±1 µmol/g reported by Fardim et al. [130] for unbleached spruce thermo-mechanical pulp.
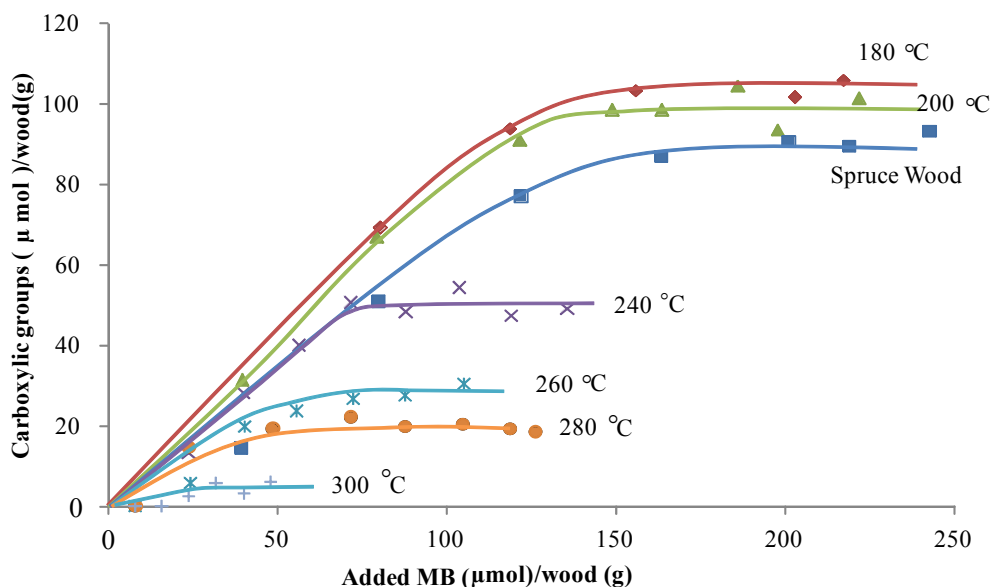

Figure 8. **Concentration of the carboxylic groups for spruce wood and spruce wood torrefied at different temperatures as determined by methylene blue sorption (Paper I)**

The content of carboxylic groups during torrefaction at 180 and 200 °C was slightly higher for untreated wood. Schafer [67] also measured the similar increase in the content of the carboxylic groups when the milled brown coal was isothermally heat treated at 150 and 200 °C.

Torrefaction of spruce wood at 240 °C, resulted in a 50% decrease in the total content of the carboxylic groups, Table 9. The concentration gradually decreased to 22, 15 and 3 µmol/g at 260, 280 and 300°C, respectively. This decrease is consistent with Schafer's results for heat treatment of coal [67]. Heat treatment of pine at 250 and 300 °C also resulted in a decrease in the concentration of carboxylic groups [131]. In another work, the degradation of carboxylic groups in straw at 250-300 ˚C has been investigated with FTIR [22].

The concentration of carboxylic groups in acid washed wood was a little over 10% higher for the raw wood. For instance, the concentration of non-torrefied acid washed wood was 103 µmol/g, while it was 18 µmol/g at 260°C and 7 µmol/g at 300°C. The increase in the concentration of the carboxylic groups after acid washing is in good agreement with an increase in the concentration of carboxylic groups from 81 to 87 µmol/g when comparing cottonwood with acid washed cottonwood [132]. The increase in the content of the carboxylic groups after acetone extraction and acid washing cannot be solely attributed to the removal of extractives. Removing the extractives, which is about 4% in spruce, can only explain 30% of the increase in the concentration of carboxylic groups. Thus, this increase is likely due to the acid-hydrolysis of the esters during the acid-washing process in the spruce wood leading to more carboxylic groups.

Table 9. The amounts of the carboxylic groups in different torrefaction temperature for spruce (single particle reactor) and birch (in moving bed at ECN) wood measured by methylene blue sorption and titration method. [1]MB: methylene blue sorption. [2]Tit: titration [3]n.m. not measured (data from Paper I and III)

Carboxylic groups (µmol/g wood)	Raw	Torrefaction Temp. °C							
		180	200	240	255	260	270	280	300
MB[1]: raw spruce	90	98	93	45	n.m.	22*	n.m.	15	3
MB: acid washing then torrefaction of spruce	103	n.m.[3]	n.m.	n.m.	n.m.	18	n.m.	n.m.	7
Tit[2]: raw spruce	87**	n.m.	n.m.	n.m.	n.m.	n.m.	n.m.	n.m.	n.m.
Tit: torrefaction then acid washing of spruce	112	n.m.	n.m.	n.m.	n.m.	29	n.m.	n.m.	9
Tit: acid washing then torrefaction of spruce		n.m.	n.m.	n.m.	n.m.	24***	n.m.	n.m.	15
MB: raw birch	40	n.m.	n.m.	25	14	n.m.	10	n.m.	10
Tit: acid washing then torrefaction of birch	42	n.m.	n.m.	31	21	n.m.	14	n.m.	14

*The results of three replicates (22, 22, 23) **The results of three replicates (80, 86, 93)*** Corrected from paper I

Table 9 also shows that at higher torrefaction temperatures, i.e., of 260 and 300 °C, the content of the carboxylic groups in both acid-washed and raw spruce are quite similar.

3.2.2. Potentiometric Titration

The content of the carboxylic groups of raw spruce was measured by potentiometric titration after triplicate runs. The measured concentration was 87 μmol/g wood. Titration curves in Figure 9 show the pH of biomass suspensions vs. the volume of the added 0.1M NaOH. Owing to some delay in reaching the equilibrium pH of the suspension, slight irregularities can be observed in the curves of biomass titration.

It can be seen that the curve of raw spruce wood is shifted to the right compared to the blank curve. The difference between the inflection points of the two curves determines the content of the weak acid in biomass. The titration curves of torrefied spruce compared to raw spruce are shifted to the left. Although, the curves of torrefied spruce show a decrease in the number of the carboxylic groups, the curves cannot be used to determine the content of the carboxylic groups without acid washing the sample first. This is likely due to the consumption of some of the initially added HNO_3 in the suspension by some inorganic anions of the salts present in biomass.

In order to remove the interference of the inorganic anions and reaction between alkaline earth metals and carboxylic groups on the titration curves, the raw and torrefied spruce at 260 and 300 °C are acid washed prior to titration. As it is seen in Figures 10 and 11, acid washing after torrefaction shifts the curves to the right side of the curve for the blank test.

Figures 10 and 11 also show the titration curve for raw spruce, spruce wood first acid washed and then torrefied and spruce wood first torrefied and then acid washed at 260 and 300 °C. The curves for the acid washed and then torrefied, and the torrefied and then acid washed are very similar during torrefaction at 260°C, Figure 10. This might show that organically bonded metals have little effect. However, for torrefaction at 300 °C, there is a significant difference in the titration curves, Figure 11. This indicates that organically bonded metals and inorganic salts might affect the mechanism of degradation of spruce wood during torrefaction at high temperatures. This idea is further investigated in section 3.5.
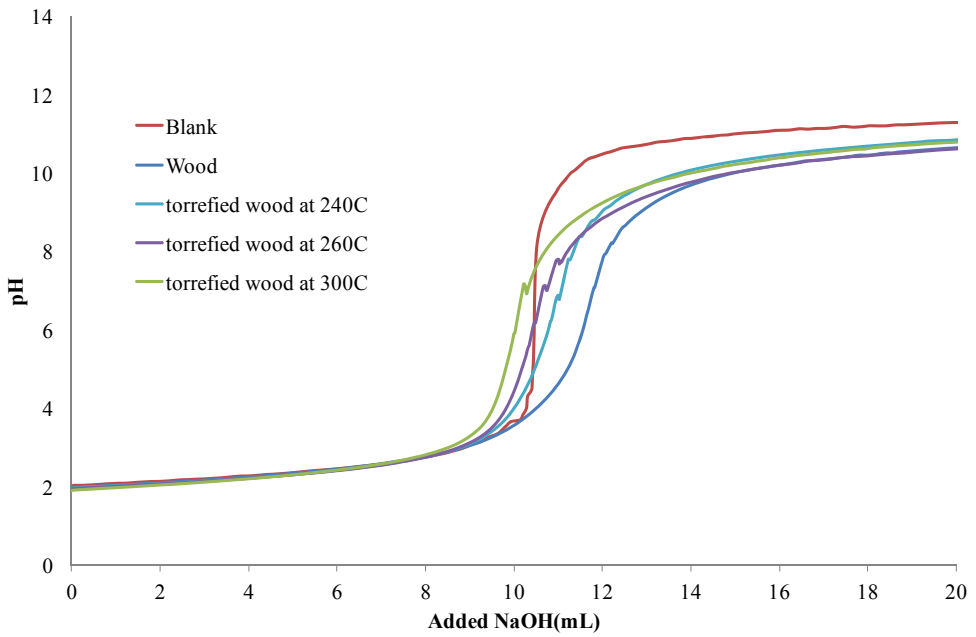
Figure 9. Potentiometric titration curve of blank, untreated wood and torrefied untreated spruce wood at different temperatures. Biomass sample was 1.50 g suspended in 150 ml of solution. The curves are for samples that have not been acid washed (Paper I)
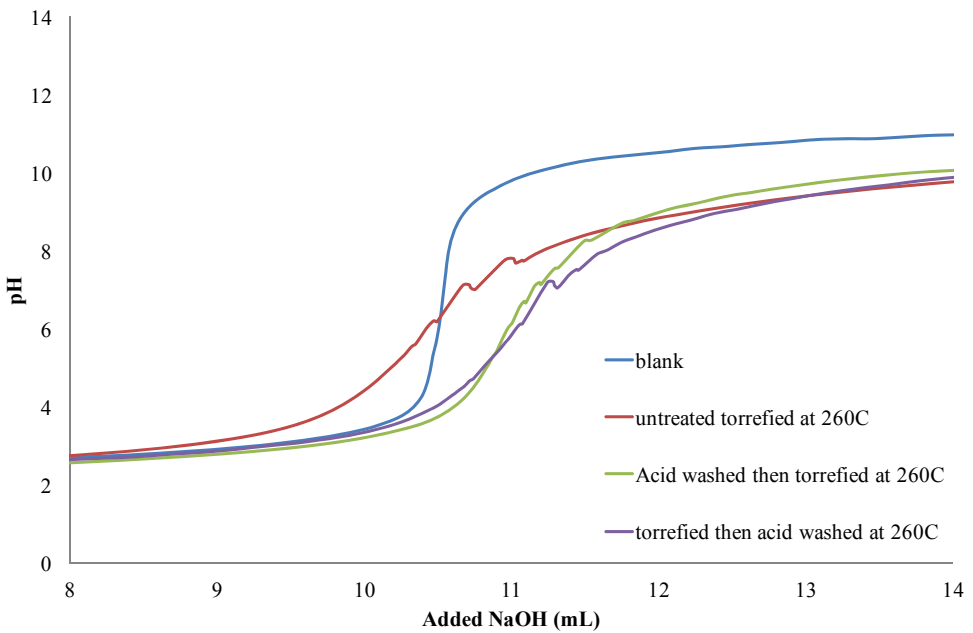

Figure10. Potentiometric titration curves for blank and torrefied spruce wood at 260 °C (Paper I)
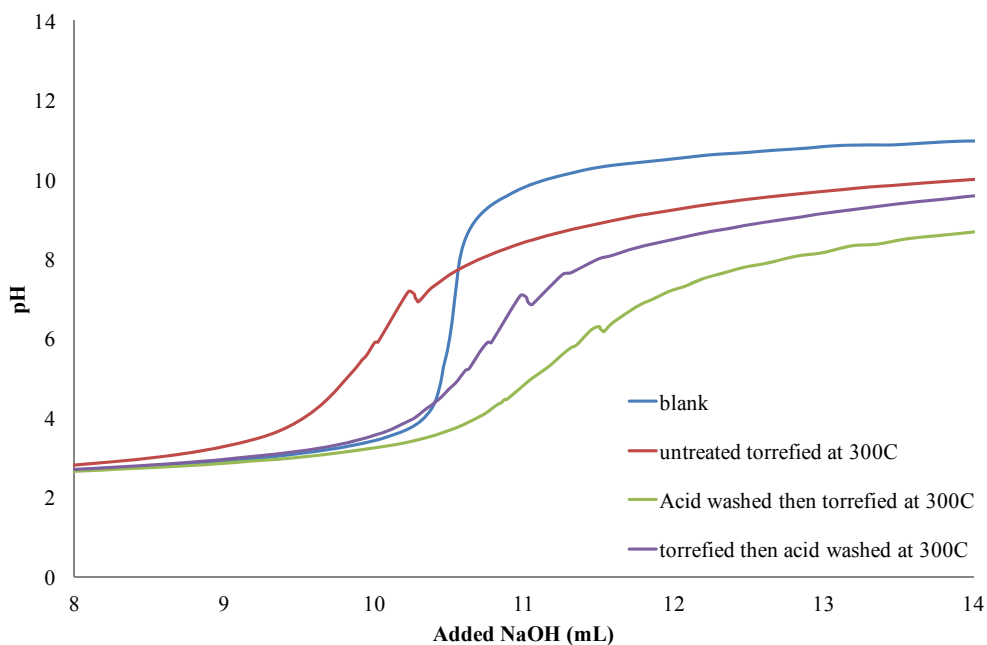
Figure11. Potentiometric titration curves for blank and torrefied spruce wood at 300 °C (data from Paper I)

Metal ions in wood are partly bonded to carboxylic groups [129,132-134]. There appears to be a difference in the destruction of carboxylic groups during torrefaction of raw and acid washed spruce, indicating that metals may have an effect on torrefaction.

3.2.3. Comparison of the Two Methods

The concentration of carboxylic groups in the acid washed spruce by potentiometric titration is 112 µmol/g, which is higher than that measured by methylene blue sorption by about 9 µmol/g, Table 9. The titration results for acid-washed wood torrefied at 260°C, agree well with the methylene blue sorption results, while at 300°C, the titration results give twice as much as the methylene blue, but the total amounts are the lowest so the actual difference is less than the difference for the acid washed wood, which has not been torrefied.

The concentration of carboxylic sites in the birch samples from ECN was analyzed by both methods. The concentration of the methods gives 40 µmol/g and 42 µmol/g for the concentration of carboxylic groups for methylene blue sorption and potentiometric titration

methods respectively, Table 9. The measured concentration is similar to the value of 52±4 µmol/g of another birch sample analyzed by methylene blue sorption [129].

Both methods have a similar decrease in the concentration of the carboxylic groups with the increase in the torrefaction temperature, Figure 12. The content of the carboxylic groups measured by titration is always slightly higher than that measured by methylene blue sorption. Applying these two methods to measure the content of the carboxylic groups in coal also results in slightly higher value by potentiometric titration [135]. This is thought to be due to two reasons: first, during acid washing of biomass, acid hydrolysis reaction produces more acidic groups, and secondly, during titration, small protons can better penetrate to biomass matrix and therefore, more of the carboxylic groups are reached. This is in comparison to sorption of the big methylene blue cations, which may not fully penetrate the biomass sample.
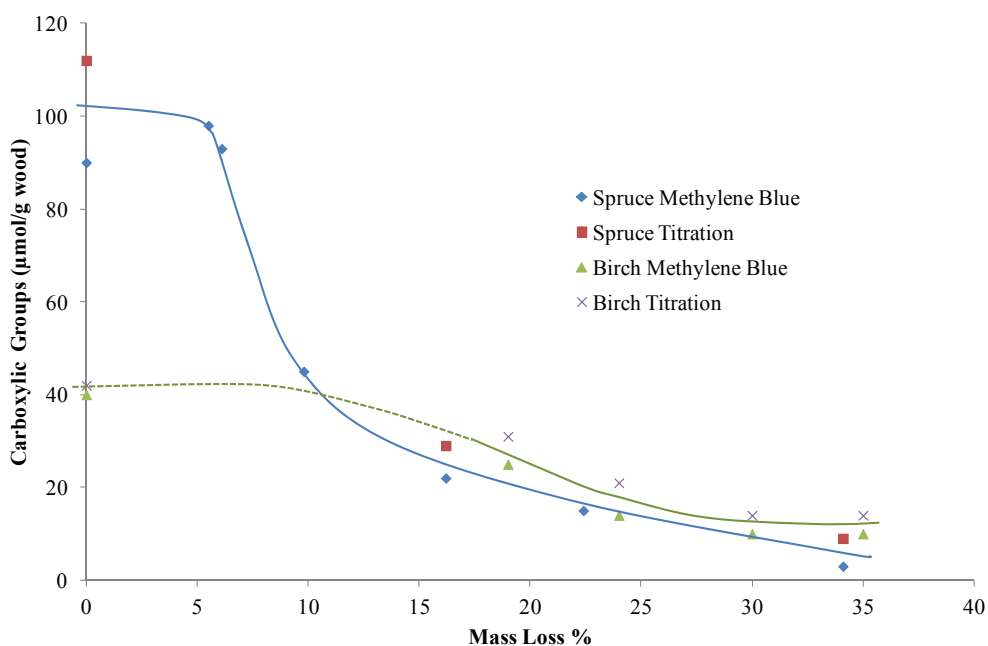

Figure 12. Comparing the results of carboxylic groups of spruce and birch wood by methylene blue sorption and potentiometric titration. Dashed lines are guessed based on spruce results (data from Paper I and III)

Figure 12 shows that the main degradation of carboxylic groups occurs below about 260 °C and it is independent of biomass type. Further decreases are modest and accompanied by more increase in mass loss.

3.3. Equilibrium Moisture Content

Changes in the equilibrium moisture content of spruce wood versus torrefaction temperature are shown in Figure 13. The moisture content decreases with increase in the torrefaction temperature at 240 ˚C and above. For 98% relative humidity, torrefaction at 180 and 200 ˚C in fact resulted in higher equilibrium moisture content when compared to raw spruce. The decrease in the equilibrium moisture content at 240 ˚C and above is consistent with results for torrefaction [1] and wet torrefaction [136]. The lower tendency to absorb moisture results in a fuel more resistant to biological decay [29,30] .

The decrease in the carboxylic group content, while torrefaction temperature increases, is shown in the secondary axis of Figure 13. A decrease in the equilibrium moisture content for torrefied spruce wood follows the degradation of carboxylic groups. Therefore, changes in the equilibrium moisture content are relevant to changes in the content of the carboxylic groups.
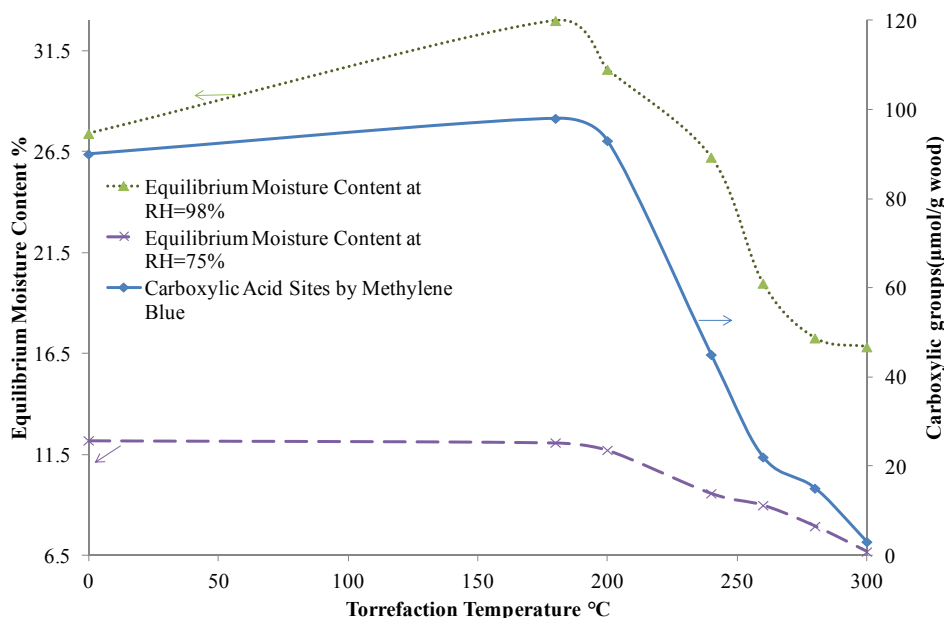

Figure 13. Equilibrium moisture content of torrefied spruce wood samples at different relative humidity and the comparison of its sensitivity with carboxylic acid sites versus temperature (Paper I)

3.4. Chemical Changes of Wood Components during Torrefaction

3.4.1. Hemicellulose

The contents of five-carbon sugars (pentoses) and six-carbon sugars (hexoses) in the hemicellulose of raw and torrefied birch are shown in Table 10. It is seen that 71% of the pentoses degrade during torrefaction at 240 °C, and the degradation increases to 84% at 255 °C and then finally increases to 96% during torrefaction of birch at 280 °C.

However, hexoses degradation is only 40% during torrefaction at 240 °C, and does not appear to degrade further. At 255 ˚C, we see decrease in all the hexoses except glucose, which we see increase in it, measured by acid methanolysis. This increase can be attributed to the depolymerization of cellulose so that it is quantified by acid methanolysis. The pentoses are more susceptible to degrade than hexoses. This probably explains some difference in mass loss between hardwood and softwood.

The uronic acids also degrade significantly during torrefaction at 240 °C. The uronic acids contain the carboxylic groups, which degrade during torrefaction. The decrease in this functional group, which exists natively in hemicelluloses and pectins, is consistent with the hemicellulose and pectin degradations found in this work. NMR results also show a clear decrease in carboxylic groups [64], which can be attributed to the decarboxylation of hemicellulose. Ben and Ragauskas [10] also observed a decrease in carboxylic groups during torrefaction using NMR analysis. Overall, the uronic acids are the most sensitive units in hemicelluloses, whereas hexoses are the most stable units during torrefaction.

The values of hemicellulose degradation, compared to mass loss during torrefaction at 240 and 255 °C, show that the hemicellulose degradation is slightly higher than the total mass loss. This is due to the degradation of hemicellulose to produce char and extractable materials rather than solely volatiles. However, above 270 °C, the char production cannot be proposed due to higher mass loss than hemicellulose degradation.

Table 10. Composition of hemicelluloses and pectins in raw and torrefied birch wood at different temperatures (as anhydrosugars) The values are the mean of 3 replicates. All values are given on original wood (mg/g wood) basis for direct comparison. 4-O-Me-GlcA =4-O-Methyl-Gluconic Acid; GlcA =Gluconic Acid; GalA =Galacturonic Acid (data from Paper II, *corrected from Paper II)

Sugars		Torrefaction Temperature °C				
		raw	240	255	270	280
Hexoses	Mannose	13.9	7.4	6.3	4.8	3.5
	Galactose	10.8	2.5	1.4	1.1	0.9
	Glucose*	28.2	23.4	26.7	33.8	40.4
Pentoses	Rhamnose	3.8	0.5	0.3	0.1	0.0
	Arabinose	4.3	0.9	0.8	0.4	0.3
	Xylose	203.7	58.9	28.3	11.5	5.3
Uronic acids	4-O-MeGlcA	18.9	1.3	0.2	0.2	0.1
	GlcA	0.5	0.1	0.1	0.1	0.0
	GalA	16.7	0.1	0.1	0.0	0.0
Hemicellulose (total)		300.9	94.9	64.2	52.1	50.8

Sugar analysis in this work shows 71% and 97% degradation in xylose during torrefaction at 240 and 280 °C, compared to 5 and 77% mass loss for xylan torrefied at 60 min at either 230 or 290 °C in a TGA [137]. The comparison between hemicellulose degradations of these two methods shows that at a lower torrefaction temperature, such as 240 °C, hemicellulose decomposition results in char and formation of extractable material, but at higher torrefaction temperatures, the majority of the decomposition products are volatiles.

3.4.2. Cellulose

Cellulose degradation is shown in Figure 14. It is seen that increasing the torrefaction temperature increases the mass loss of cellulose from 3% at 240 ˚C to 37% at 280 ˚C on an original birch wood basis.

During mild torrefaction, cellulose in biomass, which includes a strong crystalline structure, is more stable than hemicelluloses. This is due to inter- and intra-molecular hydrogen bonds in addition to glycosidic bonds between glucose units in cellulose.

Cellulose decomposition starts at 255 °C. Cellulose degradation starts with the dissociation of the accessible bonds and then continues to the more internally placed glycosidic bonds [63]. It is proposed that the more degradation of cellulose at higher temperature is likely due to acid hydrolysis of cellulose in presence of acids produced during torrefaction.

Figure 14. Cellulose content in birch and torrefied birch wood at different torrefaction temperatures (Paper II)

Comparison of the hemicellulose and cellulose loss with total mass loss during torrefaction at 240, 255, 270 and 280 °C shows that carbohydrates loss is 2.7, 4.0, 4.4, and 4.5 % more than the mass loss. This difference indicates that the carbohydrate degradation not only produces volatiles but also forms char.

Studies on grinding show that torrefaction at 255 °C has already reduced the consumed energy for grinding the pine chips and logging residues by 50%, while torrefaction at higher temperature results in mean particle size reduction up to 50% [21]. Additionally, this study shows that hemicellulose degradation occurs at the beginning of torrefaction, whereas cellulose degradation happens at relatively higher torrefaction temperatures. Therefore, it can be concluded that hemicellulose degradation can affect the grinding energy while cellulose degradation might influence the mean particle size of torrefied biomass.

3.4.3. Lignin

Three different methods, including the Klason lignin method, Py-GC-MS and DD NMR, were employed to study the changes in the lignin structure during torrefaction.

The Klason lignin method has been performed on the acetone extractive free birch samples. It is seen in Table 11 that the content of acid insoluble material increases from 17.6% in raw

birch to 26.1% in birch torrefied at 255 °C. This increase is consistent with other studies [16,21,93,138-140]. The possible explanations are firstly dissociation of polymeric cellulose, which might form acid insoluble products, including benzenoid aromatic groups and acid insoluble condensed materials; secondly, some volatile material produced from hemicellulose degradation might react to the phenolic units in lignin and then results in heavier acid insoluble products [141].

Table 11. The content of residue after acid digestion of raw birch and some of the torrefied birch samples. (* lignin, condensed materials and produced aromatics from hemicellulose and cellulose) (Paper II)

Samples(mg /g wood)	Acid insoluble lignin	Acid soluble lignin
Raw wood	175.5	22.4
Torrefied at 240 °C	224.1*	9.9
Torrefied at 255 °C	260.7*	7.8

Meanwhile, acid soluble lignin decreases from 2.2% in raw birch to 0.8% (on a wood basis) in birch torrefied at 255 °C. This shows that acid soluble materials from lignin are not formed, but degraded to insoluble materials.

Although the Klason lignin method quantifies both the acid soluble and acid insoluble material, it cannot quantify or qualify the changes in the lignin after torrefaction. Thus, two other methods, Py-GC-MS and DD NMR, were applied to determine the changes in the structure of lignin after torrefaction.

Py-GC-MS has been applied to extractive free biomass, and gave relative amounts of the *p*-hydroxyphenyl, syringyl and guaiacyl units in lignin. The analysis shows that, for example, vanillin, a guaiacyl derivative, increases during torrefaction at 240 and 255 °C (data in paper II), which is consistent with Rousset et al.'s [139] results, measuring the increase in vanillin content during heat treatment at 220 °C.

Table 12 shows that the raw birch does not have *p*-hydroxyphenyl units; however, after torrefaction the ratio of the *p*-hydroxyphenyl to syringyl and guaiacyl increases. This indicates the dissociation of methoxyl groups from lignin units during torrefaction. Earlier studies have found a release of methoxyl groups during torrefaction [140,142].

Table 12. The content of lignin-based units in Py-GC-MS chromatograms for raw and torrefied birch wood, n.d. not determined (Paper II)

Lignin's units%	Torrefaction Temperature °C				
	Raw birch	240	255	270	280
Phenyl (H)	n.d.*	3.44	5.82	6.03	14.02
Guaiacyl (G)	8.25	8.77	16.13	15.62	14.72
Syringyl (S)	25.92	28.45	32.53	29.46	29.11
H:G:S	0: 76: 24	8: 70: 20	10: 60: 30	11: 58: 31	25: 50: 25

Analysis of DD NMR has been done in Helsinki University. The analyses are in paper II.

3.4.4. Extractable Materials

The content of the acetone extractable materials have been investigated applying three different methods, including gravimetry, GC-FID followed by GC-MS and HPSEC. The gravimetric method has quantified the total content of the extractable material in biomass, whereas GC has quantified and identified the acetone extractable materials, which have low molecular weights. HPSEC has divided the acetone extractable materials based on their molecular weights.

The total amount of acetone extractable materials has been quantified using a gravimetric method. The highest content of acetone extractable materials have been found after torrefaction at 240 °C, Figure 15, and this content has decreased when the torrefaction temperature has increased. Even after torrefaction at 280 °C, the content of acetone extractable material is slightly higher than this content in raw birch wood. This increase in acetone extractable material followed by a decrease at higher torrefaction temperatures has been observed in an earlier number of studies on a heat treatment of wood [30,93,128].
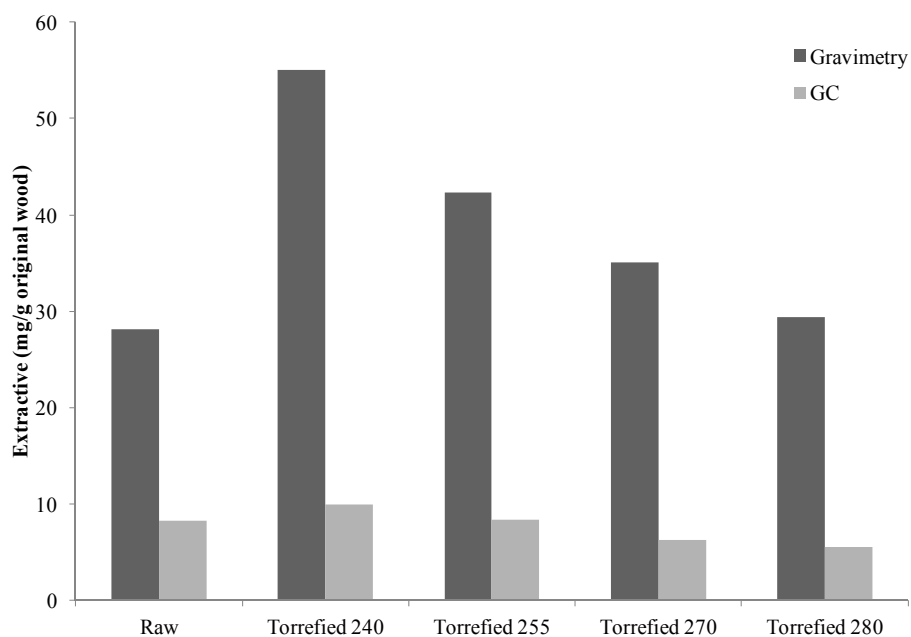
Figure 15. Acetone extractable material contents measured by GC and gravimetric method on original wood basis (Paper II)

The content of acetone extractable materials measured by GC-FID followed by GC-MS also shows the same trend observed in the gravimetric measurements. However, the fraction of the acetone extractable materials determined by this method is generally less than 20% of the total acetone extractable materials measured using gravimetric method, Figure 15. This is due to the limitation of the GC method in which the extractable materials with low molecular weights can be determined.

Some acetone extractable materials from GC results are shown in Table 13. It is seen that the extractable materials can be divided into two groups: a group of them decreases during torrefaction already at 240 °C, whereas the others are increased at the same torrefaction temperature. And, the extractable materials, increased at 240 °C, also degrade at higher torrefaction temperature. Examples include succinic acid from carbohydrate degradation, and vanillin from lignin degradation, Table 13.

Table 13. Composition of some of the acetone extractable materials of raw and torrefied birch wood quantified and qualified by GC-MS (Paper II).

Extractable material (mg/g wood)	Torrefaction temperature °C				
	Raw	240	255	270	280
Sugars derived compounds:					
Glycerol	0.058	0.006	0.007	0.005	0.005
Sugars	1.353	0.773	1.026	1.261	1.419
Sugars (total):	1.411	0.779	1.033	1.266	1.424
Acids:					
Succinic acid	0.048	0.205	0.167	0.120	0.098
Acid (total):	0.397	0.460	0.401	0.324	0.314
Lignin units and other aromatics:					
Vanillin	0.059	0.134	0.128	0.101	0.087
Hydroxyguaiacol	0.008	0.041	0.037	0.033	0.037
Hydroxysyringol		0.071	0.028	0.065	0.037
Vanillic acid	0.007	0.035	0.029	0.029	0.027
Syringic acid	0.007	0.189	0.119	0.091	0.051
3-Syringylpropenal	0.013	0.211	0.056	0.009	0.010
Syringaresinol	0.035	1.193	0.593	0.164	0.000
1-Syringyl-2-hydroxy-1-ethanone		0.056	0.050	0.023	0.012
Lignin units &other aromatics (total) :	0.527	3.754	2.394	1.362	0.877
Sterols					
Betulinol	0.530	0.287	0.303	0.018	0.055
Methyl betulinate	0.158	0.086	0.049	0.022	0.011
Sterols (total)	0.688	0.373	0.352	0.04	0.055
Unidentified compounds (total)	5.169	4.538	4.184	3.202	2.879
Sum	8.192	9.904	8.364	6.194	5.549

The increase in the content of some extractable materials like syringaresinol or vanillin is important from biorefinery perspectives. There are some other extractable materials like betulinol and methyl betulinate, which cannot form from lignin or carbohydrate degradation. These extractable materials start to degrade already at 240 °C and higher temperatures.

The molar mass distribution of acetone extractable materials in raw and torrefied birch wood, measured by HPSEC, is shown in Figure 16. In raw birch, the peaks are marked with fatty

acids, steryl esters and triglycerides. It is worth noting that the samples are stored at room temperature so it is possible that some changes will happen to the compounds during the storage. Figure 16 shows that increasing the torrefaction temperature shifts the chromatograms to the left. This indicates that torrefaction results in a decrease in high-molar-mass compounds and an increase in low-molar-mass compounds. This alteration in peak area indicates that some of the components have changed; they are either degraded from high-molar-mass compounds, or formed by any reaction of low-molar-mass compounds.
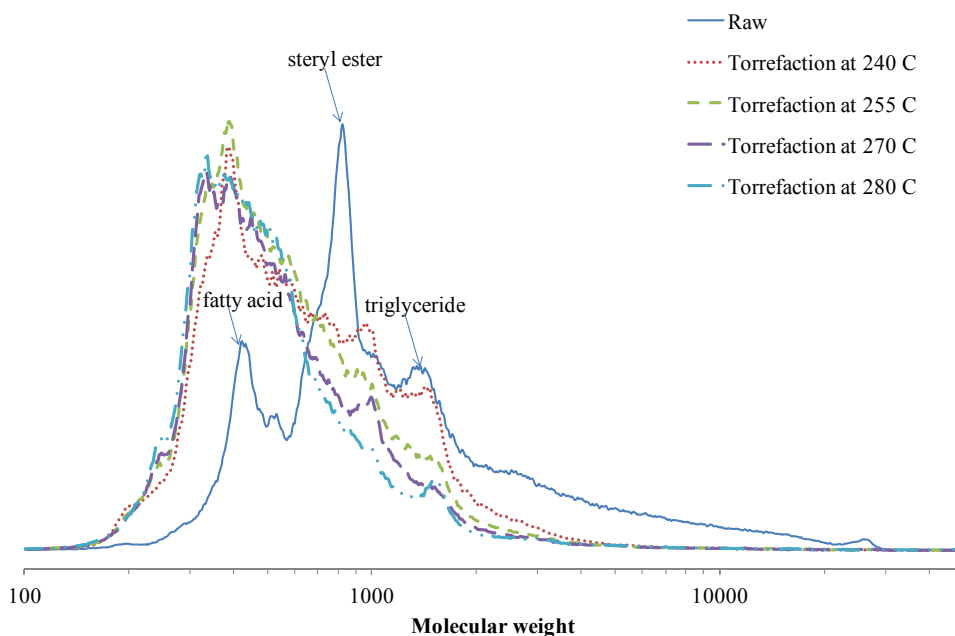
Figure 16. Molar mass distribution of acetone-soluble compounds in raw and torrefied birch wood at different torrefaction temperatures (Paper II)

In this regard, Figure 17 shows the integrated curves of molar mass distribution of extractable materials; the x-axis is the molecular weight in Dalton and the y-axis is the percentage of the extractable materials. For example, 70% of extractives from raw birch have molecular weight smaller than 1500 Dalton, whereas 70% of extractives from torrefied birch at 280 °C have molecular weight smaller than 597 Dalton. Therefore, the molecular weight of extractable materials decreases when the torrefaction temperature increases. This is due to the degradation of high molecular mass compounds in birch wood.
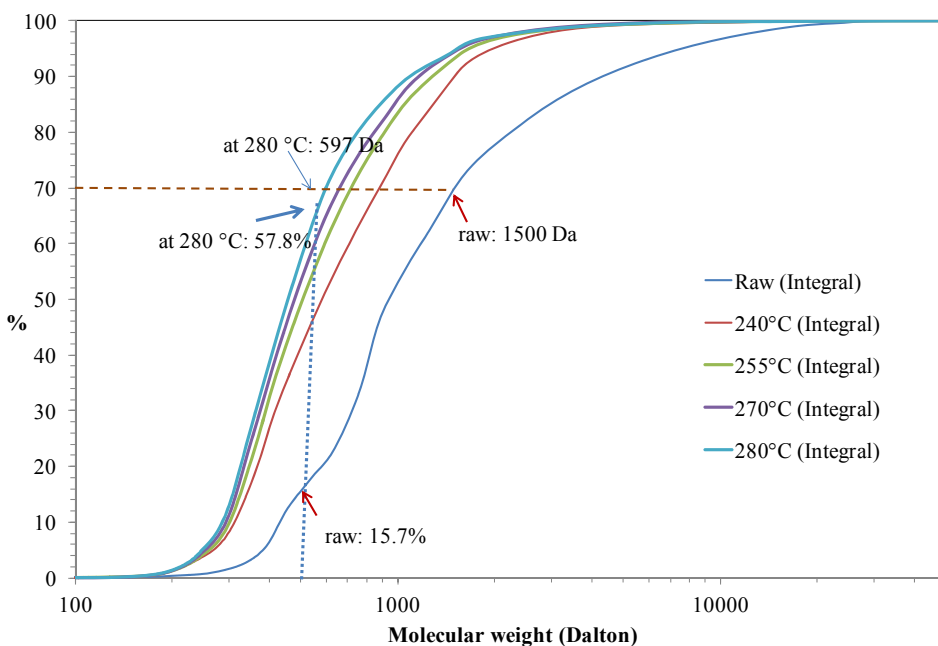
Figure 17. Integrated curves of molar mass distribution of acetone soluble compounds in raw and torrefied birch wood at different torrefaction temperatures (Paper II)

3.4.5. Ash-forming Elements

The chemical fractionation results of birch wood and birch wood torrefied at 240 and 280 °C are shown at Figure 18. Each bar shows the amount of given elements that is found in each of the fraction from stepwise leaching. The elemental analysis of the original solid material analyzed without leaching is marked with 'x'. All the values are given on a dried raw birch basis so that the total content of these elements can be directly compared. The extent of agreement between the concentration of the elements in the original fuel and the amount of the elements found in the four fractions provides a check on the accuracy of the analysis. By considering that the samples are from pilot scale reactor, there is a good agreement between solid fuel and chemical fractionation results.

Calcium, Magnesium and Manganese: These elements are not released during torrefaction. However, after torrefaction at 280 °C the water and ammonium acetate soluble contents decrease, while the acid soluble content increases. The ammonium acetate soluble calcium, magnesium and manganese are likely to be bound to carboxylic groups [143]. These groups

are mostly degraded during torrefaction [127]. Thus the degradation of carboxylic groups may partially explain decrease in the content of ammonium acetate Ca, Mg and Mn.
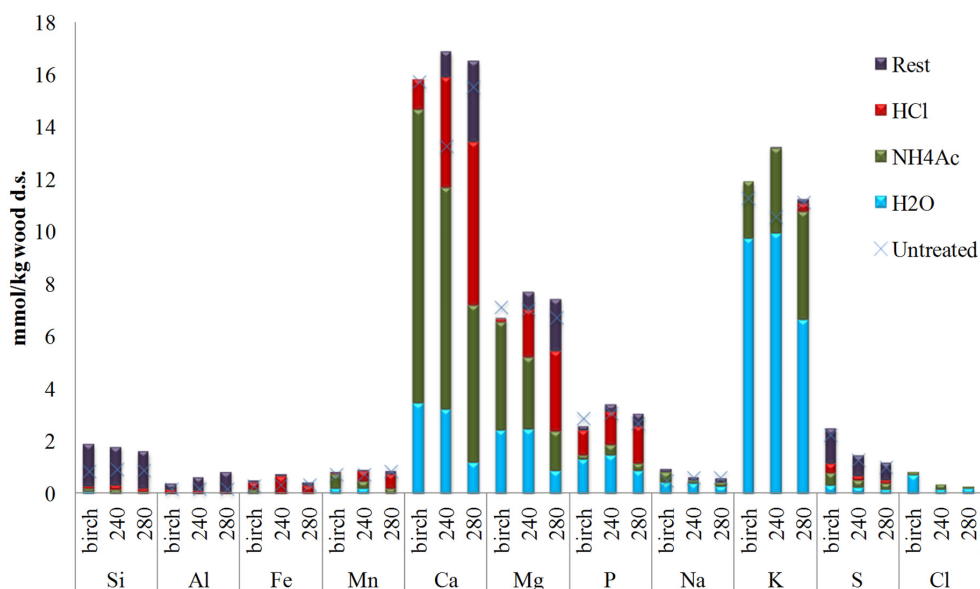

Figure 18. Comparison of ash-forming materials in birch wood and its torrefied form at 240°C and 280°C. The Cl content of solid samples was below the detection limit for the analysis method and is therefore not given (Paper III)

Increase in the amount of acid soluble phosphate or carbonate – which will be shown later in this section – is not sufficient to explain the increase in the total content of acid soluble Ca, Mg and Mn in the birch torrefied at 280 °C. Thus the acid soluble fraction is most probably bond to or blocked in the char matrix.

Potassium and Sodium: The total contents of these two elements appear to be constant during torrefaction of birch wood. The content of water soluble K decreases, while the content of ammonium acetate soluble K increases during torrefaction at 280 °C. Additionally, a small fraction of K becomes acid soluble during torrefaction at 280 °C. The K compounds in birch are chiefly K salts which are water soluble. The decrease in the content of water soluble K can be attributed to the release of Cl from alkali chloride salts [144] or reaction of phosphorous with K, which is discussed later in phosphorus section.

Chlorine: Ion chromatography was used to analyze the Cl content. All chlorines are assumed to be leached in the water leaching step. It is seen in Figure 18 that 30% of chlorine is already released at 240 °C, and about 80% is released during torrefaction of birch at 280 °C. Chlorine exists in biomass mostly in salts while a minor amount of it is present in aliphatic or aromatic compounds [88].

Eralier studies found that [88,144-146] chlorine could be released below 400 °C. For instance, it is hypothesized that [144] alkali chloride reacts with functional groups and then resulting in release of chlorine:

R-COOH(s) + KCl(s) →R-COOK(s) + HCl(g)   (reaction 2)
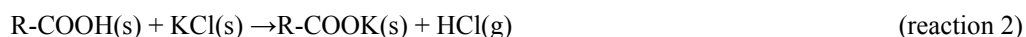
The produced organically bonded K can partly explain the decrease in water-soluble K and the increase in the ammonium acetate-soluble K during torrefaction. However, more recent studies by Hamilton et al. [147] and Saleh et al. [86] showed that the released chlorine is mostly released as methylchloride during torrefaction.

Sulfur: A high fraction of sulfur is insoluble, as seen in Figure 18. This is thought to be the organically bound sulfur. Both solid and leachate analyses show a decrease in the total content of sulfur to 65% of the initial, during torrefaction at 280 °C. The decrease is mostly seen in the insoluble fraction. The organic sulfur is thought to begin to decompose and devolatilize already at 200 °C [148]. Recent studies show a release of sulfur during torrefaction [86,89] and wet torrefaction [90]. The results of these studies for S release are consistent with our results.

Phosphorous: This element is not found to be released during torrefaction. The total amount of phosphorous (P) is remained approximately constant during torrefaction, Figure 18. The analyzed water soluble phosphate (PO_4^{3-}), Table 14, is about half of the total amount of water soluble P in raw and torrefied birch at 280 °C, meaning that water-soluble P is apparently present in a form rather than PO_4^{3-}. The content of acid soluble PO_4^{3-} after torrefaction of birch wood at 280 °C increases. However, this does not fully explain the increase in the acid soluble content of Ca, Mg, Mn.

Silicon, aluminum and iron: These elements are stable minerals in biomass at torrefaction temperatures, as shown in Figure 18. Among these non-reactive elements, silicon, which

mostly exists as silicate, has the highest concentration in the birch wood samples, compared to aluminum and iron.

Table 14. Concentration of anions measured by IC for raw and torrefied birch wood at *280*°C. n.a. not analyzed. b.d. below detection limit, *NH₄Ac: Ammonium acetate. **Carbonate is quantified by coulometry ***This value is probably too high due to the overlap of a second peak which is probably an organic ion (Paper III)

Anions	(mmol/kg wood d.s.)					
	Raw Birch			Torrefied Birch at 280°C		
	H_2O	NH₄ Ac*	HCl	H_2O	NH₄ Ac*	HCl
Cl^-	1.14	n.a.	n.a.	0.16	n.a.	n.a.
NO_3^-	0.02	0.07	0.10	b.d.	0.87	0.08
PO_4^{3-}	0.55	0.05	0.18	0.52	0.11	0.37
SO_4^{2-}	0.08	0.66	1.36***	0.16	0.32	1.53***
$C_2O_4^{2-}$	b.d.	0.61	1.13	0.21	0.69	0.66
CO_3^{2-}**		1.35			2.28[(1)]	

(1) Corrected from paper II

Nitrate: A small amount of nitrate has been dissolved in ammonium acetate from torrefied birch at 280 °C, Table 14. This amount is about 0.001 wt% of the total nitrogen in torrefied biomass, and this is even less in birch wood. This means that nitrogen is mostly in other forms in biomass than nitrate, and torrefaction does not have any significant influence on its content.

Oxalate: The content of oxalate was similar in both raw and torrefied birch at 280 °C, except for a decrease in the content of acid-soluble oxalate after torrefaction at 280 °C, Table 14. This is likely due to some decomposition of oxalate during torrefaction at 280 °C; the decomposition temperature of calcium oxalate is about 400 °C [149], meaning that this content is expected to be fairly stable.

Carbonate: Analysis of carbonate by IC is complicated, because carbonate dissolved in an acid solution apparently produces CO_2 at low pH. Additionally, the water and ammonium acetate solution containing carbonate might absorb CO_2 from the atmosphere. Therefore, coulometry has been applied to measure the carbonate in the raw and torrefied birch samples. The concentration of carbonate for raw birch is 1.35±0.33 µmol/g wood, after torrefaction at 240 °C is 4.61±2.4 µmol/g wood and after torrefaction at 280 °C is 2.28±0.65 µmol/g wood. The increase in the acid solubility of Ca, Mg and Mn after torrefaction at 280 °C cannot be

attributed to the formation of carbonates of these metals during torrefaction, mainly because carbonate content has already increased during torrefaction at 240 °C.

3.5. Effect of K on Torrefaction

3.5.1. Effect of Temperature

Figure 19 shows the experimental mass yield curves of acid washed miscanthus during torrefaction at 240, 260, 270 and 280 ˚C. At a torrefaction temperature of 240 °C, the mass loss after 30 min is 10.9% on a dry mass basis and it is 29.7% at 280 °C. At each torrefaction temperature, the rate of mass loss is comparatively rapid in the first approximately 5 minutes of torrefaction, after which the rate of mass loss slows. The mass loss does not level off within the 30 minutes and studies for very long torrefaction times – up to 6 h – have shown that mass loss continues at torrefaction temperatures [10,93]. Therefore, the rate of equation for torrefaction must account for the faster initial volatile formation and release and then the slower char forming and secondary volatile formation reactions. Increasing the torrefaction temperature increases the rate of the first step more than the second step, Figure 20.
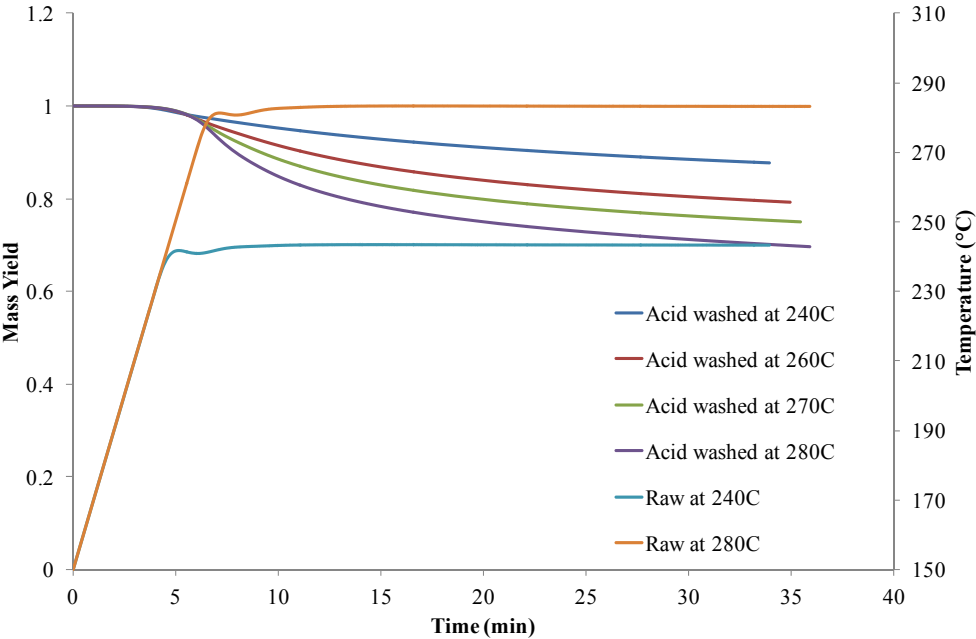

Figure 19. The effect of temperature on mass yield of acid washed and raw miscanthus during torrefaction
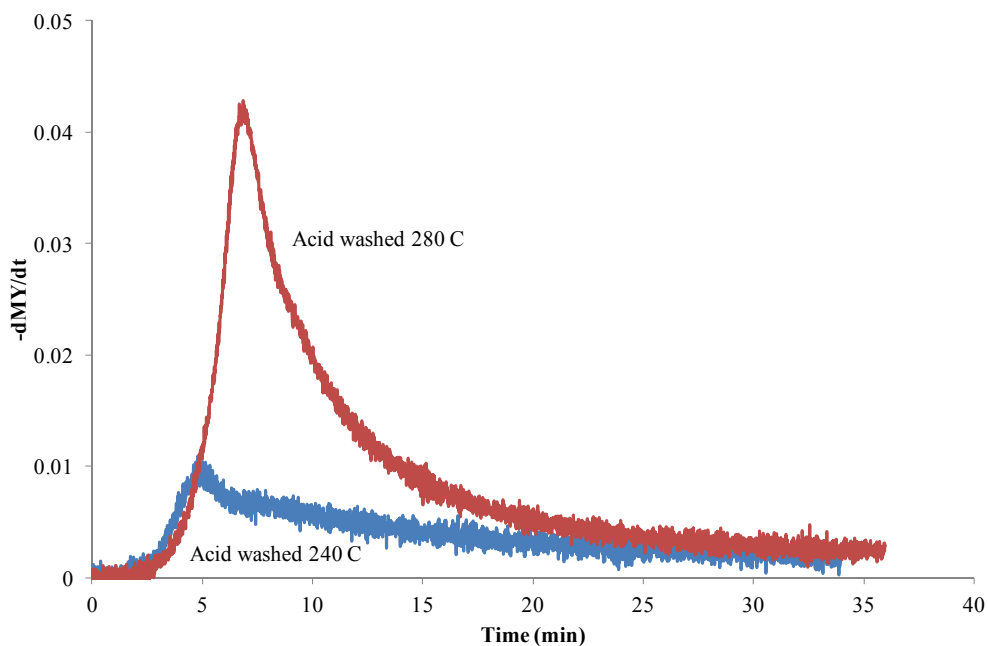
Figure 20. Comparison of reaction rate for acid washed miscanthus at 240 and 280 °C

3.5.2. Effect of K Content

Figure 21 shows the impact of the K content on spruce wood degradation during torrefaction. For the demineralized sample the mass loss after 30 min at 240 °C is about 7.6%, while the increase of K content to 1.2% increases the mass loss to 16.2%. This effect can also be observed at 280 °C. The mass loss is 24.9% for the demineralized wood and 48.2% for the samples doped with 1.2 wt% K. In general, increasing the K content increases the mass loss; however, it is seen in Figure 21 that up to 0.6 wt% K, there is a clear increase in the mass loss of biomass. Above this level, there is some leveling off in the influence of K.

In K-low and K-medium spruce, the K is chiefly bonded to carboxylic groups. As shown in section 3.2, these groups degrade during torrefaction with approximately 50% degradation at 240 °C and over 90% degradation after torrefaction at 280 °C. During torrefaction, the total content of alkali and alkaline earth metals remain constant, but their chemical association changes and their solubility decreases, as shown by the fuel fractionation results in section 3.4.5. It can be hypothesized that these metals, during carboxylic group degradation, leave their original positions and form new bonds in the biomass matrix. It has been suggested that

the mechanism of torrefaction includes the cleavage of homolytic bonds to produce free radicals and the formation of free radicals is facilitated by inorganics [68]. For the higher content of K, K>0.6 wt.% – for instance in K-high spruce, wherein K is bonded to carboxylic groups as well as to phenolic groups – there is not a significant increase in the mass loss compared to K-medium spruce. One interpretation of these results is that any increase in the mass loss mainly depends on the K bonded to carboxylic groups rather than the K bonded to phenolic groups. Potassium participated as K_2CO_3 at a level of 0.33 wt.% K behaved similarly to the K that was doped onto carboxylic sites. It was not done in this work, but depositing higher levels of K as K_2CO_3 would help clarify if there is saturation level of K where additional K has little effect or if it is simply K doped to the phenolic groups that is not very active.
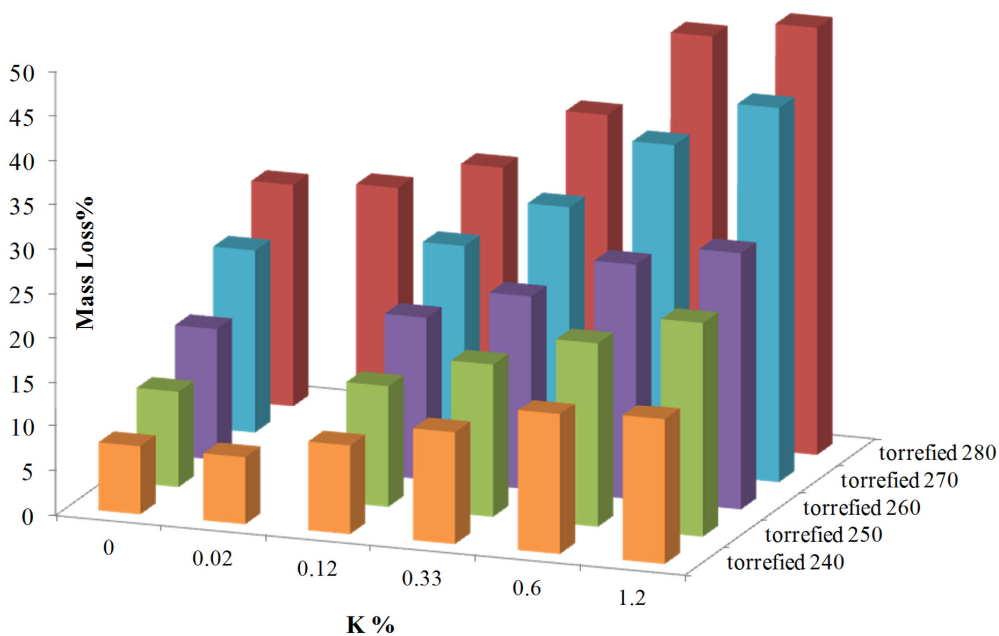

Figure 21. The effect of K on mass loss of spruce at different torrefaction temperature (data from paper IV)

65

3.5.3. Effect of Na

Aspen doped with K or Na at two levels: 61 (K)/61 (Na) and 210 (K)/222 (Na) was torrefied at 240 °C and 280 °C. The mass loss during the torrefaction of the doped aspen is almost identical for the Na and K doped at the same level, Figure 22, indicating that the two behave in a similar manner. This is reasonable as both have been also found to affect pyrolysis in a similar way.

The results show that increasing the concentration of K or Na had little to no effect on the mass loss during torrefaction of aspen at 240 °C. During torrefaction at 280 °C, there is a clear impact of the K and Na concentration on mass loss. It is seen that increasing the K or Na content from 61 to 210 (or 222 for Na) µmol/g increases the mass loss from 27% to 53%.
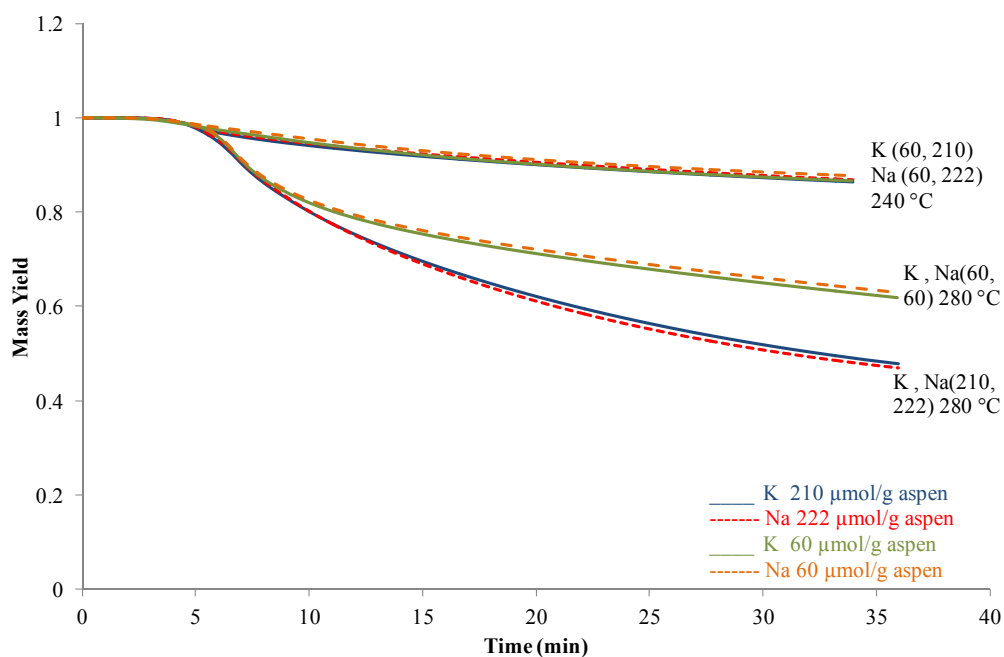

Figure 22. Impact of Na and K on torrefaction of aspen (data from Paper IV)

3.5.4. Effect of Mn & Ca

Figure 23 compares the effect of Mn and Ca cations on the mass yield curves during torrefaction at 280 °C. The mass yield decreases from 75.1% for demineralized spruce to 71% for the same Mn doped spruce wood (20 µmol/g wood). In this regard, K doped spruce wood (31 µmol/g wood) results in 70.4% mass yield during the same torrefaction condition (section 3.5.2).

The lower level of Ca doping (62 µmol/g wood) seems to increase the mass yield, while at the highest level of Ca doping (115 µmol/g wood), the mass yield curve follows the raw spruce behavior, Figure 23. The differences between the mass yields are very small and could not be explained by the standard deviations of the repeated TGA tests (section 2.1.1). Therefore, the effect of Ca on torrefaction is not clear and needs further research.
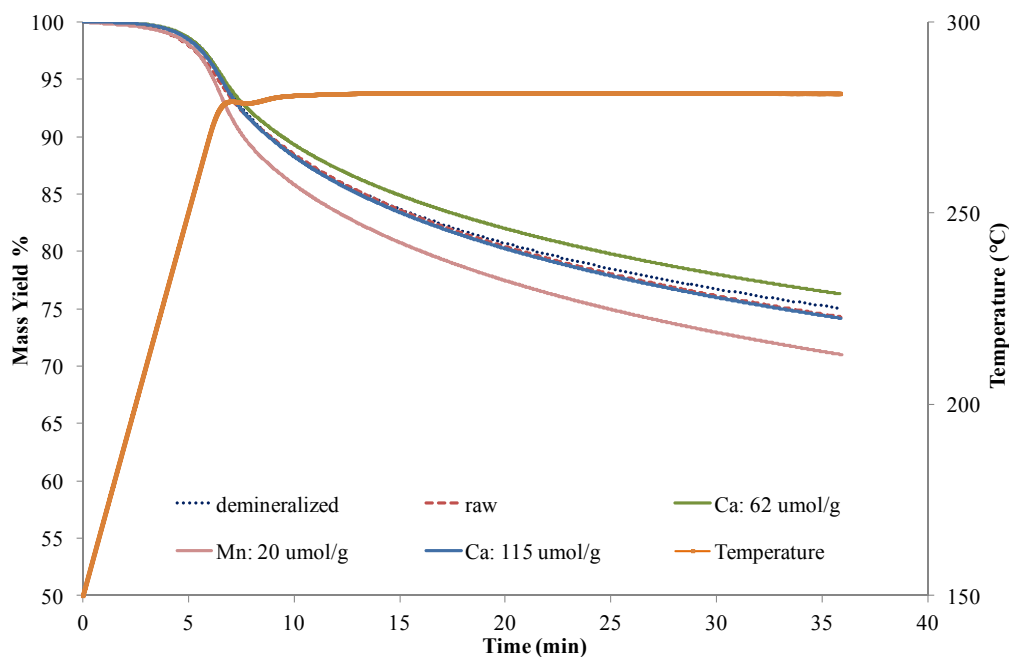

Figure 23. The effect of different cations on torrefaction of spruce at 280 °C. (data from paper IV)

Mn and Ca are both added as divalent cations to the doping solution; and thus they are both organically bonded divalent cations in this work; however, these results would indicate that Mn and Ca do not behave similarly during torrefaction. It has been found that Mg is

catalytically active during pyrolysis [150] while Ca is not [151]. Further research to understand the difference in behavior between cations, when they are divalent, is required.

3.5.5. Effect of Biomass Type

The mass yields of acid washed and raw spruce, aspen and miscanthus during torrefaction at 240 °C are shown in Figures 24. The higher mass loss for aspen and miscanthus compared to spruce can be attributed to a higher percentage of five-carbon sugars, which exists in aspen and miscanthus hemicelluloses. Five-carbon sugars start to decompose more, compared to six-carbon sugars during torrefaction [64].
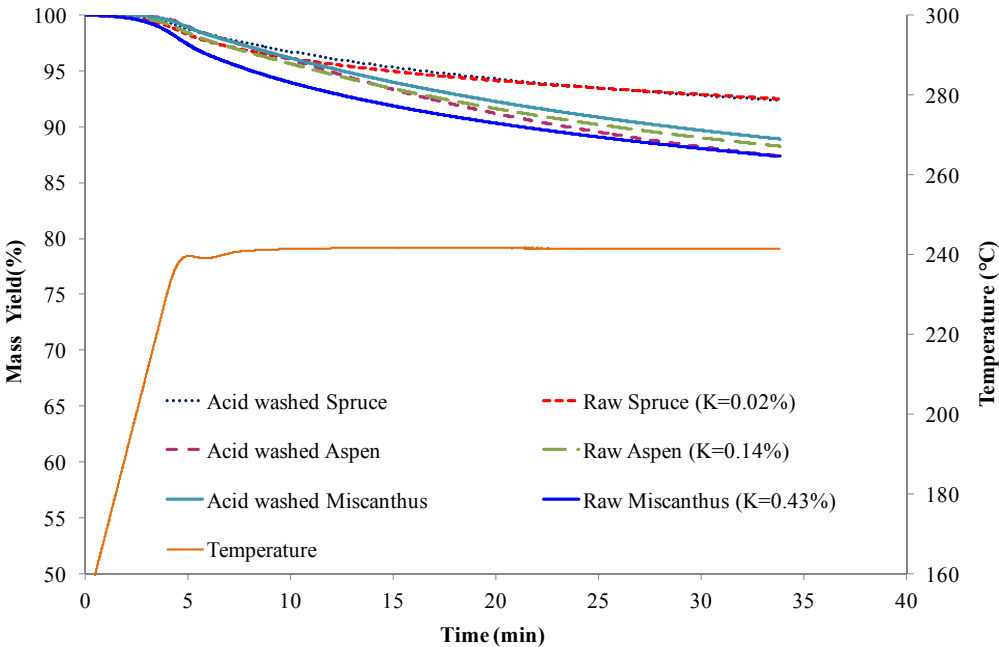

Figure 24. Mass yield curves of acid washed and raw spruce, aspen and miscanthus during torrefaction at 240°C (data from paper IV)

During torrefaction at 240 °C, the mass loss of raw spruce and aspen are quite the same as acid washed spruce and aspen; however, acid washed miscanthus has slightly lower mass loss compared to raw miscanthus, Figure 24. This could be attributed to higher content of K in raw miscanthus (K=0.43%) than raw spruce and aspen (K=0.02% and K=0.14%, respectively).

The mass loss of different biomass types doped with K is shown in Figure 25. The x-axis shows the weight percentage of K in biomass, and the y-axis shows the mass loss during

torrefaction. At 280 °C, the effect of K is more than the effect of biomass type on mass loss. This finding can help to predict the mass loss of different biomasses when the K content is known. An earlier work also showed similar trend between the mass loss and K content for different biomasses torrefied at 270 and 300 ˚C [58]. They also observed that after torrefaction at 270 ˚C for the concentration of K higher than 0.5 wt.%, the mass loss curve starts to level off. This is consistent with our results when the mass loss curve of all biomass types start to level off above 0.6 wt.% K.
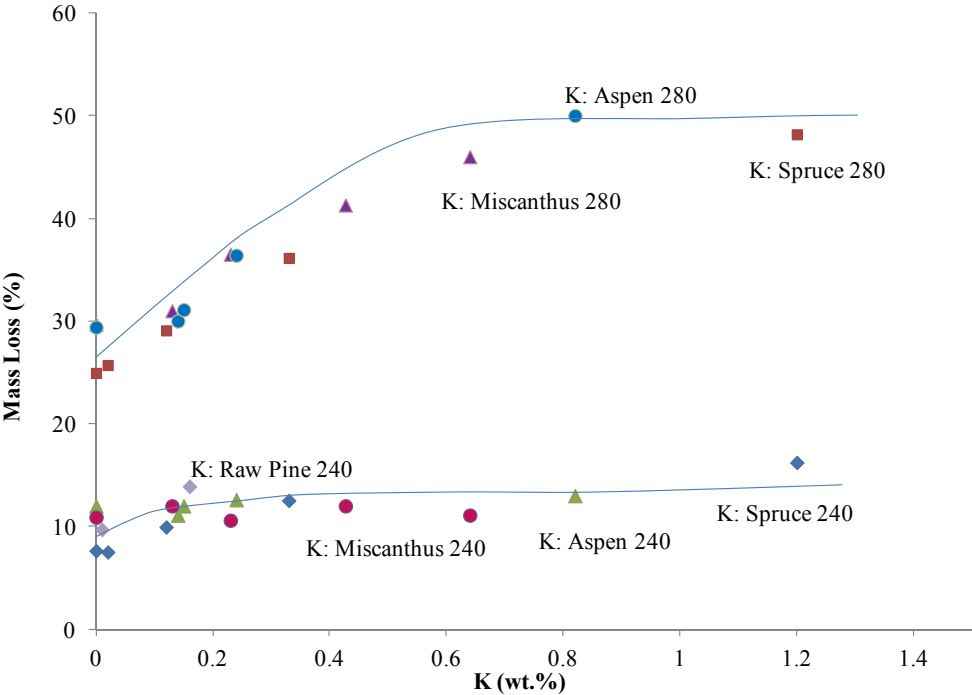

Figure 25. Effect of biomass type on mass loss during torrefaction at 240 and 280°C (Paper IV)

3.5.6. Effect of K on Spruce Components

Figure 26 shows the impact of 1.2 wt.% K (impregnated with K_2CO_3) on the wood components: cellulose, galactoglucomannan and lignin, during torrefaction at 280 °C. It is seen that the addition of K accelerates cellulose degradation mostly at the beginning of torrefaction meaning that the mechanism of cellulose degradation in the presence of K has

changed. The mass loss of cellulose after torrefaction at 280 °C increases from 8% to 55%. Earlier research [152] showed that the addition of K_2CO_3 to cellulose decreased the initial degradation temperature of cellulose from 315 to 200 °C during pyrolysis.

In the presence of K, galactoglucomannan degradation at the beginning of torrefaction occurs sooner, and the degradation rate is much higher. Its final mass loss increases from 51% to 72% during torrefaction at 280 °C.

The mass loss of both original lignin and the K_2CO_3 doped lignin are essentially the same during torrefaction at 280 °C. This is consistent with an earlier study [152] in which K did not result in any mass loss in lignin during mild pyrolysis. Thus, it can be concluded that the higher mass losses in the biomass samples doped with K and torrefied at 280 °C is due to both increased hemicellulose and cellulose decomposition.
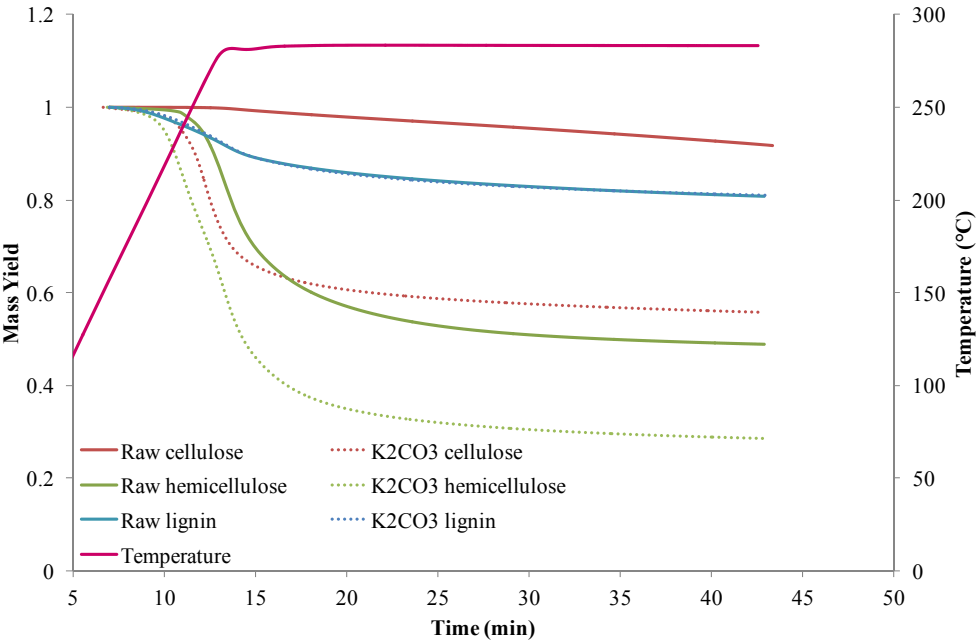

Figure 26. Effect of K-impregnation (1.2wt. %) on the wood components during torrefaction at 280 °C (data from paper IV)

The spruce wood used in this work contains 24% hemicellulose and 38% cellulose. The increase in mass loss of hemicellulose and cellulose in K-high spruce containing 1.2% K are predicted 5% and 18%, respectively, based on the results in Figure 26. The overall increase in

mass loss of K-high spruce would be 23%, which is in good agreement with 23% increase in the mass loss between acid washed and K-high spruce at 280 °C.

The thermal gravimetric curves for non-isothermal pyrolysis of the acid-washed and K-low spruce are given, Figure 27. As can be seen, at a temperature as low as 230 °C, the K-low spruce starts degradation which is presumeably due to degradation of hemicelluloses. The peak associated with cellulose degradation is higher and narrower for the acid washed spruce than the doped spruce. this is probably due to the lowering of the temperature at which cellulose starts to degrade.
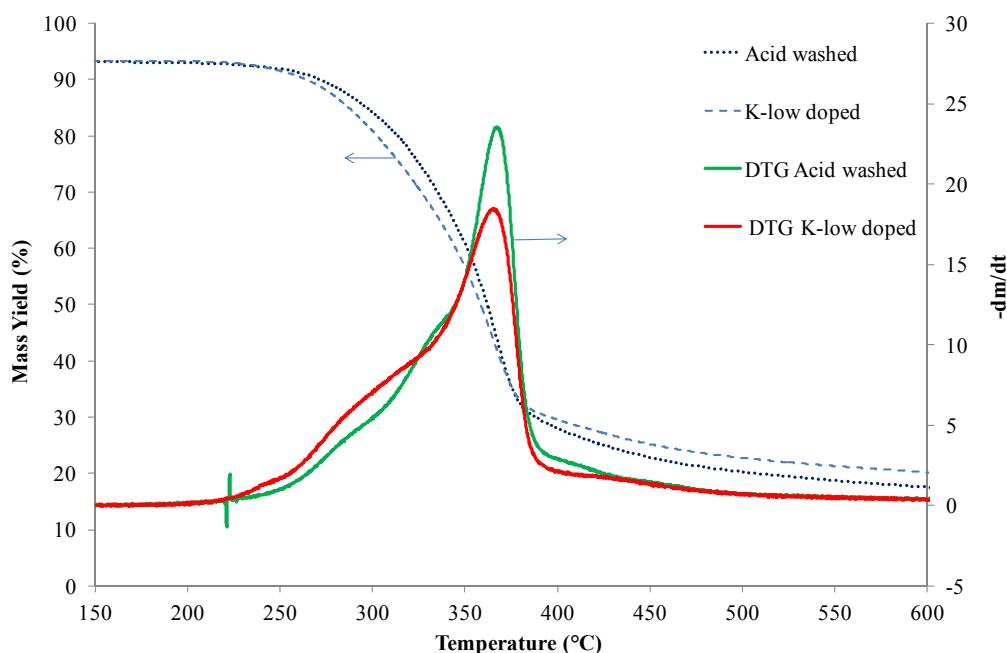

Figure 27. TG and DTG pyrolysis curves of acid washed and K-low doped spruce (Paper IV)

Additionally, the results in Figure 27, show that below 360 °C, the K-low spruce has a higher mass loss, whereas above this temperature the mass loss of K-low becomes less than the acid-washed spruce. A number of studies [79,82,153] have shown that K increases the char yield during pyrolysis at temperatures of 400 °C or higher. Our results indicate that the effect of K on increased char yield during pyrolysis happens at temperatures between 360 and 390 °C for non-isothermal pyrolysis. For isothermal pyrolysis, this transition point may occur between 300 and 350 °C [154].

3.6.   Effect of K on Torrefaction: Modeling

3.6.1. Torrefaction Kinetics of Spruce with Different K Content

The kinetic parameters for equation (6) to (8) were determined by torrefying the demineralized, raw and K doped spruce samples at 240, 250, 260, 270 and 280 °C in a TGA, Table 15. Figure 28 is an example of the good consistency between the modeled results and experimental data for the torrefaction of K-impregnated spruce at temperatures from 240 to 280 °C. The sum of the squares is 0.996 for the results shown in Figure 28.
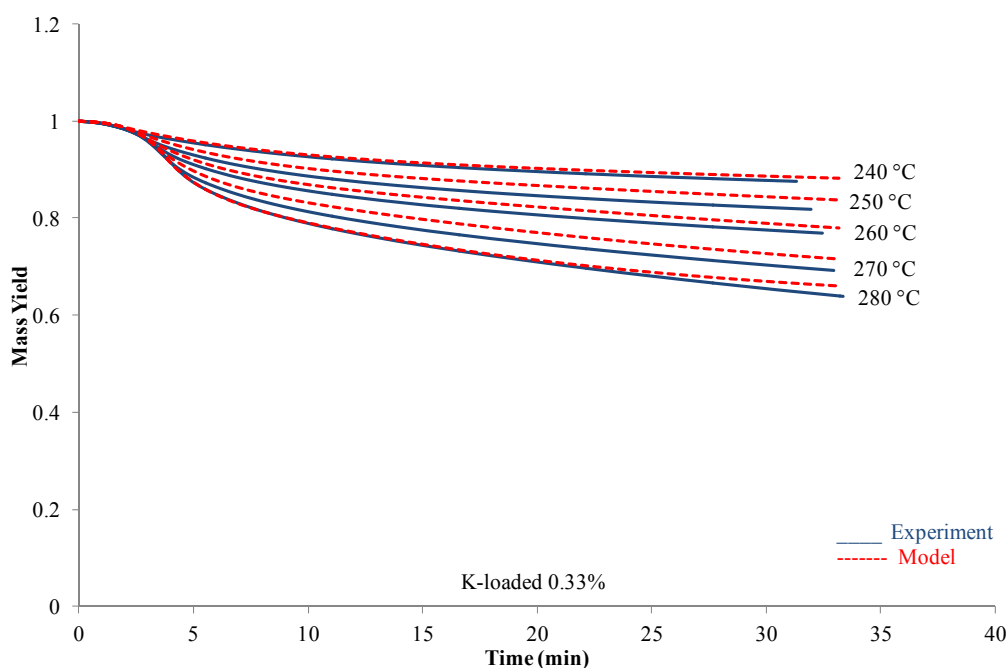

Figure 28. The experimental data and modeled results of the K-impregnated spruce at 240, 250, 260, 270 and 280 °C (R^2=0.996), t=0 corresponds to the time at which the temperature is 200 °C (Paper V)

The kinetic parameters of each five different spruce samples are shown in Table 15. It is seen that the sum of the squares vary between 0.988 and 0.998, and there is slightly better fit for the samples with a lower content of K than for those with the highest content of K. The kinetic parameters in Table 15 also show that there is a reasonable agreement between our results for spruce and an earlier study by Prins et al. [19] for the torrefaction of willows.

3.6.2. Unified Torrefaction Kinetic Model for Spruce

The results in Table 15 show that for the different contents of K in spruce wood, the values for the activation energies of each of the reaction steps are relatively close to each other, while the values of pre-exponential factors vary significantly. An earlier study [155] showed that the determination of activation energies at high temperatures contains a vast uncertainty, and thus in this work, it is reasonable to unify these relatively close activation energies by averaging them. These averaged activation energies are used to determine the new pre-exponential factors (A), Table 16.

Table 15. kinetic parameters obtained by fitting the experimental data of K-contained spruce at 240, 260, 250, 270 and 280 °C torrefaction (E_a is the activation energies and A is the pre-exponential factors) (Paper V)

Spruce	Kinetics constants (units)	Reaction $B \rightarrow C$	Reaction $C \rightarrow D$	Reaction $C \rightarrow V_1$	Reaction $D \rightarrow V_2$	R^2
Acid washed	E_a (kJ/mol)	67	152	131	139	0.996
	A (s^{-1})	2.15×10^4	3.44×10^{11}	4.84×10^9	6.08×10^9	
K: 0.12 wt.%	E_a (kJ/mol)	72	144	114	159	0.998
	A (s^{-1})	3.74×10^4	3.58×10^{10}	1.15×10^8	4.99×10^{11}	
K: 0.33 wt.%	E_a (kJ/mol)	75	214	136	91.7	0.996
	A (s^{-1})	1.02×10^5	3.80×10^3	2.57×10^{10}	1.38×10^5	
K: 0.60 wt.%	E_a (kJ/mol)	73	167	110	147	0.996
	A (s^{-1})	6.97×10^4	1.38×10^{10}	8.60×10^7	4.30×10^{10}	
K: 1.20 wt.%	E_a (kJ/mol)	71	145	113	150	0.988
	A (s^{-1})	8.54×10^4	3.18×10^{10}	3.16×10^8	1.69×10^{11}	

Table 16. Determined new pre-exponential factors as a function of potassium content assuming the mean activation energies of Table 15 (Paper V)

Spruce	Kinetics constants (units)	Reaction $B \rightarrow C$	Reaction $C \rightarrow D$	Reaction $B \rightarrow V_1$	Reaction $C \rightarrow V_2$	R^2
	$\bar{E}_a$ (kJ/mol)	72	164	121	137	
Acid washed	A (s⁻¹)	3.87×10^4	3.00×10^{12}	4.19×10^8	2.92×10^9	0.996
K: 0.12 wt.%	A (s⁻¹)	3.81×10^4	2.21×10^{12}	5.48×10^8	3.11×10^9	0.999
K: 0.33 wt.%	A (s⁻¹)	5.94×10^4	2.91×10^{12}	9.76×10^8	5.56×10^9	0.995
K: 0.6 wt.%	A (s⁻¹)	6.53×10^4	5.92×10^{11}	1.34×10^9	5.76×10^9	0.996
K: 1.2 wt.%	A (s⁻¹)	8.46×10^4	4.63×10^9	1.73×10^9	7.44×10^9	0.986

The new pre-exponential factors are then modeled as a linear function of K content which can be expressed as follows:

Reaction B→C: $A_B = 4.0 \times 10^4 \times [K] + 3.9 \times 10^4$ equation (13a)

Reaction C→D: $A_C = -3 \times 10^{12} \times [K] + 3 \times 10^{12}$ equation (13b)

Reaction B→V₁: $A_{V1} = 1 \times 10^9 \times [K] + 5 \times 10^8$ equation (13c)

Reaction C→V₂: $A_{v2} = 4 \times 10^9 \times [K] + 3 \times 10^9$ equation (13d)

where pre-exponential factor A is (s⁻¹) and potassium content $[K]$ is (wt.%).

The pre-exponential factors' equations show that for reactions B→V₁ and C→V₂, increasing the K content leads to the formation of higher amounts of volatiles This is consistent with earlier studies in which CO, CO_2 and water productions increased in the presence of K in experiments above 250 ˚C [154].

The averaged activation energies in Table 16 and equations (13a-13d) are used to model the mass loss for the spruce wood samples doped with different levels of K. The resulted R^2 from

the unified model, varying between 0.986 and 0.997, shows the reasonable accuracy of the model.

3.6.3. Validating the Torrefaction Kinetic Model for Some Other Biomasses

The model developed with the spruce wood results is applied to raw and K-high aspen, raw and K-high miscanthus, raw straw and bark, Figure 29 a-e.

Figure 29a shows that the final mass yields of both the experiment and model are about 0.88 and 0.68 for raw aspen torrefied at 240 and 280 °C, respectively, with a minimum least square of 99% for the full mass loss curve. However, Figure 29b for K-loaded aspen (0.82 wt.% K) shows a small difference between the mass yields of model and experiments. It is seen that the model predicts more decomposition, particularly at the beginning of torrefaction.

The results for raw miscanthus show a good agreement between model and experiment at 240 °C; however, for the experimental data at 280 °C, the mass loss is about 4% higher than predicted by the model. Like aspen, mass loss is over-predicted by model for K-loaded miscanthus; however, overall degree of explanation is still quite good with a minimum least square of 96.7%.

Raw straw, with a higher content of K compared to other raw biomasses in this work shows relatively a good agreement between the modeled results and experimental data, Figure 29e. The difference between the modeled and experimental mass yields after torrefaction at 240 and 280 °C is about 2% and 7% respectively, with the minimum least square of 98%.
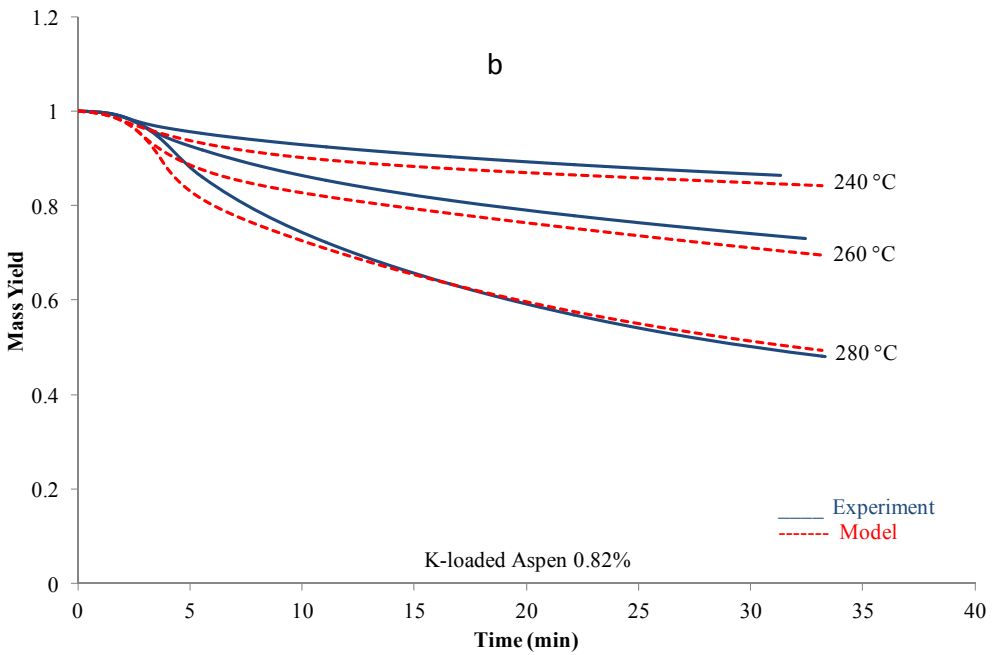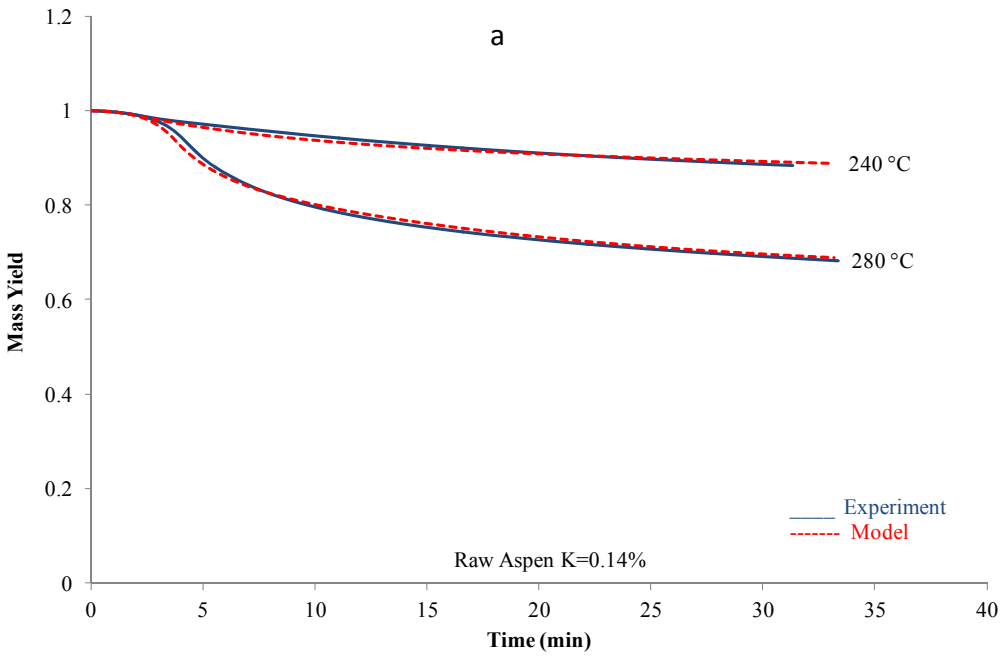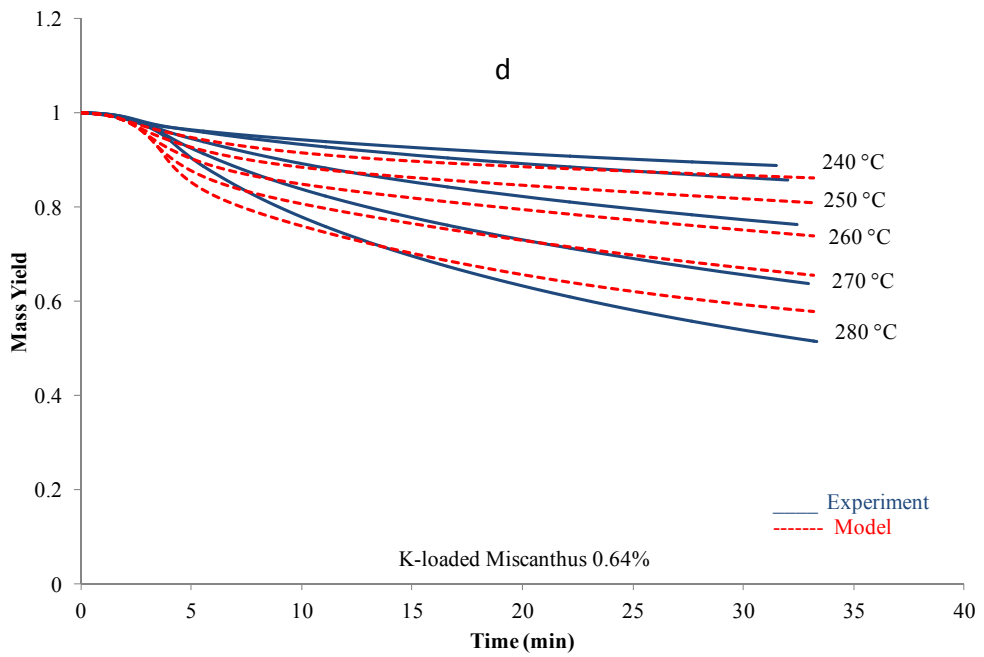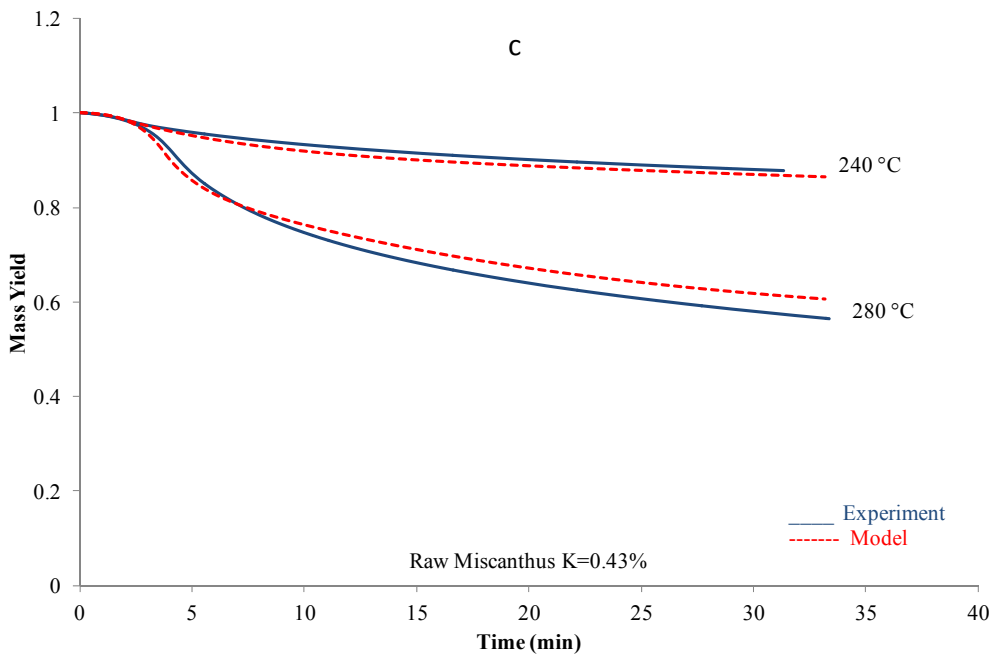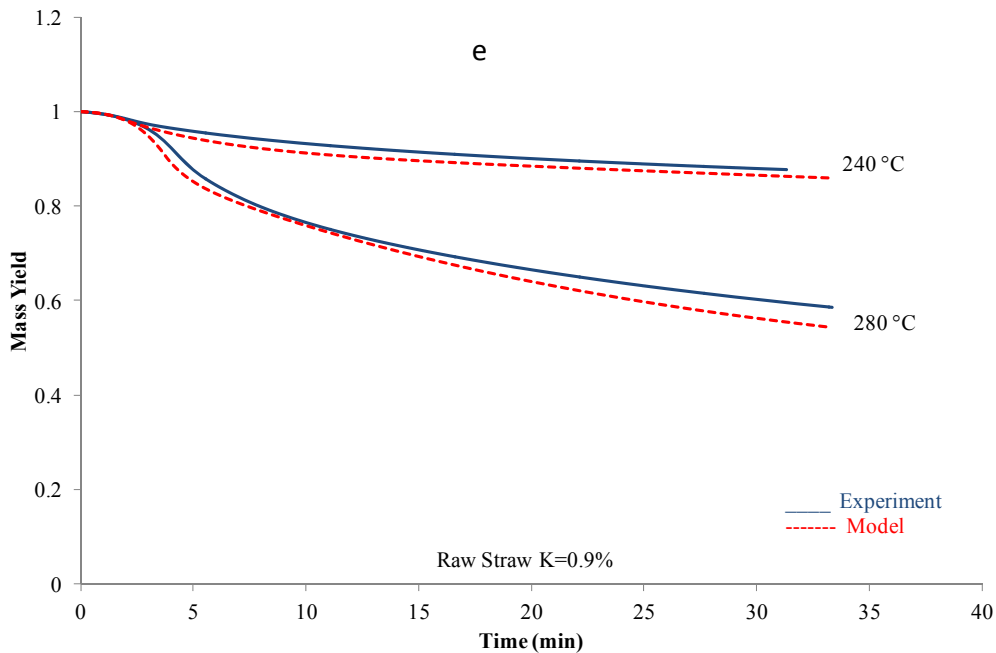
Figure 29. experimental data and modeled results of

a) Raw aspen, K=0.14%. R^2:0.994   b) K-high aspen, K=0.82 %. R^2:0.979
c) Raw miscanthus, K=0.43 %. R^2:0.982   d) K-high miscanthus, K=0.64 %. R^2:0.967
e) Raw straw, K=0.90%, R^2:0.982 (Paper V)

Figure 30a shows the mass yield curves of raw and K-high miscanthus at 240 and 280 °C. At 240 °C, the K has no clear effect on mass yield during torrefaction. At 280 °C, the raw miscanthus at the beginning of torrefaction has higher degradation than the K loaded biomass, while the final mass loss for the K-high miscanthus is higher. This is due to K affecting the secondary volatile formation. This is different from spruce wood where K had more of an impact on the early volatiles formation. Therefore, further work is required if the kinetic parameters of this model are also determined based on a hardwood and then the difference between them would be investigated.
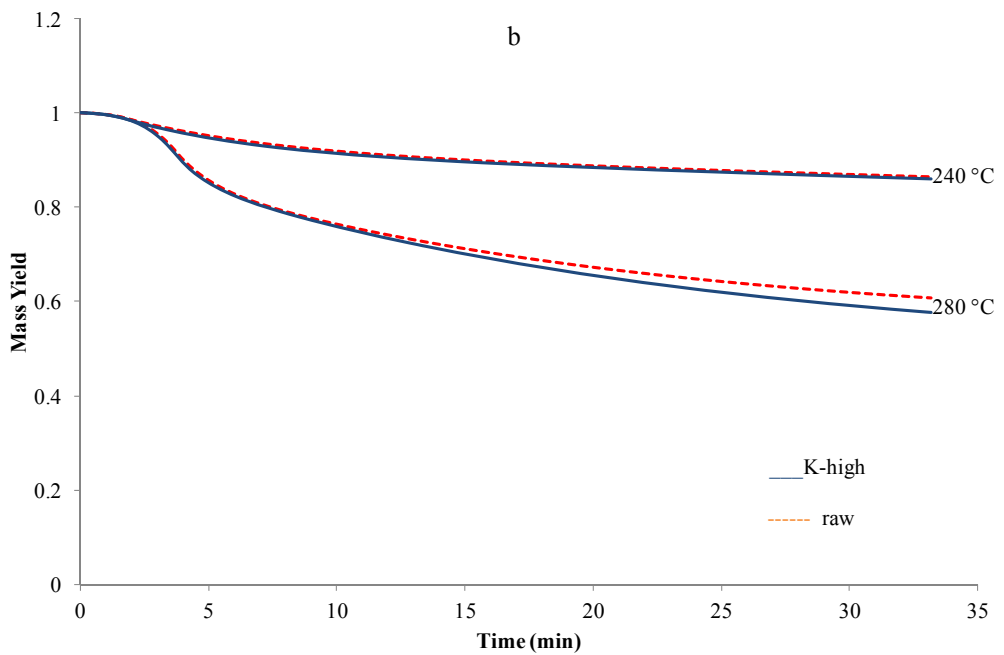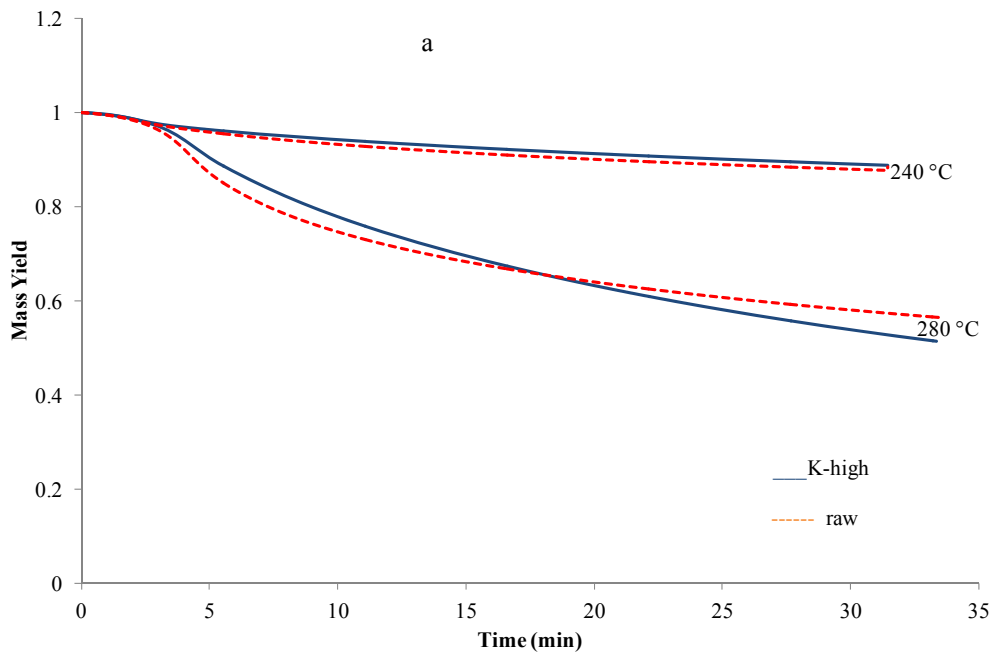
Figure 30. Mass Yield of raw (K=0.43 wt.%) and K-high (K=0.64 wt.%) miscanthus during torrefaction a) Experimental results b) Modeled data (Paper V)

The fact that the highest levels of K seem to result in some delay in the onset of mass loss for miscanthus and aspen compared to spruce is probably due to a difference in the form of the hemicelluloses. The model is obtained from spruce containing mainly six-carbon sugars in the hemicelluloses. Aspen and miscanthus mainly contain xylan, a five-carbon sugars. This probably results in a different mechanism for the degradation and cracking of the hemicelluloses in the presence of high content of K. At K levels seen in the raw miscanthus, the final mass loss appears to behave similarly for spruce, aspen and miscanthus.

Interestingly, for straw, which contained more K than the doped miscanthus or the doped aspen, there is a better agreement between the model and experimental data throughout the full mass yield curve. There does appear to be some delay in the onset of decomposition in comparing the experimental and modeling, but it is much smaller than for the doped miscanthus or the doped aspen.

Figure 31a shows the comparison between the modeled results and experimental data for raw bark when the reactive biomass is considered the sum of hemicellulose and cellulose. In Figure 31b, the model uses the sum of hemicellulose, cellulose and extractives. The measured mass loss for the raw bark is significantly higher than that calculated by the model when using only hemicellulose and cellulose at both 240 and 280 °C (R^2= 0.94), Figure 31a. There is a good agreement between the model and experiment at both 240 and 280 °C (R^2= 0.96) if the acetone extractable material is also considered as part of the reactive fraction, Figure 31b. This is due to the relatively high content of tannins and other compounds found in bark (ex. Krogell et al. [156]) that are reactive and at least partially volatile at torrefaction temperatures. The fate of the acetone extractable material during torrefaction is complicated [64]. Some components are volatilized during torrefaction, while the decomposition of hemicellulose, cellulose and lignin forms the new acetone extractable material. The decomposition of acetone extractable material is clearly required for the modeling of bark. As a first approximation, it seems it can simply be included as part of the reactive components in the model developed in this work.
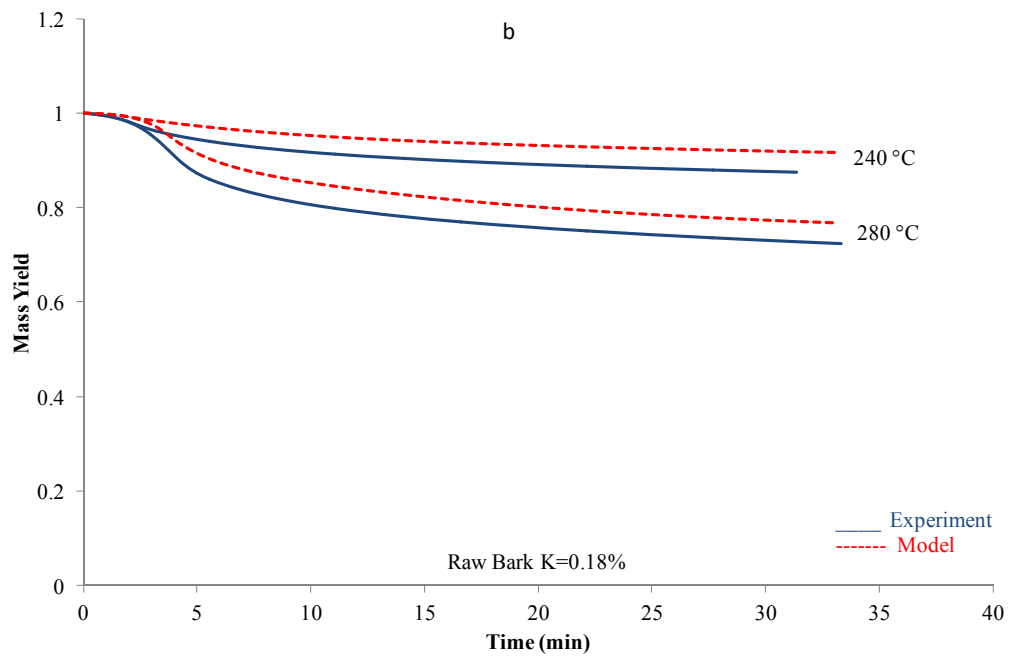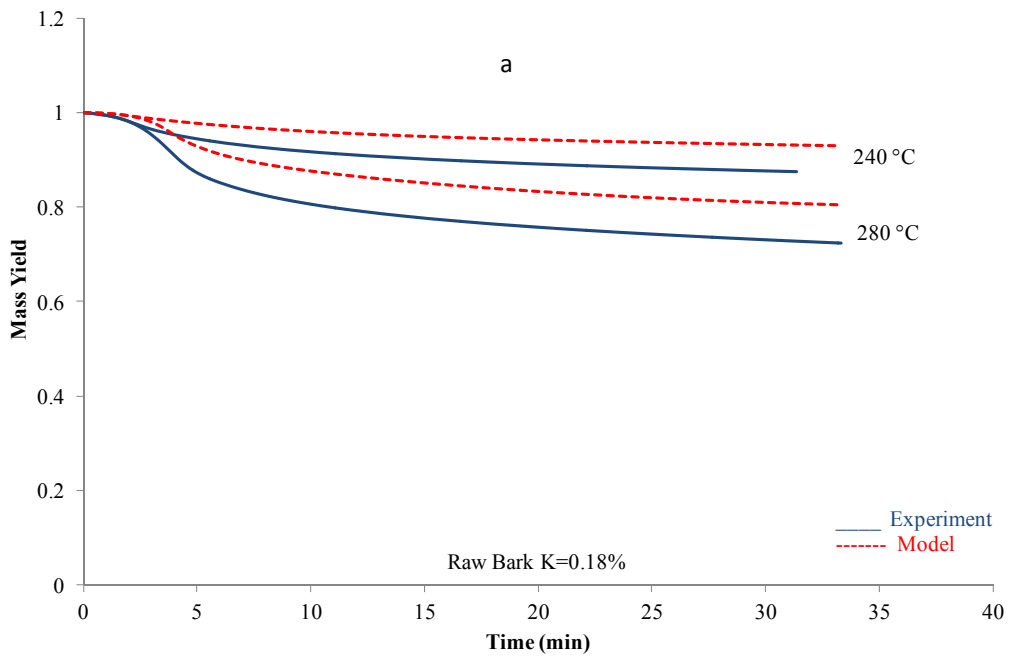
Figure 31. Comparison between the experimental results and modeled data of bark (K=0.18 wt.%) where the reactive biomass is considered as: a) sum of hemicellulose and cellulose b) sum of hemicellulose, cellulose and extractives (Paper V)

Conclusion

Torrefaction is a technology that is trying to emerge as a means of providing a higher grade biomass fuel for use in combustion systems. This work is a study of the chemical changes in biomass during torrefaction. A more complete understanding of the chemical changes in biomass can be used by industry to choose operational conditions. Changes in the organic biomass components as well as changes in the chemical association of ash-forming matters are investigated. Additionally, the effect of alkali metals – with a focus on K – are studied experimentally and the mass loss is modeled. The dependence of the kinetic parameters on the concentration of K is determined.

Carboxylic groups degrade during torrefaction, which appears to result in a decrease in the hydrophilic characteristic of the biomass. This can be seen in the decrease in equilibrium moisture content that follows the decrease in carboxylic groups with increasing torrefaction temperature. It is worth noting that even after torrefaction at elevated temperatures, when almost all the carboxylic groups are degraded, torrefied biomass still absorbs moisture. This could be due to presence of hydroxyl groups in the phenolic structure of lignin units and/or the absorption of non-bonded water to the matrix of torrefied biomass. This provides some understanding of the relationship between torrefaction temperature and the resultant equilibrium moisture content. This is useful since reduced equilibrium moisture content is one benefit of torrefaction.

Hemicellulose degrades significantly at low torrefaction temperatures while cellulose degradation is significant at high torrefaction temperatures at or above about 270 °C. During hemicellulose degradation, the five-carbon sugars in biomass decompose more at the lower torrefaction temperature than the six-carbon sugars. A part of the hemicellulose and cellulose degradation results in char formation during torrefaction as well as the formation of extractives and volatiles. Only a small amount of mass is lost during torrefaction due to lignin degradation. One of the main decomposition reactions of lignin during torrefaction is the dissociation of methoxyl groups from lignin. This may be important to Cl and S release as the methoxyl groups can react to form volatile compounds containing Cl and S. Some extractable compounds are also formed from lignin degradation.

Some acetone extractable materials are released or degraded, while some others are produced during torrefaction. The final molar mass distribution of the acetone extractable materials becomes narrower and the average molar mass is lowered by increasing the torrefaction temperature. Production of some extractable materials can be interesting from a biorefinery perspective, but lower temperatures than those studied in this work are probably desired.

This study provides new data on the changes in the association of ash-forming elements in birch wood during torrefaction. These results show that the metals are not released during torrefaction. A significant fraction of the elements including calcium, magnesium, manganese and phosphorous is shifted from being ammonium acetate soluble to being acid soluble especially after torrefaction at 280 °C. Analysis of the phosphate anion indicates that this does not explain the reaction of water soluble phosphates to form acid soluble compounds. Instead, other phosphorous compounds appear to form acid soluble phosphorous.

The concentration of chlorine and sulfur decreases during torrefaction. This study shows that chlorine and sulfur are released up to 80% and 65%, respectively, during torrefaction of birch at 280°C. Sulfur and chlorine in fuel result in corrosion and emissions. Therefore, the release of sulfur and chlorine is an additional benefit to the usage of torrefied biomass as a fuel, particularly for lower grade biomasses such as agricultural residues.

The metals K, Na and to a lesser extent Mn have a catalytic effect on the decomposition of biomass during torrefaction, while Ca does not. The mass loss at a given temperature increases with increasing K or Na concentration. This effect is more pronounced at higher torrefaction temperatures. The presence of these elements appears to affect both hemicellulose and cellulose decomposition. At lower temperatures, the effect is probably mostly on hemicellulose decomposition. But as the temperature increases, the contribution of cellulose decomposition increases. For K, there appears to be an upper limit where increasing the K content results in little to no increase in mass loss. In this work, that level is about 0.6 wt% K on a dry biomass basis. The practical impact is that if a plant shifts from a low K biomass feedstock to a higher one, the torrefaction temperature or time can be decreased.

A two-step reaction model is applied to describe the kinetics of torrefaction. The kinetic parameters are determined for spruce wood doped with different levels of K assuming carbohydrates as the reactive fraction during torrefaction. The focus is on K because along with Ca, it tends to be the main inorganic element in biomass. The model is successfully

applied to both raw and doped samples of aspen, miscanthus and straw. For biomasses containing more xylan and a higher content of K, the mechanism of degradation and cracking early in the torrefaction is slightly different from the spruce, which contains more galactoglucomannan.

Bark has a comparatively high concentration of extractives, which are to some extent volatile. This is not accounted for in this model, although some might react and degrade during torrefaction. Therefore, for spruce bark, when the extractives are considered as part of the reactive fraction along with hemicellulose and cellulose, the model gives reasonable results for the mass loss. Overall, the model can predict the mass loss during torrefaction for different types of biomasses. This is important for designing future reactors, which will likely be designed to be fuel flexible.

This work has provided new information about the chemical changes of biomass during torrefaction, which can help to adjust the operating conditions to achieve the optimum conditions in the torrefaction reactors. Additionally, the better understanding of the torrefaction mechanism is beneficial for designing and operating future torrefaction reactors used to process different types of biomass. There are still plenty of interesting questions to be studied.

Additional work should be carried out to determine the impact of torrefaction at different reaction times and temperatures on the fate of carboxylic sites of different biomass feedstock. This combined with Equilibrium Moisture Content (EMC) work could clarify the observation in this work that EMC seems to follow the fate of the carboxylic acid sites well.

Changes in the chemistry of hemicellulose, cellulose, lignin and acetone extractable materials in biomass can likely explain its grindability and pellet production characteristic. Linking chemical changes to these physio-chemical properties would be an important topic for future work.

The content of soluble Ca, Mg and Mn in water and ammonium acetate shifts to acid and non-soluble matters with increasing torrefaction temperature. This transformation cannot be explained by the formation of Ca, Mg and Mn carbonates. Thus, further studies are required to clarify the decrease in water and ammonium acetate soluble Ca, Mg and Mn and increase in the acid and non-soluble Ca, Mg and Mn. This might help to predict the mechanism of

alkaline earth metals during torrefaction, because for instance, Ca is nonreactive or Mn is reactive during torrefaction.

The effect of alkali and alkaline earth metals are studied; however, further work is needed to clarify the chemistry behind the observed changes in decomposition in presence of these metals. It would be beneficial if the effect of these metals on a larger particle size and pilot scale reactors is investigated when using the new conditions to do the modeling. It would be valuable if the kinetic parameters from a hardwood or herbaceous biomass are also determined to compare them with the spruce results. It makes sense to have a different model for hardwood and/or herbaceous biomass, even if the spruce model works reasonably well.

Bark has a comparatively high concentration of extractives, which are to some extent volatile. This is not accounted for in this model. More work would be needed to clarify the fate of extractives to extend the model to biomasses with high extractive content.

References

[1] Almeida G, Brito JO, Perre P. Changes in wood-water relationship due to heat treatment assessed on micro-samples of three Eucalyptus species. Holzforschung 2009;63:80-8.

[2] Chaouch M, Petrissans M, Petrissans A, Gerardin P. Use of wood elemental composition to predict heat treatment intensity and decay resistance of different softwood and hardwood species. Polym Degrad Stab 2010;95:2255-9.

[3] Arias B, Pevida C, Fermoso J, Plaza MG, Rubiera F, Pis JJ. Influence of torrefaction on the grindability and reactivity of woody biomass. Fuel Process Technol 2008;89:169-75.

[4] Shafizadeh F. Thermal conversion of cellulosic materials to fuel and chemicals. Wood Agric Residues: Res Use Feed, Fuels, Chem , Proc Conf Feed, Fuels, Chem , Wood Agric Residues 1983:415-38.

[5] Bridgeman TG, Jones JM, Shield I, Williams PT. Torrefaction of reed canary grass, wheat straw and willow to enhance solid fuel qualities and combustion properties. Fuel 2008;87:844-56.

[6] Zevenhoven M, Yrjas P, Skrifvars B, Hupa M. Characterization of ash-forming matter in various solid fuels by selective leaching and its implications for fluidized-bed combustion. Energy Fuels 2012;26:6366-86.

[7] Bourgeois J, Doat J, Egnéus H, Ellegård A. Torrefied wood from temperate and tropical species. Advantages and prospects. Bioenergy 84. 1984:153-9.

[8] Lipinsky ES, Arcate JR, Reed TB. Enhanced wood fuels via torrefaction. Prepr Symp - Am Chem Soc , Div Fuel Chem 2002;47:408-10.

[9] Felfli FF, Luengo CA, Suárez JA, Beatón PA. Wood briquette torrefaction. Energy for Sustainable Development 2005;9:19-22.

[10] Ben H, Ragauskas AJ. Torrefaction of Loblolly pine. Green Chem 2012;14:72-6.

[11] Grigiante M, Antolini D. Experimental Results of Mass and Energy Yield Referred to Different Torrefaction Pathways. Waste and Biomass Valorization 2014;5:11-7.

[12] Bergman P, Boersma A, Zwart R, Kiel J. Torrefaction for biomass co-firing in existing coal-fired power stations. Energy Research Centre of the Netherlands, ECN-C--05-013 2005:1-71.

[13] Tumuluru JS, Sokhansanj S, Wright CT, Hess JR, Boardman RD. A review on biomass torrefaction process and product properties. Industrial Biotechnology 2011;7:384-401.

[14] Agar D, Wihersaari M. Bio-coal, torrefied lignocellulosic resources–Key properties for its use in co-firing with fossil coal–Their status. Biomass Bioenergy 2012;44:107-11.

[15] Vasquez V, Coronella C. A simple model for vapor-moisture equilibrium in biomass subtrates. AIChE J 2009;55:1595-603.

[16] Medic D, Darr M, Shah A, Rahn S. Effect of torrefaction on water vapor adsorption properties and resistance to microbial degradation of corn stover. Energy Fuels 2012;26:2386-93.

[17] Li H, Liu X, Legros R, Bi XT, Lim CJ, Sokhansanj S. Pelletization of torrefied sawdust and properties of torrefied pellets. Appl Energy 2012;93:680-5.

[18] Björk H, Rasmuson A. Moisture equilibrium of wood and bark chips in superheated steam. Fuel 1995;74:1887-90.

[19] Prins MJ, Ptasinski KJ, Janssen FJJG. Torrefaction of wood: Part 1. Weight loss kinetics. J Anal Appl Pyrolysis 2006;77:28-34.

[20] Repellin V, Govin A, Rolland M, Guyonnet R. Modelling anhydrous weight loss of wood chips during torrefaction in a pilot kiln. Biomass Bioenergy 2010;34:602-9.

[21] Phanphanich M, Mani S. Impact of torrefaction on the grindability and fuel characteristics of forest biomass. Bioresour Technol 2011;102:1246-53.

[22] Shang L, Ahrenfeldt J, Holm JK, et al. Changes of chemical and mechanical behavior of torrefied wheat straw. Biomass Bioenergy 2012;40:63-70.

[23] Wu K, Tsai C, Chen C, Chen H. The characteristics of torrefied microalgae. Appl Energy 2012;100:52-7.

[24] Bergman PCA, Kiel JHA. Torrefaction for biomass upgrading. Energy Research Centre of the Netherlands, ECN-RX--05-180 2005:1-8.

[25] Deng J, Wang G, Kuang J, Zhang Y, Luo Y. Pretreatment of agricultural residues for co-gasification via torrefaction. J Anal Appl Pyrolysis 2009;86:331-7.

[26] Bridgeman T, Jones J, Williams A, Waldron D. An investigation of the grindability of two torrefied energy crops. Fuel 2010;89:3911-8.

[27] Stamm AJ. Thermal degradation of wood and cellulose. Industrial & Engineering Chemistry 1956;48:413-7.

[28] Kamdem D, Pizzi A, Jermannaud A. Durability of heat-treated wood. Holz als Roh-und Werkstoff 2002;60:1-6.

[29] Kamdem DP, Pizzi A, Triboulot MC. Heat-treated timber: potentially toxic byproducts presence and extent of wood cell wall degradation. Holz als Roh-und Werkstoff 2000;58:253-7.

[30] Hakkou M, Petrissans M, Gerardin P, Zoulalian A. Investigations of the reasons for fungal durability of heat-treated beech wood. Polym Degrad Stab 2005;91:393-7.

[31] Weiland J, Guyonnet R. Study of chemical modifications and fungi degradation of thermally modified wood using DRIFT spectroscopy. Holz als Roh-und Werkstoff 2003;61:216-20.

[32] Li J, Brzdekiewicz A, Yang W, Blasiak W. Co-firing based on biomass torrefaction in a pulverized coal boiler with aim of 100% fuel switching. Appl Energy 2012;99:344-54.

[33] Alobaid F, Busch J, Ströhle J, Epple B. Investigations on torrefied biomass for co-combustion in pulverized coal-fired furnaces. VGB powertech 2012:50-4.

[34] Clausen LR, Elmegaard B, Houbak N. Technoeconomic analysis of a low CO_2 emission dimethyl ether (DME) plant based on gasification of torrefied biomass. Energy 2010;35:4831-42.

[35] Wilén C, Jukola P, Järvinen T, Sipilä K, Verhoeff F, Kiel J. Wood torrefaction–pilot tests and utilisation prospects. Espoo, VTT technology report 2013;122:73.

[36] Prins MJ, Ptasinski KJ, Janssen FJJG. More efficient biomass gasification via torrefaction. Energy 2006;31:3458-70.

[37] Bergman PC, Boersma AR, Kiel JH, Prins MJ, Ptasinski KJ, Janssen F. Torrefaction for entrained-flow gasification of biomass. Energy Research Centre of the Netherlands, ECN-C-05-067 2005:1-50.

[38] Khazraie Shoulaifar T, DeMartini N, Zevenhoven M, Verhoeff F, Kiel J, Hupa M. Ash-Forming Matter in Torrefied Birch Wood: Changes in Chemical Association. Energy Fuels 2013;27:5684-90.

[39] Kannan M, Richards G. Potassium catalysis in air gasification of cellulosic chars. Fuel 1990;69:999-1006.

[40] Zheng A, Zhao Z, Chang S, et al. Effect of torrefaction on structure and fast pyrolysis behavior of corncobs. Bioresour Technol 2013;128:370-7.

[41] Gilbert P, Ryu C, Sharifi V, Swithenbank J. Effect of process parameters on pelletisation of herbaceous crops. Fuel 2009;88:1491-7.

[42] Stelte W, Clemons C, Holm JK, et al. Pelletizing properties of torrefied spruce. Biomass Bioenergy 2011;35:4690-8.

[43] Mišljenović N, Bach Q, Tran K, Salas-Bringas C, Skreiberg Ø. Torrefaction influence on pelletability and pellet quality of Norwegian forest residues. Energy Fuels 2014;28:2554-61.

[44] Uslu A, Faaij AP, Bergman P. Pre-treatment technologies, and their effect on international bioenergy supply chain logistics. Techno-economic evaluation of torrefaction, fast pyrolysis and pelletisation. Energy 2008;33:1206-23.

[45] Bergman PCA. Combined torrefaction and pelletisation: The TOP process. Energy Research Center of the Netherlands, ECN-C-05-073 2005:1-29.

[46] Du S, Chen W, Lucas JA. Pretreatment of biomass by torrefaction and carbonization for coal blend used in pulverized coal injection. Bioresour Technol 2014;161:333-9.

[47] Chen W, Du S, Tsai C, Wang Z. Torrefied biomasses in a drop tube furnace to evaluate their utility in blast furnaces. Bioresour Technol 2012;111:433-8.

[48] Acharya B, Sule I, Dutta A. A review on advances of torrefaction technologies for biomass processing. Biomass Conversion and Biorefinery 2012;2:349-69.

[49] Amos WA. Report on biomass drying technology; National Renewable Energy Laboratory NREL/TP-570-25885 1998:1-35.

[50] Koppejan J, Sokhansanj S, Melin S, Madrali S. Status overview of torrefaction technologies. 2012;32:1-54.

[51] Eyre A. Torrefaction demonstration plants. WPAC Conference, AGM Quebec City 2012;2015:27.

[52] van der Berg P. Topell on torrefaction. 2012:1-9. http://www.bioenergytrade.org/downlaods/topell.pdf

[53] Ratte J, Fardet E, Mateos D, Héry J. Mathematical modelling of a continuous biomass torrefaction reactor: TORSPYD™ column. Biomass Bioenergy 2011;35:3481-95.

[54] Mateos D. TORSPYD torrefaction by depolymerization. IEA Bioenergy Task 32 2012.

[55] Ren S, Lei H, Wang L, et al. Microwave torrefaction of Douglas Fir sawdust pellets. Energy Fuels 2012;26:5936-43.

[56] Kleinschmidt C. Overview of international developments in torrefaction; Central European Biomass Conference, 26-28 January, Graz, Austria 2011;1-16 http://www.ieabcc.nl/workshops/task32_2011_graz_torrefaction/Kleindschmidt_Paper.pdf

[57] Fengel D, Wegener G. Chemical composition and analysis of wood. In: Anonymous Wood: chemistry, ultrastructure, reactions. : Walter de Gruyter, 1984:26-65.

[58] Saleh SB, Hansen BB, Jensen PA, Dam-Johansen K. Influence of biomass chemical properties on torrefaction characteristics. Energy Fuels 2013;27:7541-8.

[59] Alen R. Structure and chemical composition of wood. In: Stenius P, editor. Forest products chemistry. 2000:350.

[60] Sjöström E. Wood chemistry: fundamentals and applications. Elsevier, 1993.

[61] Fengel D, Wegener G. Polyoses (Hemicellulose). In: Wood: chemistry, ultrastructure, reactions : Walter de Gruyter, 1984:106-131.

[62] Willför S, Pranovich A, Tamminen T, et al. Carbohydrate analysis of plant materials with uronic acid-containing polysaccharides–a comparison between different hydrolysis and subsequent chromatographic analytical techniques. Industrial Crops and Products 2009;29:571-80.

[63] Gaur S, Reed TB. Thermal data for natural and synthetic fuels. : CRC Press, 1998.

[64] Khazraie Shoulaifar T, DeMartini N, Willför S, et al. Impact of Torrefaction on the Chemical Structure of Birch Wood. Energy Fuels 2014;28:3863-72.

[65] Prins MJ, Ptasinski KJ, Janssen FJJG. Torrefaction of wood Part 2. Analysis of products. J Anal Appl Pyrolysis 2006;77:35-40.

[66] Lv P, Almeida G, Perré P. TGA-FTIR Analysis of Torrefaction of Lignocellulosic Components (cellulose, xylan, lignin) in Isothermal Conditions over a Wide Range of Time Durations. BioResources 2015;10:4239-51.

[67] Schafer HNS. Pyrolysis of brown coals. 1. Decomposition of acid groups in coals containing carboxyl groups in the acid and cation forms. Fuel 1979;58:667-72.

[68] Shafizadeh F. Introduction to pyrolysis of biomass. J Anal Appl Pyrolysis 1982;3:283-305.

[69] Pastorova I, Arisz PW, Boon JJ. Preservation of D-glucose-oligosaccharides in cellulose chars. Carbohydr Res 1993;248:151-65.

[70] Patai S, Halpern Y. Pyrolytic Reaction of Carbohydrates. Part IX the Effect of Additives on the Thermal Behavior of Cellulose Samples of Different Crystallinity. Isr J Chem 1970;8:655-62.

[71] Mohan D, Pittman CU, Steele PH. Pyrolysis of wood/biomass for bio-oil: a critical review. Energy Fuels 2006;20:848-89.

[72] Müller-Hagedorn M, Bockhorn H, Krebs L, Müller U. A comparative kinetic study on the pyrolysis of three different wood species. J Anal Appl Pyrolysis 2003;68:231-49.

[73] Grønli MG. A theoretical and experimental study of the thermal degradation of biomass. PhD thesis, 1996.

[74] Fengel D, Wegener G. Constituents of bark. In: Wood: chemistry, ultrastructure, reactions : Walter de Gruyter, 1984:240-267.

[75] Fengel D, Wegener G. Extractives. In: Wood: chemistry, ultrastructure, reaction : Walter de Gruyter, 1984:182-226.

[76] Välimaa A, Honkalampi-Hämäläinen U, Pietarinen S, Willför S, Holmbom B, von Wright A. Antimicrobial and cytotoxic knotwood extracts and related pure compounds and their effects on food-associated microorganisms. Int J Food Microbiol 2007;115:235-43.

[77] Knudsen JN, Jensen PA, Dam-Johansen K. Transformation and release to the gas phase of Cl, K, and S during combustion of annual biomass. Energy Fuels 2004;18:1385-99.

[78] Zevenhoven-Onderwater M, Blomquist J-, Skrifvars B-, Backman R, Hupa M. The prediction of behaviour of ashes from five different solid fuels in fluidised bed combustion. Fuel 2000;79:1353-61.

[79] Aho A, DeMartini N, Pranovich A, et al. Pyrolysis of pine and gasification of pine chars– Influence of organically bound metals. Bioresour Technol 2013;128:22-9.

[80] Eom I, Kim J, Kim T, et al. Effect of essential inorganic metals on primary thermal degradation of lignocellulosic biomass. Bioresour Technol 2012;104:687-94.

[81] Jensen A, Dam-Johansen K, Wójtowicz MA, Serio MA. TG-FTIR study of the influence of potassium chloride on wheat straw pyrolysis. Energy Fuels 1998;12:929-38.

[82] Nowakowski DJ, Jones JM, Brydson RM, Ross AB. Potassium catalysis in the pyrolysis behaviour of short rotation willow coppice. Fuel 2007;86:2389-402.

[83] Patwardhan PR, Satrio JA, Brown RC, Shanks BH. Influence of inorganic salts on the primary pyrolysis products of cellulose. Bioresour Technol 2010;101:4646-55.

[84] Pan WP, Richards GN. Influence of metal ions on volatile products of pyrolysis of wood. J Anal Appl Pyrolysis 1989;16:117-26.

[85] Saddawi A, Jones J, Williams A, Le Coeur C. Commodity fuels from biomass through pretreatment and torrefaction: effects of mineral content on torrefied fuel characteristics and quality. Energy Fuels 2012;26:6466-74.

[86] Saleh SB, Flensborg JP, Shoulaifar TK, et al. Release of chlorine and sulfur during biomass torrefaction and pyrolysis. Energy Fuels 2014;28:3738-46.

[87] Jensen PA, Frandsen F, Dam-Johansen K, Sander B. Experimental investigation of the transformation and release to gas phase of potassium and chlorine during straw pyrolysis. Energy Fuels 2000;14:1280-5.

[88] Björkman E, Strömberg B. Release of Chlorine from Biomass at Pyrolysis and Gasification Conditions1. Energy Fuels 1997;11:1026-32.

[89] Medic D, Darr M, Shah A, Rahn S. The Effects of Particle Size, Different Corn Stover Components, and Gas Residence Time on Torrefaction of Corn Stover. Energies 2012;5:1199-214.

[90] Yan W, Hastings JT, Acharjee TC, Coronella CJ, Vásquez VR. Mass and Energy Balances of Wet Torrefaction of Lignocellulosic Biomass. Energy Fuels 2010;24:4738-42.

[91] Kotilainen R, Alen R, Arpiainen V. Changes in the chemical composition of Norway spruce (Picea abies) at 160-260 C under nitrogen and air atmospheres. Paperi ja Puu 1999;81:384-8.

[92] Wilk M, Magdziarz A, Kalemba I. Characterisation of renewable fuels' torrefaction process with different instrumental techniques. Energy 2015,87:259-60.

[93] Pierre F, Almeida G, Brito JO, Perré P. Influence of torrefaction on some chemical and energy properties of maritime pine and pedunculate oak. BioResources 2011;6:1204-18.

[94] Wannapeera J, Worasuwannarak N. Upgrading of woody biomass by torrefaction under pressure. J Anal Appl Pyrolysis 2012;96:173-80.

[95] Nhuchhen DR, Basu P. Experimental Investigation of Mildly Pressurized Torrefaction in Air and Nitrogen. Energy Fuels 2014;28:3110-21.

[96] Agar D, DeMartini N, Hupa M. The influence of elevated pressure on the torrefaction of wood. Submitted 2015.

[97] Almeida G, Brito JO, Perre P. Alterations in energy properties of Eucalyptus wood and bark subjected to torrefaction: The potential of mass loss as a synthetic indicator. Bioresour Technol 2010;101:9778-84.

[98] Uemura Y, Omar W, Othman NA, Yusup S, Tsutsui T. Torrefaction of oil palm EFB in the presence of oxygen. Fuel 2013;103:156-60.

[99] Lu K, Lee W, Chen W, Liu S, Lin T. Torrefaction and low temperature carbonization of oil palm fiber and eucalyptus in nitrogen and air atmospheres. Bioresour Technol 2012;123:98-105.

[100] Chen W, Lu K, Lee W, Liu S, Lin T. Non-oxidative and oxidative torrefaction characterization and SEM observations of fibrous and ligneous biomass. Appl Energy 2014;114:104-13.

[101] Wang C, Peng J, Li H, et al. Oxidative torrefaction of biomass residues and densification of torrefied sawdust to pellets. Bioresour Technol 2013;127:318-25.

[102] Eseltine D, Thanapal SS, Annamalai K, Ranjan D. Torrefaction of woody biomass (Juniper and Mesquite) using inert and non-inert gases. Fuel 2013;113:379-88.

[103] Thanapal SS, Chen W, Annamalai K, Carlin N, Ansley RJ, Ranjan D. Carbon dioxide torrefaction of woody biomass. Energy Fuels 2014;28:1147-57.

[104] Di Blasi C, Lanzetta M. Intrinsic kinetics of isothermal xylan degradation in inert atmosphere. J Anal Appl Pyrolysis 1997;40:287-303.

[105] Di Blasi C. Modeling chemical and physical processes of wood and biomass pyrolysis. Progress in Energy and Combustion Science 2008;34:47-90.

[106] Branca C, Di Blasi C. Kinetics of the isothermal degradation of wood in the temperature range 528–708 K. J Anal Appl Pyrolysis 2003;67:207-19.

[107] Rousset P, Turner I, Donnot A, Perré P. The choice of a low-temperature pyrolysis model at the microscopic level for use in a macroscopic formulation. Ann For Sci 2006;63:213-29.

[108] Chen W, Kuo P. Isothermal torrefaction kinetics of hemicellulose, cellulose, lignin and xylan using thermogravimetric analysis. Energy 2011;36:6451-60.

[109] Shang L, Ahrenfeldt J, Holm JK, et al. Intrinsic kinetics and devolatilization of wheat straw during torrefaction. J Anal Appl Pyrolysis 2013;100:145-52.

[110] Khazraie Shoulaifar T, DeMartini N, Karlström O, Hupa M. Impact of organically bonded potassium on torrefaction: Part 1. Experimental. Fuel 2016;165:544-52.

[111] Werkelin J, Skrifvars B, Hupa M. Ash-forming elements in four Scandinavian wood species. Part 1: Summer harvest. Biomass Bioenergy 2005;29:451-66.

[112] Demartini N, Monedero E, Yrjas P, Hupa M. Co-firing black liquor and biomass in a laboratory single droplet reactor - effects on emissions and combustion characteristics. Tappi J 2010;9:29-33.

[113] Kiel J, Verhoeff F, Gerhauser H, Meuleman B. BO2-technology for biomass upgrading into solid fuel-pilot-scale testing and market implementation. 16th European Biomass Conference and Exhibition: 2-6 June, Valencia, Spain 2008:1-7.

[114] Harris DC. Quantitative chemical analysis. 1995:787.

[115] Fardim P, Holmbom B. Fast determination of anionic groups in different pulp fibers by methylene blue sorption. Tappi J 2003;2:28-32.

[116] Mehta S, Singh A. Adsorption isotherms for red chilli (Capsicum annum L.). European Food Research and Technology 2006;223:849-52.

[117] Greenspan L. Humidity fixed points of binary saturated aqueous solutions. Journal of Research of the National Bureau of Standards 1977;81:89-96.

[118] Sundberg A, Sundberg K, Lillandt C, Holmbom B. Determination of hemicelluloses and pectins in wood and pulp fibres by acid methanolysis and gas chromatography. Nordic Pulp and Paper Research Journal 1996;216-9.

[119] Smeds AI, Eklund PC, Monogioudi E, Willför SM. Chemical characterization of polymerized products formed in the reactions of matairesinol and pinoresinol with the stable radical 2, 2-diphenyl-1-picrylhydrazyl. Holzforschung 2012;66:283-94.

[120] Willför S, Hemming J, Reunanen M, Eckerman C, Holmbom B. Lignans and lipophilic extractives in Norway spruce knots and stemwood. Holzforschung 2003;57:27-36.

[121] Holmbom B. Extractives. In: Sjöström E and Alén R, editors. Analytical methods in wood chemistry, pulping, and papermaking. : Springer Series in Wood Science, 1999:125-48.

[122] Örsa F, Holmbom B. A convenient method for the determination of wood extractives in papermaking process waters and effluents. J Pulp Paper Sci 1994;20:J361-6.

[123] Bialczak S, Willför S, Sundberg A. The effect of storage conditions on extraction efficiency and identification of extractives in wood-containing paper. Nordic Pulp & Paper Research Journal 2013;28,541-6.

[124] Baxter LL, Miles TR, Jenkins BM, et al. The behavior of inorganic material in biomass-fired power boilers: field and laboratory experiences. Fuel Process Technol 1998;54:47-78.

[125] EPA 200.7, http://www.caslab.com/EPA-Method-200_7/ ; last access 12.2015.

[126] EPA 200.8. http://www.caslab.com/EPA-Method-200_8/ ;last access 12.2015.

[127] Khazraie Shoulaifar T, DeMartini N, Ivaska A, Fardim P, Hupa M. Measuring the concentration of carboxylic acid groups in torrefied spruce wood. Bioresour Technol 2012:338-343.

[128] Windeisen E, Strobel C, Wegener G. Chemical changes during the production of thermo-treated beech wood. Wood Sci Technol 2007;41:523-36.

[129] Werkelin J, Skrifvars BJ, Zevenhoven M, Holmbom B, Hupa M. Chemical forms of ash-forming elements in woody biomass fuels. Fuel 2010;89:481-93.

[130] Fardim P, Holmbom B, Ivaska A, Karhu J, Mortha G, Laine J. Critical comparison and validation of methods for determination of anionic groups in pulp fibres. Nord Pulp Pap Res J 2002;17:346-51.

[131] Rutherford DW, Wershaw RL, Reeves JB, Geological Survey (US). Development of acid functional groups and lactones during the thermal degradation of wood and wood components. : US Geological Survey, 2008; 1-52.

[132] DeGroot WF. Preliminary investigation of the association of inorganic cations with carboxylic acid groups in wood. Carbohydr Res 1985;142:172-8.

[133] Sjöström E. The origin of charge on cellulosic fibres. Nordic Pulp and Paper Research Journal 1989;4:90-93.

[134] Sundén A, Brelid H, Rindby A, Engström P. Spatial distribution and modes of chemical attachment of metal ions in spruce wood. J Pulp Paper Sci 2000;26:352-7.

[135] Maher TP, Schafer HNS. Determination of acidic functional groups in low-rank coals: comparison of ion-exchange and non-aqueous titration methods. Fuel 1976;55:138-40.

[136] Acharjee TC, Coronella CJ, Vasquez VR. Effect of thermal pretreatment on equilibrium moisture content of lignocellulosic biomass. Bioresour Technol 2011;102:4849-54.

[137] Chen W, Kuo P. Torrefaction and co-torrefaction characterization of hemicellulose, cellulose and lignin as well as torrefaction of some basic constituents in biomass. Energy (Oxford, UK) 2011;36:803-11.

[138] Inari GN, Petrissans M, Gerardin P. Chemical reactivity of heat-treated wood. Wood Sci Technol 2007;41:157-68.

[139] Rousset P, Lapierre C, Pollet B, Quirino W, Perre P. Effect of severe thermal treatment on spruce and beech wood lignins. Ann For Sci 2009;66:110 (p1-p8).

[140] Park J, Meng J, Lim KH, Rojas OJ, Park S. Transformation of lignocellulosic biomass during torrefaction. J Anal Appl Pyrolysis 2013;100:199-206.

[141] Pastorova I, Botto RE, Arisz PW, Boon JJ. Cellulose char structure: a combined analytical Py-GC-MS, FTIR, and NMR study. Carbohydr Res 1994;262:27-47.

[142] Bourgois J, Guyonnet R. Characterization and analysis of torrefied wood. Wood Sci Technol 1988;22:143-55.

[143] Benson SA, Holm PL. Comparison of inorganics in three low-rank coals. Industrial & engineering chemistry product research and development 1985;24:145-9.

[144] Zintl F, Strömberg B, Björkman E. Release of chlorine from biomass at gasification conditions. 1998:1608-1611.

[145] Jensen PA, Frandsen F, Dam-Johansen K, Sander B. Experimental investigation of the transformation and release to gas phase of potassium and chlorine during straw pyrolysis. Energy Fuels 2000;14:1280-5.

[146] van Lith SC, Alonso-Ramírez V, Jensen PA, Frandsen FJ, Glarborg P. Release to the gas phase of inorganic elements during wood combustion. Part 1: development and evaluation of quantification methods. Energy Fuels 2006;20:964-78.

[147] Hamilton JT, McRoberts WC, Keppler F, Kalin RM, Harper DB. Chloride methylation by plant pectin: an efficient environmentally significant process. Science 2003;301:206-9.

[148] Johansen JM, Jakobsen JG, Frandsen FJ, Glarborg P. Release of K, Cl, and S during Pyrolysis and Combustion of High-Chlorine Biomass. Energy Fuels 2011;25:4961-71.

[149] Freeman ES, Carroll B. The application of thermoanalytical techniques to reaction kinetics: the thermogravimetric evaluation of the kinetics of the decomposition of calcium oxalate monohydrate. J Phys Chem 1958;62:394-7.

[150] Fuentes M, Nowakowski D, Kubacki M, Cove J, Bridgeman T, Jones J. Survey of influence of biomass mineral matter in thermochemical conversion of short rotation willow coppice. Journal of the Energy Institute 2008;81:234-41.

[151] Kleen M, Gellerstedt G. Influence of inorganic species on the formation of polysaccharide and lignin degradation products in the analytical pyrolysis of pulps. J Anal Appl Pyrolysis 1995;35:15-41.

[152] Yang H, Yan R, Chen H, Zheng C, Lee DH, Liang DT. Influence of mineral matter on pyrolysis of palm oil wastes. Combust Flame 2006;146:605-11.

[153] Darvell LI, Hrycko P, Jones JM, Nowakowski DJ, Pourkashanian M, Williams A. Impact of minerals and alkali metals on willow combustion properties. World Renewable Energy Congress, Editors M. S. Imbabi and C. P. Mitchell, Elsevier 2005:584-9.

[154] Wang Z, Wang F, Cao J, Wang J. Pyrolysis of pine wood in a slowly heating fixed-bed reactor: potassium carbonate versus calcium hydroxide as a catalyst. Fuel Process Technol 2010;91:942-50.

[155] Karlström O, Brink A, Hupa M, Tognotti L. Multivariable optimization of reaction order and kinetic parameters for high temperature oxidation of 10 bituminous coal chars. Combust Flame 2011;158:2056-63.

[156] Krogell J, Holmbom B, Pranovich A, Hemming J, Willför S. Extraction and chemical characterization of Norway spruce inner and outer bark. Nordic Pulp and Paper Research Journal 2012:6-17.

RECENT REPORTS FROM THE COMBUSTION AND MATERIALS CHEMISTRY GROUP OF THE JOHAN GADOLIN PROCESS CHEMISTRY CENTRE AT ÅBO AKADEMI UNIVERSITY:

10-01	Markus Engblom	Modeling and Field Observations of Char Bed Processes in Black Liquor Recovery Boilers
11-01	Leena Varila et al.	Fyrtio År Oorganisk Kemi vid Åbo Akademi
11-02	Johan Lindholm	On Experimental Techniques for Testing Flame Retardants in Polymers
11-03	Minna Piispanen	Characterization of Functional Coatings on Ceramic Surfaces
11-04	Sonja Enestam	Corrosivity of Hot Flue Gases in the Fluidized Bed Combustion of Recovered Waste Wood
12-01	Xiaoju Wang	Enzyme Electrode Configurations: for Application in Biofuel Cells
12-02	Patrycja Piotrowska	Combustion Properties of Biomass Residues Rich in Phosphorus
12-03	Dorota Bankiewicz	Corrosion Behavior of Boiler Tube Materials during Combustion of Fuels Containing Zn and Pb
12-04	Mikael Bergelin, Jan-Erik Eriksson, Xiaoju Wang, Max Johansson, et al.	Printed Enzymatic Power Source with Embedded Capacitor on Next Generation Devices, Tekes-PEPSecond
12-05	Susanne Fagerlund	Understanding the in vitro dissolution rate of glasses with respect to future clinical applications
13-01	Oskar Karlström	Oxidation rates of carbon and nitrogen in char residues from solid fuels
13-02	Juho Lehmusto	The Role of Potassium in the Corrosion of Superheater Materials in Boilers Firing Biomass
13-03	Bingzhi Li	Modeling of Fireside Deposit Formation in Two Industrial Furnaces
13-04	Frida Jones	Characterisation of Waste for Combustion –with Special Reference to the Role of Zinc

RECENT REPORTS FROM THE COMBUSTION AND MATERIALS CHEMISTRY GROUP OF THE JOHAN GADOLIN PROCESS CHEMISTRY CENTRE AT ÅBO AKADEMI UNIVERSITY:

Johan Gadolin
Process Chemistry Centre